SKBF TEKNISK
KBS RAPPORT

83-57

Neotectonics in northern Sweden – geophysical investigations

H Henkel
K Hult
L Eriksson

Geological Survey of Sweden

L Johansson

Swedish Geological
May 1983

NEOTECTONICS IN NORTHERN SWEDEN -

Geophysical Investigations

Herbert Henkel
Karin Hult
Leif Eriksson
Geological Survey of Sweden

Lars Johansson
Swedish Geological

May 1983

NEOTECTONICS IN NORTHERN SWEDEN -

Geophysical Investigations

Herbert Henkel

Karin Hult

Leif Eriksson

Geological Survey of Sweden

Lars Johansson

Swedish Geological

May 1983

Neotectonic phenomena, i.e. recent or contemporary faulting and block movement, are of cruical interest for the choice of methods and sites for the disposal of radioactive waste.

During the last decade, attention has been drawn to the occurrence of late quaternary faults in the Norrbotten district. These faults and their related effects have been studied by several methods, e.g. air photo interpretation, ground geological investigation, and geophysics.

This paper is a compilation of geophysical surveys over late quaternary faults in Norrbotten made during1982 at the geological survey of Sweden (SGU). The work has been made by commission of PRAV and KBS.

The results have previously been presented in the reports 8218 (Herbert Henkel, Karin Hult and Leif Eriksson), and in FM 8231 (Lars Johansson). These papers are in Swedish.

ABSTRACT

The report treats the geophysical aspects of the late quaternary faults in the Norrbotten district, and the connection between these faults and older fracture zones. The older fracture zones are mapped out mainly by aeromagnetic interpretation.

Three late quaternary fault complexes are included, namely the Lansjärv fault, the Kärkejaure fault and the Pärvie fault.

Around the Lansjärv fault, older regional and local fault systems have been mapped out by aeromagnetic interpretation. The interpretation in the vicinity of the fault was made from high resolution aeromagnetic data, augmented with ground geophysical surveys. The technique and the limitations of the aeromagnetic interpretation are discussed.

Maps and trend distribution diagrams of the older fault zones are presented, together with interpretation of the displacements at some of these zones.

It has been found that the late quaternary faults at Lansjärv are largely influenced by the older fault zones, but that fracturing outside of these zones is quite common. It is also supected that recent movements may have occurred within major older fault zones, but escaped detection in these places.

Possible mechanisms, i.e. post-glacial uplift and plate tectonic motion, of the late quaternary fault movements are preliminarily discussed.

Also around the Kärkejaure fault, aeromagnetic interpetation from high-resolution data has been made. This has revealed that the fault entirely follows an older fault zone, that previously has escaped detection. It has also been found that the late quaternary fault has been influenced by the local fracture system belonging to the Kärkejaure gabbro.

At the Lansjärv fault, also seismic refraction investigation has been made. The results indicate that late quaternary block motion has occurred at several events. The throw of the fault is estimated from the thickness of weathered rock, preserved on the downthrown side.

Airborne electromagnetic (RAMA) surveys over late
quaternary faults are discussed and compared with
ground electromagnetic methods. It is shown that
the late quaternary faults generally are represen-
ted by conductive zones in the bedrock, i.e.
water-bearing fracture zones. A case of Slingram
survey over a late quaternary fault, where it is
shown that the recent fault apparently has engaged
the central part of an older fracture zone, is
presented.

In the Tjårrojåkka and Aitejåkka areas, where
ground geophysical data from earlier ore prospect-
ing are available, these have been used, together
with supplementary surveys, for the investigation
of the faults of the Pärvie compelx. It has been
found that at Tjårrojåkka, the Pärvie fault coin-
cides with an older tectonic zone. The seismic
survey undertaken indicates that substantial
preglacial displacement has occurred at the zone.

Also the fault at Aitejåkka has been found to
follow an older tectonic zone.

CONTENTS: page

1. INTRODUCTION

The present report is a follow-up on a formerly published preliminary study on the relation between late quaternary faults and surrounding structures (Lagerbäck and Henkel 1977). In order to augment the knowledge of geophysical methods as a tool for the investigation of these faults, an evaluation of ground geophysical measurements, made for ore prospecting purposes in the areas Tjårrojåkka and Aitejåkka, has been undertaken. This work is presented in chapter 8.

A very thorough study of the regional and local faults surrounding the Lansjärv area has been carried out. The purpose of this is to closer map out the connection between older structures (faults and tectonic zones) and the more recent faults. The available aeromagnetic maps (on the scale of 1:50 000) along with an improved revision of the aeromagnetic survey in the vicinity (20 x 45 km) of Lansjärv, form the basis of the study. To improve the knowledge of geophysical features of regional and late quaternary faults, ground geophysical measurements have been made along some 30 profiles in the Lansjärv area. Within an area where airborne electromagnetic (RAMA) data are available, an evaluation of the electric (i.e. conductivity) properties of the fault has been made.

The late quaternary faults are usually associated with distinct electric and electromagnetic (Slingram, RAMA) anomalies. In addition to these indications, older faults and fracture zones exhibit magnetic anomalies (linear minima). These are missing where the recent faults do not follow older zones. The closer geophysical investigation also establishes that the late tectonic movement has occurred in several ways and at, in the least, two separate occasions. The interplay between younger and older faults suggests that reactivation of older zones also has occurred outside of the main paths of late quaternary faults.

The discussion on the kinematic interpretation of the observed neo-tectonic phenomena is very preliminary. This field requires further study, in cooperation with other geosciences (i.e. tectonics, rock mechanics and seismology). The causes of the late quaternary faults are as yet uncertain, deglaciation and plate movement being two possible alternatives. For the estimation of future block movements, it is necessary not only to explain the features of historic tectonic events, but also to evaluate the causing local stress conditions in the earth's crust.

The geophysic survey of the Lansjärv area has shown that a fairly detailed mapping of younger and older fracture zones is feasible with present technique. However, our knowledge of recent tectonic phenomena and their causes is not yet sufficient for prognoses concerning the future stability of the bedrock. This calls for considerably more observation of the studied phenomena.

figure 1.

Subdivision of Sweden
in map areas. (RAK)
Shaded area represents
fig. 2

Figure 2
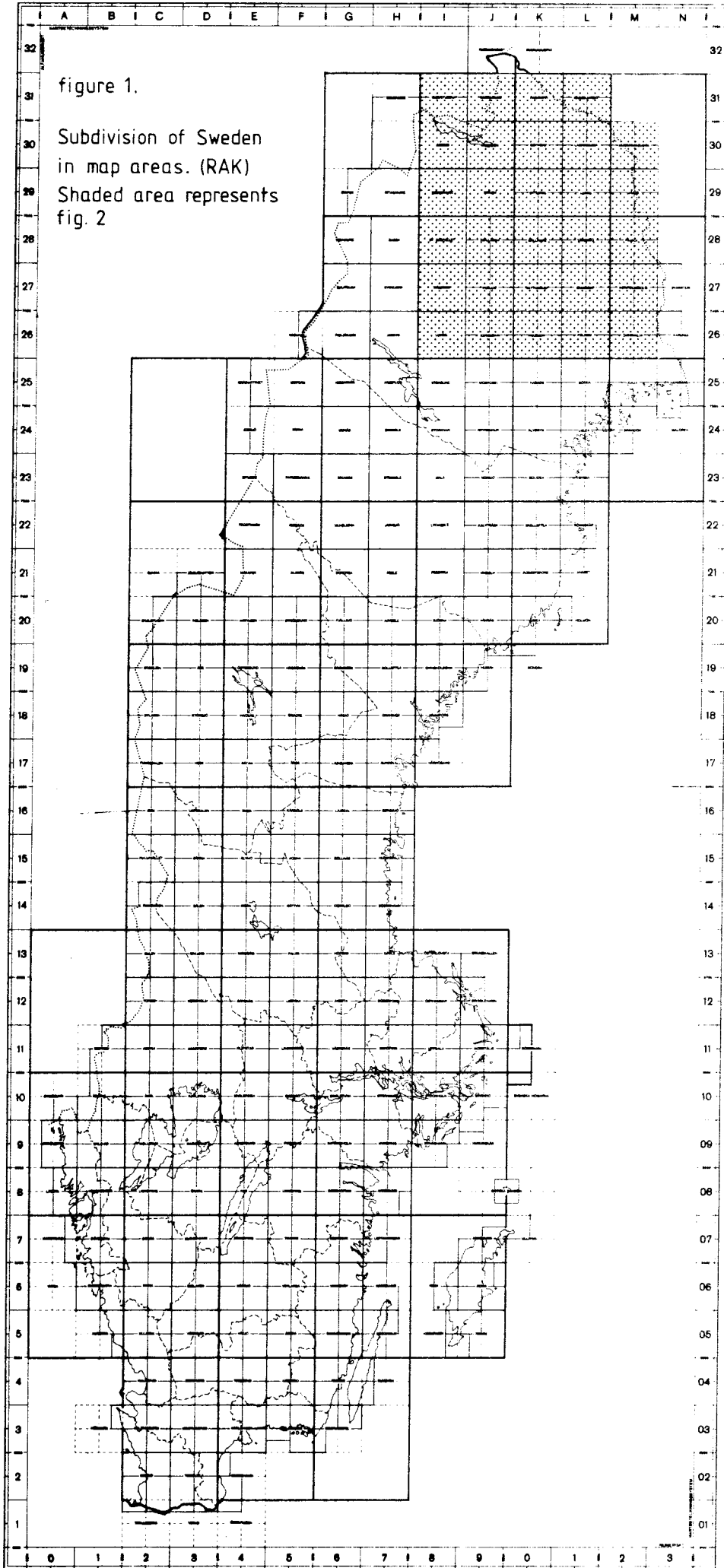
LATE QUATERNARY FAULTS IN NORRBOTTEN
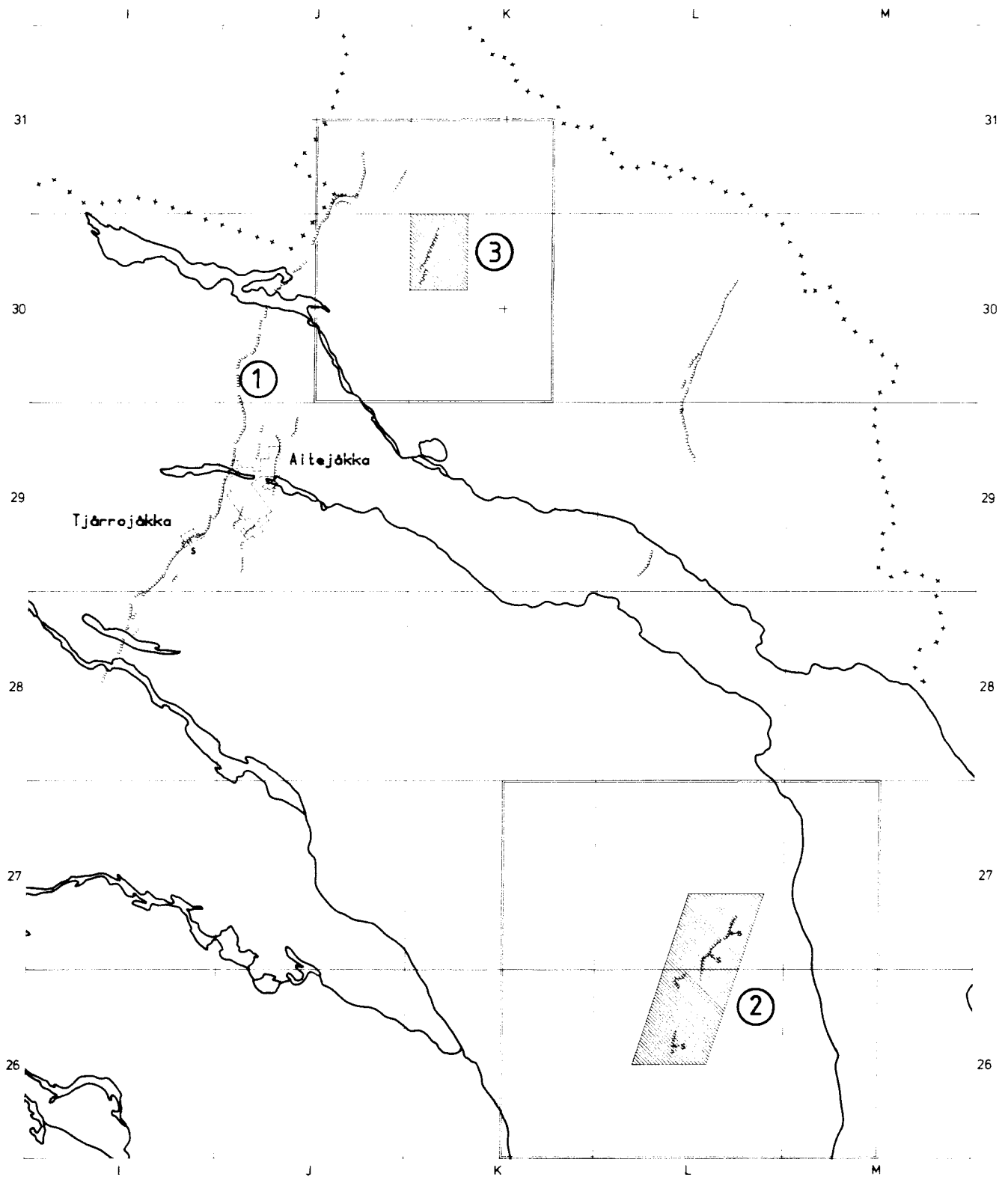
①	PÄRVIE FAULT
②	LANSJÄRV FAULT
③	KÄRKEJAURE FAULT

s SEISMIC PROFILES

2. MAGNETIC MAPPING OF LARGE-SCALE REGIONAL DISLOCATION SYSTEMS IN THE LANSJÄRV REGION

(By Karin Hult)

2.1 Background

As a background and complement to the detailed magnetic and neotectonic survey of the Lansjärv area (cf. fig. 3), an aeromagnetic interpretation of major fault systems within the map areas 26-27 K-M (100 x 100 km) has been made.

2.2 Methods

The prevalent magnetic total intensity map (on the scale of 1:50 000, flight altitude 30 m, flight line spacing 200 m, equidistance 100 nT) has been the basis of the work. The flight direction in the area was east-westerly. In total, 16 sub-areas have been interpreted, namely: 26 and 27K (the eastern sub-areas), L and M (the western sub-areas).

The dislocations have been recognized from the following features (Henkel 1979):

1. Zones containing low magnetic material, producing elongated, narrow, linear magnetic minima.

2. Interruption of the anomaly pattern.

3. Displacement of characteristic anomalies.

4. Changes in magnetic horizontal gradients.

Magnetic dislocations that satisfy one or several of the above criteria are taken as representing faults or fracture zones. The low magnetic zones are caused by the oxidation of magnetite into hematite (Henkel and Guzmán 1977).

For convenient statistic treatment, the mapped dislocations have been digitized. The digitized material was used for construction of strike frequency distribution diagrams.

2.3 Comparison with topographic features

Topographic maps of the investigated area have been scrutinized for linear structures, i.e. precipices, ravines, valleys and straight lake shores. These topographic lineaments have a prominent NW-SE trend, in good accordance with the main trend of the magnetic dislocations. Often the topographic lineaments follow magnetic dislocations. Occasionally, they occur as extensions or connections of the latter, but mostly as parallel or totally separate features.

The maps of glaciation grooves and bedrock drumlinization worked out by R. Lagerbäck (1981) show, when compared with the magnetic maps, good agreement between the assumed bedrock drumlinization and northwesterly trending magnetic dislocations.
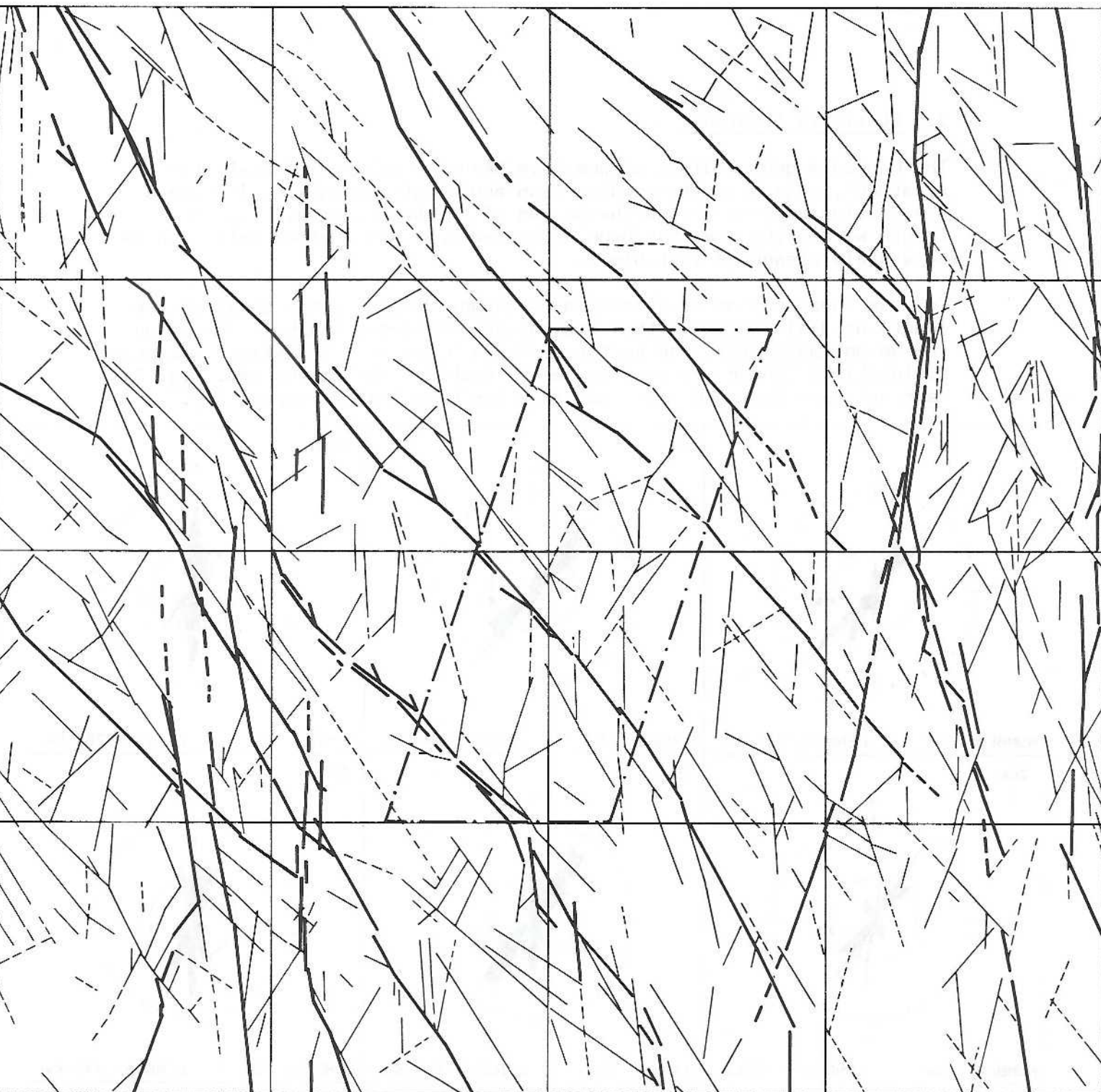
LANSJÄRV MAGNETIC DISLOCATIONS   Scale 1:500 000

Area of detailed survey — · —

Index: Figure 3.

distinct regional dislocations

less distinct regional dislocations

distinct dislocations

less distinct dislocations
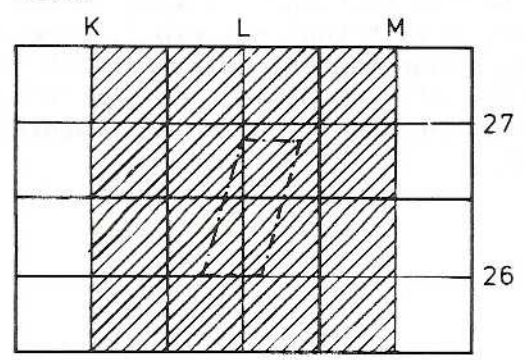
2.4 Statistic treatment

The mapped magnetic dislocations have been the subject of statistic treatment, regarding strike direction and length extension. In case a dislocation extends beyond the bounds of the survey area, only the length within the area has been accounted for. The further extension is separately presented in table 2.

For the construction of direction frequency diagrams, the total strike length of dislocations within each direction sector has been chosen as the weight parameter. The sector width is 5 degrees. Indistinct magnetic dislocations (these are represented by dashed lines on the map, fig. 3) have not been included. Each map area has been treated separately.

27K	27L	27M
NUMBER: 132 LENGTH: 531 Km	NUMBER: 190 LENGTH: 640 Km	NUMBER: 206 LENGTH: 708 Km
26K	26L	26M
NUMBER: 130 LENGTH: 515 Km	NUMBER: 227 LENGTH: 854 Km	NUMBER: 130 LENGTH: 443 Km
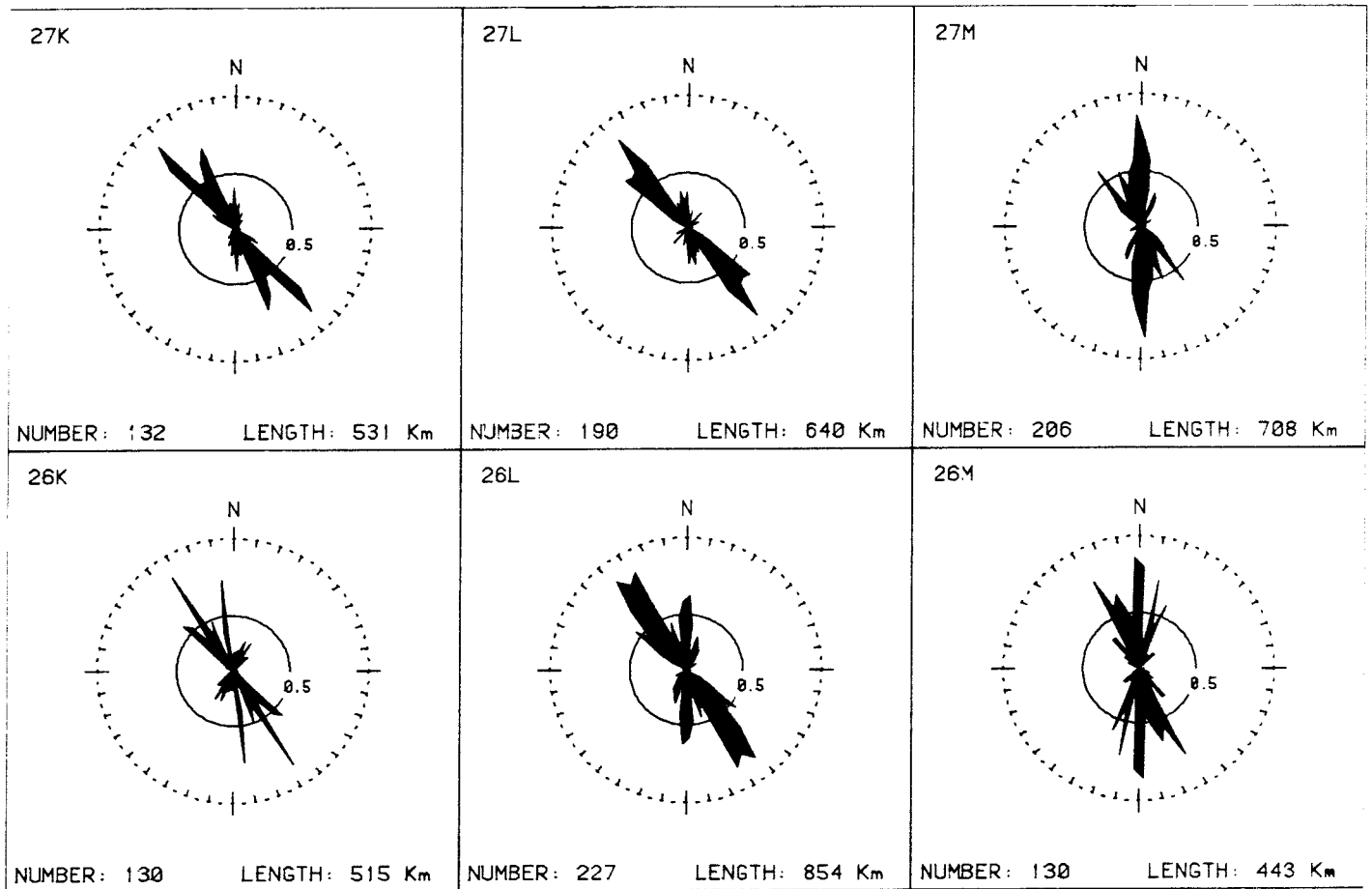
Fig. 4. Trend frequency diagrams of the mapped magnetic dislocations.

From the diagrams, the dominating trends are evident. Dislocations with east-westerly strike have very rarely been detected. As the flight direction of the magnetic survey of this area has been east-westerly, the resolution of narrow features striking in this direction is substantially lower, a fact that may explain the absence of detected east-west striking, minor magnetic dislocations. However, major dislocation zones are of such dimensions that they will be detected regardless of the flight direction. No east-westerly trending such zones have been observed.

The dominating trend of the dislocations changes from the western to the eastern map areas. In the western part, the main trend is to the northwest, while a prominent northerly trend supervenes in the eastern areas, cf. fig. 4.

The NE-striking dislocations are often interrupted or disturbed by northwesterly trending zones. No tendency of forming prominent zones exist among them. (However, the southern parts of zones nr. 1 and nr. 8 strike to the northeast.)

The many shorter dislocations of different strike directions appear as 'random noise' in the frequency-distribution diagrams. The trends of the frequency maxima, clearly discernible above the 'noise level' are listed in table 1.

TABLE 1. Prominent trends of magnetic dislocations within each map area. Underscored trends dominate.

AREA	Prominent trends												
27 K	N60W		N45W			**N20W**			N				
27 L		N50W		**N40W**				N5W					N40E
27 M				**N40W**		N20W		**N5W**		N5E		N20E	
26 K		**N50W**			N30W	N20W	**N10W**						N30E
26 L		**N50W**		N40W		N20W			N				
26 M				**N40W**	N30W				N		N10E	N20E	

2.5 Large-scale regional dislocation zones

From the map of magnetic dislocations, 13 major zones have been interpreted. These consist of sequences of dislocations, trending in roughly the same direction. The width of the zones varies from about 100 m up to barely 1 km. Often, the widest zones are bordered by parallel magnetic dislocations at a separation of up to 2.5 km.

The spacing between the regional zones is from 4 to 25 km, the mean distance being about 17 km. The extensions of the zones are given in table 2.

TABLE 2. Extension in kilometers of dislocation zones within and outside of the survey area.

Zone nr	1	2	3	4	5	6	7	8	9	10	11	12	13
in the area	75	85	80	40	30	115	115	95	90	65	55	45	85
north / west			24	38		10	80	29	6	14		30	11
south / east	5	5	36			5	17				2		
total length	80	90	140	78	30	130	212	124	96	79	57	75	96
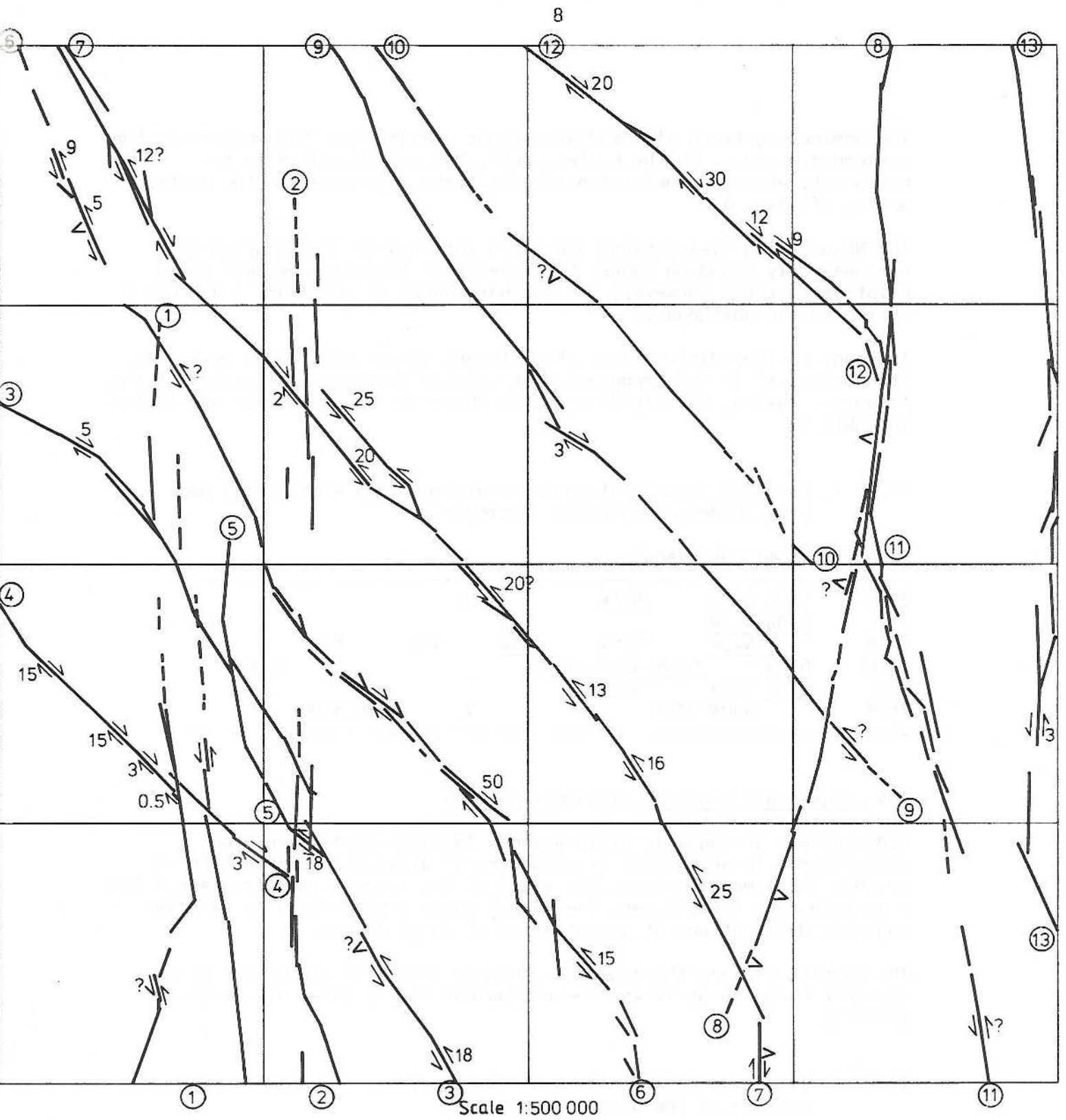
LANSJÄRV MAGNETIC DISLOCATIONS   MAJOR REGIONAL ZONES

Index:

Figure 5

distinct regional dislocations

--- less distinct regional dislocations

(1) end of zone nr. 1

→15 displacement, 1500 m

V downthrown block

? uncertain interpretation

Scale 1:500 000
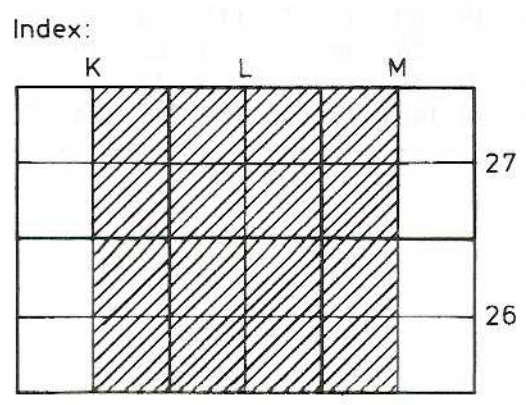
The dominating strike direction of the major zones is SE-NW. In the western- and easternmost parts of the survey area, north-trending zones occur. These disturb some of the above-mentioned zones, which may indicate that the north-trending zones are more recently formed. Seemingly, they delimit a 50 km wide, less magnetic area, apparently lacking north-striking dislocations. Interpretation of the displacements at the major zones has been attempted, and the results will be presented below.

Descriptions of individual major zones: (See fig. 5.)

1. The zone, trending N-S, consists of two parallels at a mutual distance of c. 2.5 km. The southern part is very prominent, but in the northernmost map area, the zone dwindles. Its extension within the area is 75 km, and it continues for 5 km to the south. Apparently, it disturbs the southernmost of the SE-NW-trending dislocations. The block displacement can hardly be ascertained. Probably, it has been vertical, which is common among north-striking dislocations.

2. This zone, striking north-south, apparently forms the western boundary of the above-mentioned low magnetic area. It extends for 85 km within the survey area, and for an additional 5 km to the south. However, it is not discernible in the northern part of map-area 26L NW, where the zone nr. 6 dominates. In places, the zone consists of parallel dislocations at a separation of 2 - 2.5 km. No distinct block displacement is demonstrable, but probably, vertical movement has occurred.

3. This zone appears mainly as a sequence of SE-NW-trending, linear minima. Its length within the area is 80 km, and it extends for 24 km to the north and for 36 km to the south. It is affected by the zones 1, 2, and 5. In the southern part, an apparent sinistral displacement, amounting to 1.8 km, possibly along with a downthrow of the southeastern block, appears. The central part is complicated by the interference of zones 5 and 2. The northern part shows a sinistral displacement of 500 m.

4. The zone, appearing as a sequence of linear minima, strikes to the NW. It is bounded to the east by zone nr. 2. The length is 40 km within the area, extending for a further 38 km to the NW. In several places along the zone, dextral displacement appears, amounting to c. 1.5 km in the northwestern part.

5. It is somewhat difficult to separate this rather short (30 km) zone from zone nr. 3. Seemingly, the zone is curved, its strike varying from NNW in the southern part to N in the north. No interpretation of the displacement has been achieved.

6. This very prominent zone crosses the entire area in a north-westerly direction. Within the survey area, it extends for 115 km. Towards the northwest, it continues for a further 10 km, and, towards the southeast, for 5 km. The separation of the parallel dislocations in the southern section varies, but is on the average 500 m. The zone

appears mainly from the change of anomaly pattern across it. In the
northwest, linear minima are the most prominent features of the zone.
In the south-eastern part of sub-area 26L NW, a dextral displacement
of 5 km is indicated. This is probably the resultant of several
movements in somewhat different directions. At the western extremity,
after the passage of zone nr. 1, several minor sinistral
displacements, at places including a vertical component, appear.

7. This NW-trending zone is largely a parallel of nr. 6, at a
   distance varying from 12 km in the south to 7 km in the north.
   It extends for 115 km within the area. To the NW, it is traceable
   for a further 80 km, and, to the SE, 17 km. The dislocation zone
   appears from the displacements of characteristic anomalies. It
   crosses the zones nr. 2 and nr. 8, and is the dominating one
   at these sites. The displacement is sinistral and amounts up to
   2.5 km. In the north, however, minor dextral displacement appears.

8. This northerly trending dislocation zone diminishes towards the
   south. It extends for 95 km within the survey area, and, to the
   north of it, for another 29 km. In the southern section, a vertical
   displacement with a downthrown eastern block is indicated. Vertical
   displacement is also indicated in the north, where the zone is more
   prominent, but here, the western block has subsided. This
   interpretation relies on anomaly patterns and -levels, as distinct
   reference structures are missing. The zone constitutes the eastern
   border of the formerly mentioned low magnetic central part of the
   survey area. The regional zones 10, 11, and 12 are discontinued at
   this zone, while the zones 7 and 9 cross it.

9. The zone strikes to the NW and is 90 km long. To the NW of the
   area, it can be followed for another 6 km. It appears as linear
   minima, though at its southern extremity, by a change of the
   anomaly pattern. In the southern part, it is affected by zone
   nr. 8. No major displacement is discernible. A minor dextral
   displacement of 300 m is found in the middle of the zone.

10. This zone, appearing as linear minima, strikes to the NW, and is
    bounded to the SE by zone nr. 8. It extends for 65 km within the
    survey area, and for a further 14 km towards the NW. No
    displacement has been interpreted. In the sub-area 27L NE, a
    possible downthrow of the southeastern block appears.

11. This zone consists of several short dislocations. The strike is
    to the NNW, i.e. in between of the two main trends, north and
    northwest. Its northern part appears as a change of the anomaly
    pattern, the southern part mainly as linear minima. The length
    of the zone is 55 km, and the width varies from some hundred
    meters in the south to a km in the north. Here, the zone is
    interrupted by zone nr. 8, and, to the south, it is discernible
    for 2 km outside of the survey area. No displacement has
    been interpreted.

12. The zone strikes to the NW, and is limited to the SE by zone nr.
    8. In the southeastern part, parallel dislocations at a separation

of 1.5 km occur. The northern part of the zone is narrower. It
is visible mainly on account of differences in the anomaly pattern.
It is 45 km long within the survey area, and continues for 30 km
to the NW. Several dextral displacements can be gauged. The dis-
placement is at its greatest, 3 km, in the central part of the
zone, and diminishes to 2 km in the northwest, and to 0.9 km in
the southeast.

13. This N-trending zone is situated at the eastern extremity of the
    survey area. It extends for 85 km within the area, and for an
    additional 11 km northwards. To the south, it is interrupted by a NW-
    striking magnetic dislocation. The width of the zone varies around
    300 m. Probably, vertical displacement has occurred, though this has
    not been proved. In one locality at the zone, a sinistral
    displacement of 300 m has been interpreted.

2.6 Comments

The described displacements are the results of a succession of block
movements which may have amplified or cancelled each other. It may,
partly on account of this complex course of events, be difficult to find
the right connections of reference structures. Sometimes, the dip of a
reference structure is difficult to estimate, which obstructs the
interpretation, particularly of vertical block movement and amount of
displacement. Additionally, the reference structures may be of different
age, and thus, their relations are difficult to make out.

At a straight-forward study of the correlation of displacement direction
to strike of the magnetic dislocations, it was found that the north-
trending zones have been engaged in vertical block movement, possibly
with a horizontal component, in this case mainly a sinistral one.

The zones which show dextral displacement seem to lie within a narrower
direction interval than those showing sinistral displacement.
Principally, their trend is somewhat more westerly, between N65W and
N40W.

Consequently, sinistral displacement occurs at dislocations within a
wider trend interval, from N65W to N15W. The greater part of the
sinistral displacements occur at the more northerly trending
dislocations.

An attempt has been made to evaluate the age relation of the zone nr. 8
to the zones crossing it, one criterion being that the younger zones
disturb the older ones. The plausible interpretation is that the zone
is younger than the zones 9, 11, and 12, but older than zone nr. 7.
This estimation of relative age has not been practicable for the
other zones.

3. ANALYSIS OF FRACTURE SYSTEMS IN THE VICINITY OF THE LANSJÄRV FAULT
   (by Herbert Henkel)

3.1 Description and trend-statistics

In the vicinity of the Lansjärv fault (see fig. 3), a detailed
interpretation of fracture zones and faults was made. For this work, a
revised version of the aeromagnetic map, with 40 nT equidistance, has
been employed. This, and the corresponding topographic map, is shown in
fig. 6.

The bedrock around the Lansjärv fault has a rather high and varying
magnetization. These conditions are favourable for the study of fracture
zones and faults. Thus, the location, width, extension, and sometimes
the dip of the zones can be assessed. Where unambiguous reference
structures are at hand, it is also possible to estimate the relative
displacement and the age of the faults.

Fracture zones cause linear, negative magnetic anomalies due to the
oxidation of the magnetite in the bedrock into hematite (Henkel and
Guzman 1977). The oxidation, in turn, is caused by circulating subsoil
water. The faults cause displacement or interruption of the magnetic
structural features. The magnetic interpretation of the fracture zones
and faults has been made according to the methods presented in Henkel
(1979), and in chapter 2, above. The results are shown in figure 7.

This interpretation reveals faults and fracture zones within the survey
area that are indicated by their magnetic effects. The zones must be of
a certain minimal magnitude (i.e. width, length, and displacement and/or
depth of weathering) to appear from the magnetic anomaly picture. The
magnitude necessary depends on the distance between measured points, and
on the profile direction. Thus, zones trending perpendicularly to the
flight direction may be identified if their width amounts to 20 m and/or
the displacement exceeds 50 m, while for zones running parallel to the
direction of flight, the required width is about 100 m. The length of
the zones must exceed c. 500 m if their trend deviates from the strike
of the magnetic reference structures. For positive identification of
dislocation zones parallel to the strike, a substantially greater length
(often more than the length extension of the reference structures) is
required. Besides faults and tectonic zones, linear escarpments in the
bedrock surface (beneath the quaternary deposit or as rock terraces)
will have magnetic effects, interpretable as dislocations. Among the
magnetic dislocations in the Lansjärv area, low magnetic zones
predominate, and distinct block displacement is observable only at a few
places along the major, regional faults.

The dislocations occur in characteristic trends and at characteristic
spacing. Table 3 below gives an overview of features of the major
faults, and fig. 8 shows the trend distribution of the dislocations
presented in fig.7.
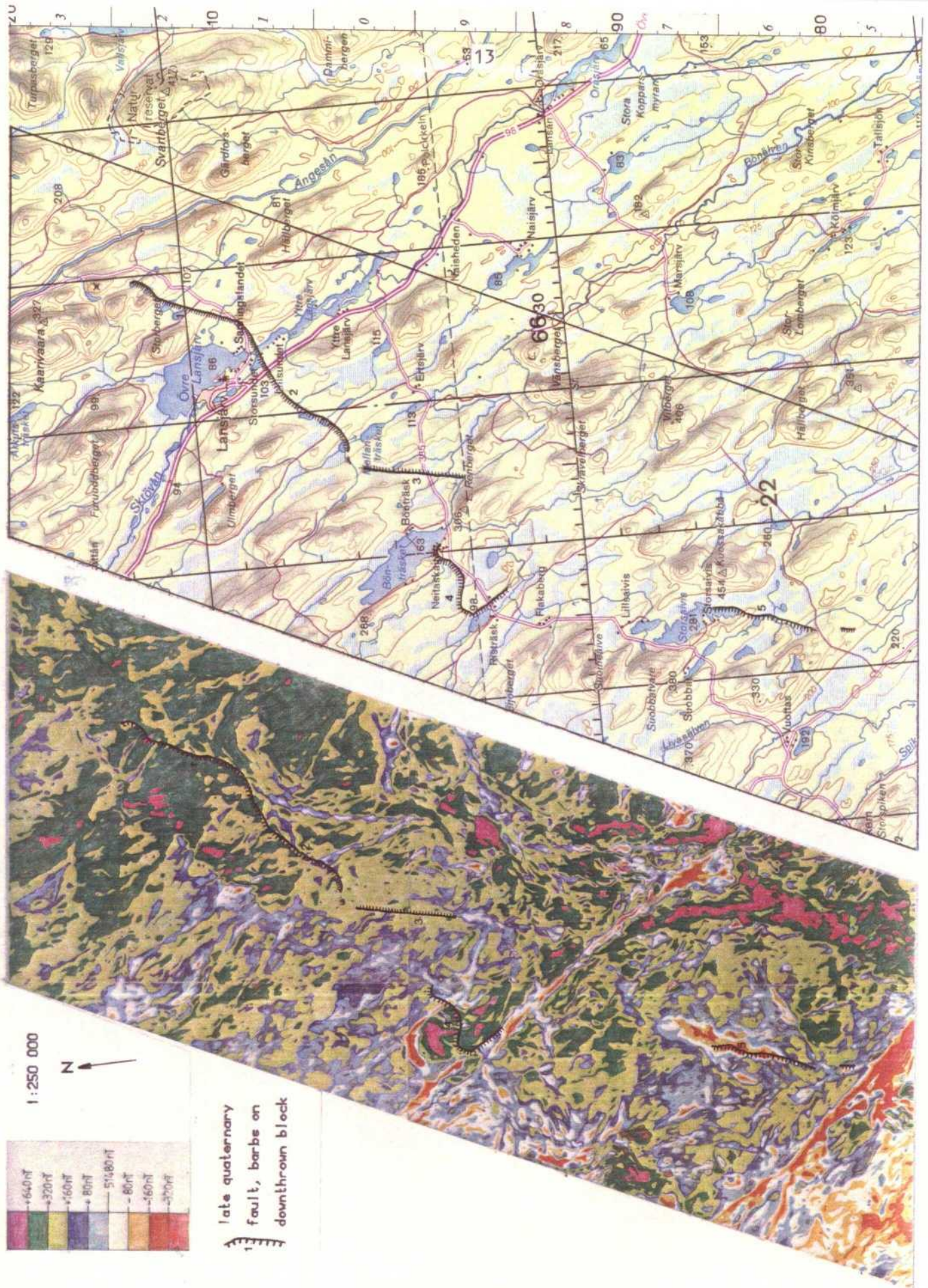
Figure 6. The vicinity of the Lansjärv fault. Aeromagnetic map of 40 nT resolution (bottom) and the corresponding topographic map.
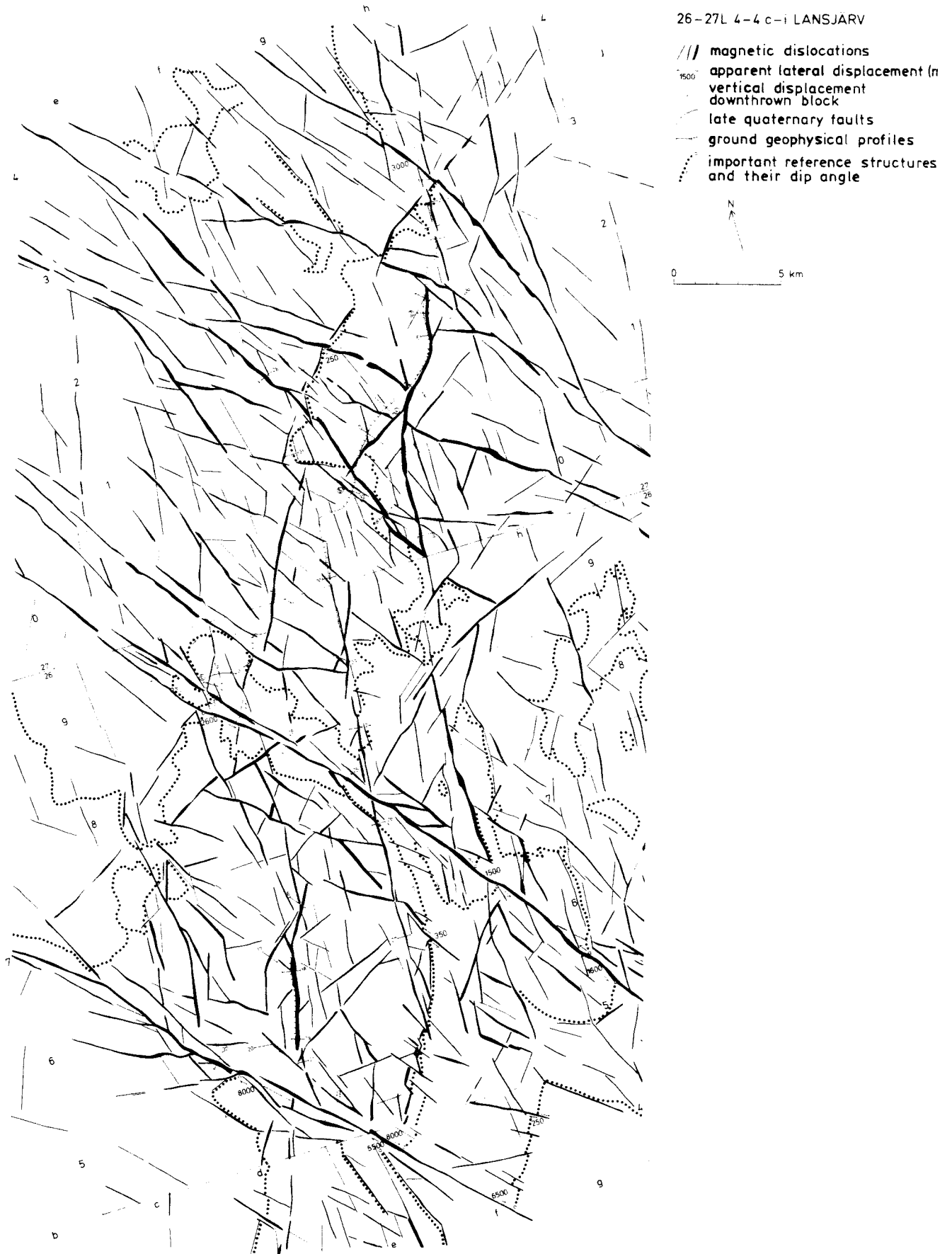
Figure 7. Magnetic interpretation map of dislocations and certain
reference structures of the surroundings of Lansjärv.

TABLE 3. Features of dislocations in the Lansjärv region.

Trend	percentage	spacing (km)	displacement	length (km)
N40W (N50W N20W)	45	12-15	sinistral and dextral	>25
N	45	4-6	vertical	c. 20
N55E	10	–	–	c. 15

Figure 8. Direction frequency
spectrum of all
magnetic dislocations
within the area shown
in figures 6 and 7.
Angular resolution
is 5 degrees.
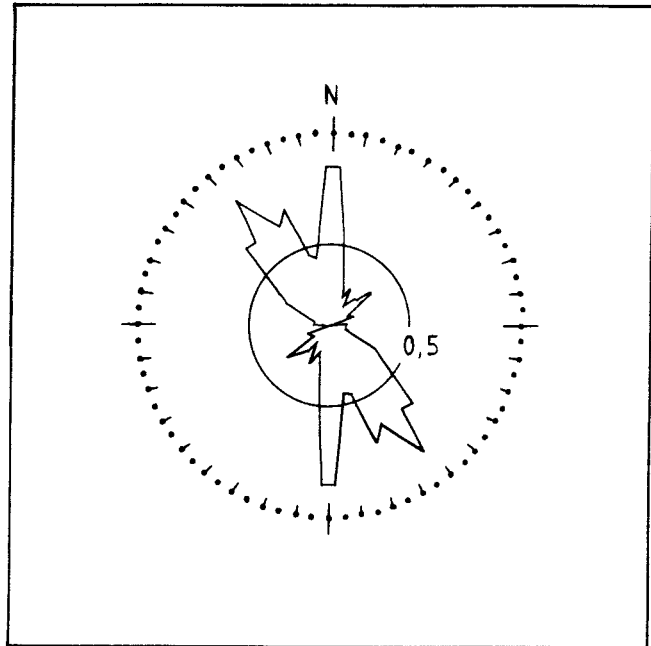
3.2 Age of the dislocations:

All magnetic dislocations are younger than the reference structures
forming the basis of their interpretation. The structures (i.e. magnetic
contacts, zoning etc.) are about 1500 million years old, and it is
plausible that they have not been affected by younger influence other
than metamorphosis, block displacement, and fracturing. In areas of more
recent reference structures, such as impact craters, dolerite dikes, and
sedimentary strata, one may establish that these too have been heavily
affected by dislocations. The youngest dated impact structure in Sweden,
the lake Mien, 119 million years of age, is considerably affected by a
fault, disturbing its western part (Stanfors 1973). Thus, it is probable
that the dislocations observed in this context are substantially younger
than the Precambrian. An important cause of faulting is the present
plate motion of the earth's crust (Hill 1982).

During separate epochs, block displacement in several directions may
have engaged the same dislocation system, and today only the accumulated
effect is visible. This hampers the analysis of the relative ages of
dislocation systems.

Nevertheless, it is evident that in the Lansjärv region, the NW-trending zones are the latest activated, as these are not displaced by any other zones. In the next place, the north-trending zones appear the most distinct, while dislocations trending in other directions are subordinate, the shorter of these being merely linear, low-magnetic zones.

Indications, distinct enough to serve for relative age-determination, occur only at a few places within the survey area. Neither are these indications wholly unambiguous. This situation results from the independent activation of single faults. To unravel such problems, further surveys of larger areas (in order to increase the number of reliable estimations of displacements), are necessary. Areas favourable for such investigation are those where magnetic rocks and distinct magnetic reference structures occur. Also, mathematic modelling of the involved structures will be called for.

TABLE 4. Estimation of relative ages of dislocations.

dislocation trend	near the Lansjärv fault	within the survey area
NW (zone 7)	1	1
NW other regional	3	3
NW local	4	4
N (zone 8)	–	2
N other regional	–	2
N local	4	4
NE	4	4

1 youngest .... 4 oldest

3.3 Tentative interpretation of block movements in the different fault systems observed in the Lansjärv area

3.3.1 Major, regional faults

These are zones (lineaments) of substantial length (often in excess of 100 km), great width (more than 200 m), with observable block displacements at several places. The youngest block movement apparently has occurred at the NW-trending zone nr. 7 (cf. fig. 5), since this zone disturbs zone nr. 8 at 26L 2i. Furthermore, a late-quaternary thrust (cf. chapter 4) occurs in direct connection to the zone This thrust may be a side-effect of a sinistral reactivation of zone nr. 7, which is the only wholly continuous fault. It is also very extended, its length exceeding 200 km, and exhibits a consistent sinistral displacement, amounting to 1 2 - 2 5 km. This apparent displacement cannot be

accounted for by vertical block movement alone, as the adjacent blocks are similarly magnetized, and thus probably represent comparable erosion levels.

Among the other zones, the N-S-trending nr. 8 appears to be the most recently activated, since it interrupts other regional zones. It is of great length (over 100 km), and shows consistent displacement, the western bock being downthrown by a substantial amount, as indicated by differences in magnetization and structure of adjacent blocks. In the southern part of the zone, an unambiguous, minor downthrow of the eastern block is indicated over a distance of 15 km. This shows that the zone has been engaged by at least two phases of block movement. Thus, large displacement along the NW-trending regional zones has preceded the vertical displacement at the major N-S-trending zones.

Among these, nr. 6 and nr. 12 exhibit consistent dextral accumulated displacement amounting to 1.2 - 5 km. A third, nr. 9, shows a somewhat smaller accumulated dextral displacement.

3.3.2 Conclusions regarding block movement at the regional faults:

-Different zones have, at least partly, moved independently during separate epochs of different stress field.

-Different lateral block movement (i.e. dextral and sinistral) seems to have engaged different, rather than the same, fault systems.

-All zones may have been activated by vertical block displacement, possibly in different direction at different sites. This is most pronounced for the N-S-trending zones.

-In the event of large lateral block displacement, secondary fracture systems are formed or activated.

-Generally, only a limited number of fracture zones are developed. Their spacing depends on the thickness of the brittle part of the earth's crust, and on the character of the stress field.

-The lateral displacement at the N-S-trending faults is older than the displacement of the NW-trending faults, and older than the vertical displacement of the N-S-trending faults.

3.3.3 Local fracture systems

These are minor zones, generally not traceable across the regional faults. it is no longer possible to decide whether they once have been parts of regional zones. Their length extent is less than 25 km, and their width is most often substantially less than that of regional faults (i.e. less than 200 m). This pattern of occurrence, together with the minor (often unsignificant) displacement observable at these zones, leads to the conclusion that they are secondary fracture systems, caused by lateral block movement along the regional faults.

Among the local fracture systems, a number of fairly long (c.25 km) N-S-trending faults predominate. In the next place, a few longer NW- and NE-ENE-trending zones, along with several shorter zones, striking to the NW, N, and NE, are observed. The longer zones do not cross the major NW-trending faults. The observable block displacement is small. Their systematic occurrence as regards trend and spacing is explained by their interpretation as being secondary to lateral movement along the two major, NW- and N-trending regional fault zones. Thus, the NW- and NE-trending fracture zones are connected to lateral block displacement along N-S-faults, and , correspondingly, N- and NE-trending fracture zones to lateral motion along the NW-faults. Depending on which of these movements is the youngest, the corresponding secondary fracturing is the relatively more prominent. Hence, it appears that lateral movements in the NW-faults are younger than those in the N-S-faults. Furthermore, these movements must have taken place in two phases, one of mainly dextral motion, and another of mainly sinistral (cf. the preceding paragraph).

Figure 9 gives a summary of the types of block movement deducted, and their relative ages. It is, however, not possible to assess the absolute ages of the block movements. A reasonable assumption is that the greater part of the visible displacement has taken place in connection with the local plate tectonic activity, i.e. the opening of the Atlantic, and the preceding rift phase during the transition Carbonaceous-Permian. Furthermore, the present plate motion demands that also the internal form of the plates changes.
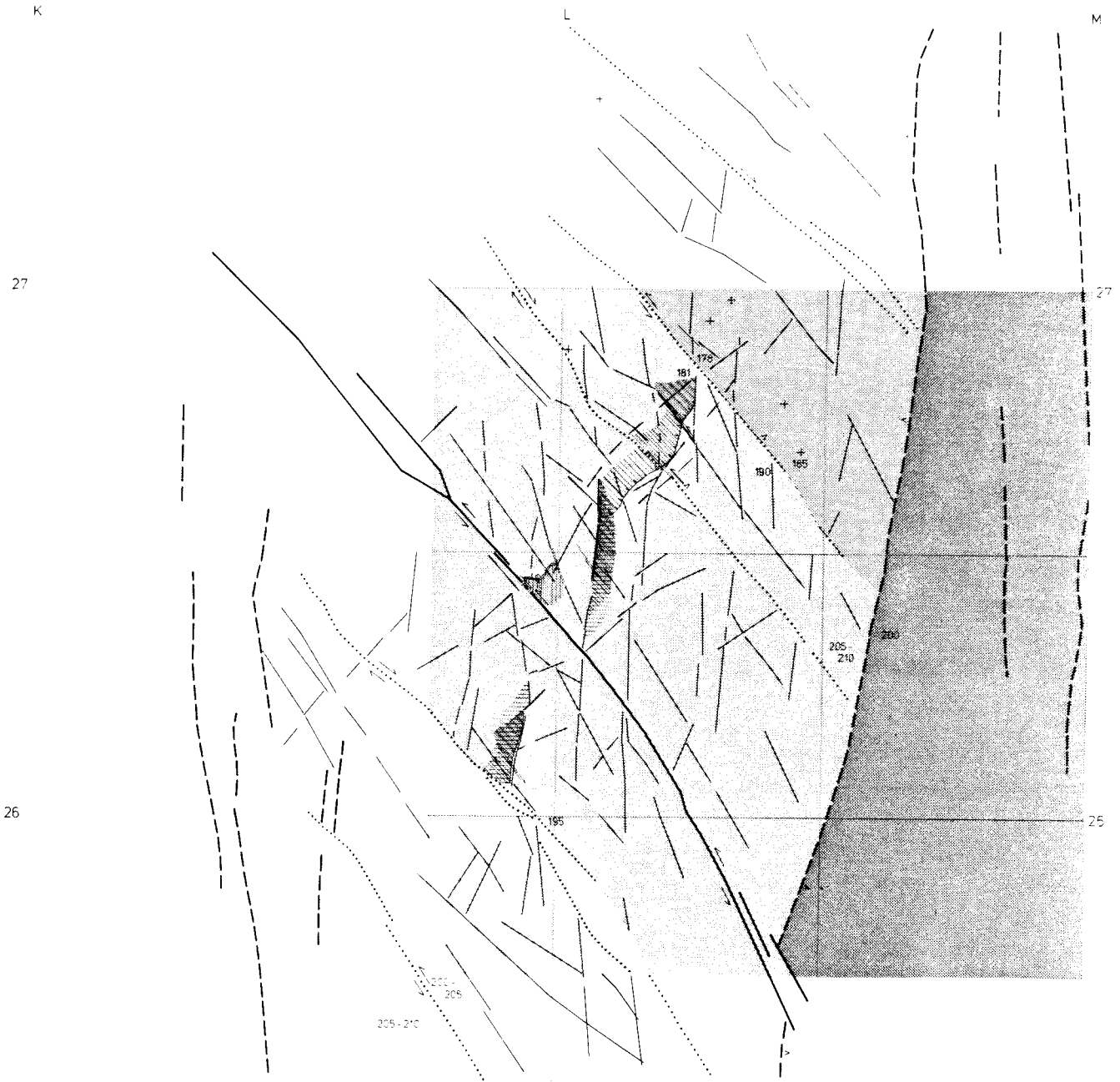
K   L   M

RECENT BLOCK MOVEMENTS

interpreted from changes of the highest coastline level:

→ increasing subsidence

possible relative subsidence c 5 m

most recent subsidence 5 - 10 m

interpreted from late quaternary faults.

→ increasing post glacial subsidence

0 - 2   2 - 5   5 - 8 m

possible preglacial subsidence

possible thrust

late quaternary fault
change of scarp height

+   landslide

195   highest coastline level

OLDER BLOCK MOVEMENTS

——— most recent ⎫
－ － －   ⎬ major regional fault
········ oldest ⎭

block displacement

——— major secondary fracture systems

Figure 9. Older faults and fracture zones. Tectonic interpretation.

3.3.4 Summary of the occurrence of minor fracture zones

-They can be interpreted as secondary fracture systems formed around the
major regional faults during shear stress in connection to large lateral
block movement.

-The fracture systems of the major faults overlap in such a manner that
the secondary fractures of one type of fault also is involved at
secondary block movement, caused by the other type.

-The block displacements at the minor fracture systems are rather small,
and complex as regards direction and date.

4. FEATURES OF THE LANSJÄRV FAULT (By Herbert Henkel)

4.1 Geophysical description of the separate parts of the Lansjärv fault

The fault, having a total length of 35 km, can be divided into 5
separate branches. (Though branches 1 and 2 are closely connected.)
The branches differ in appearance and by type of block displacement.

The northern and southern limitations of the fault show that it ends
within N-trending dislocation zones, that after a further 1.5 - 3 km
encounter with major regional NW-trending faults with, respectively,
sinistral (in the north) and dextral (in the south), apparent block
displacement. These faults are of substantial width (200 - 500 m), and
great extension (60 - 110 km).

All fault branches end within or at some magnetic dislocation. There is a
difference of 3 - 4 m in scarp height between branches 1 and 2, across a
NW-trending dislocation. The separate branches of the fault closely
follow N-S-trending dislocations for a total length of about 5 km, and a
NW-trending major regional zone for 2 km. The rest of the fault does not
coincide with such zones. Thus, about 50 % of the fault has been
released in major older fracture zones, while the rest apparently has
caused new fracturing (or possibly has followed subordinate fracture
zones).

The fault crosses 6 NW-trending larger dislocations without change of
direction. However, its throw changes in several instances. For 6 km, it
runs almost parallel to a NE-trending zone at a distance of 500 m, which
is distinctly indicated, both magnetically and electrically. The recent
fracture, on the other hand, though situated in high magnetic rock,
lacks magnetic indication. Thus, in the fracture zone caused by the
recent fault, the rock is not yet enough oxidized to appear as a low-
magnetic zone.

In the following, an account is given of the ground geophysical survey
that closer illustrates the electric and magnetic features of the fault.
The seismic survey is treated separately. The locations of the different
profiles are given in figure 2. In the following illustrations, the
measured ground geophysical profiles are stacked (from the north to
the south) within each of the separate branches of the fault. The common
reference is the location of the mapped fault, alternatively the zero-
crossing of the VLF anomaly, or, in some cases, the location of the
magnetic dislocation zone. (The length coordinates given refer to the
starting point of the profile in question.)

All the Slingram indications are asymmetric, implying a steep easterly
dip of the fault branches. Generally, the recent fault is an
electrically conductive structure, the conductivity being brought about
by an increased water content. This also holds for the magnetic
dislocations.
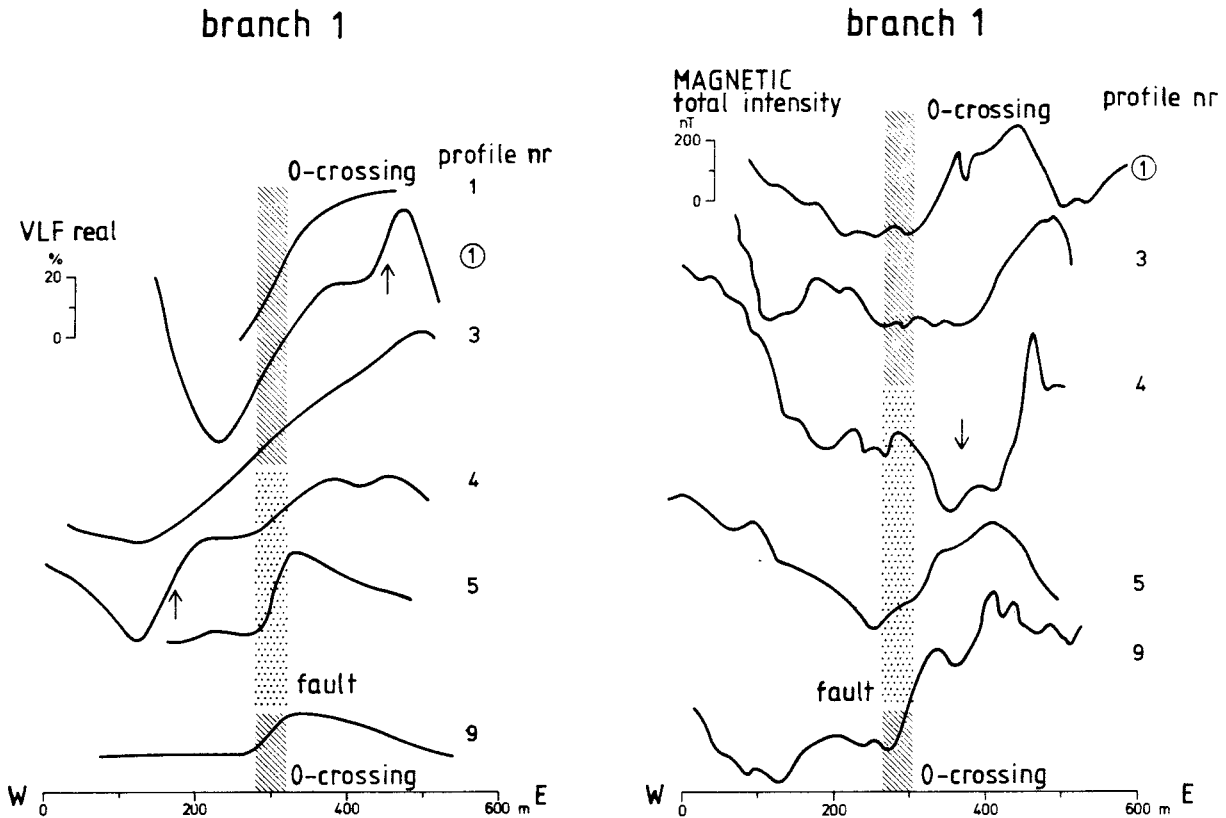
branch 1   branch 1

Fig.10. Branch 1. Since this branch of the fault ceases within a
N-S-trending dislocation, attempts were made to trace the fault
further towards the NW-trending major regional dislocation. In
profile 1, a strong electric indication appears after c. 40 m E,
where the magnetic indication is weak. In the next profile to
the south, a still stronger electric indication is obtained at
about 140 m E. The same indication appears in profile 1 at 0 m
E, together with a weaker indication at 250 m E (arrow). Here,
also a clear-cut, about 120 m wide magnetic minimum occurs. In
profile 4, a conductive zone appears at 240 m E and at c. 40 m
east of the fault.The magnetic zone sets out at about 40 m to
the east of the fault. The discrepancy, amounting to a few tens
of meters, probably depends on differences in the morphology of
the fault in relation to the zone in the bedrock. Profile 5
exhibits an unambiguous magnetic and VLF anomaly, and a strong
Slingram indication.

The measurements over the fault fault branch nr.1 show that,
when the fault coincides with the dislocation, the geophysical
signature is similar to the indications obtained at the north
extension of the fault, where only magnetic dislocations occur.
This may be interpreted as that the movement along the fault
gradually decreases within an older fracture zone, whose water
content remains unchanged. The measured scarp height decreases
somewhat towards the north.

branch 2
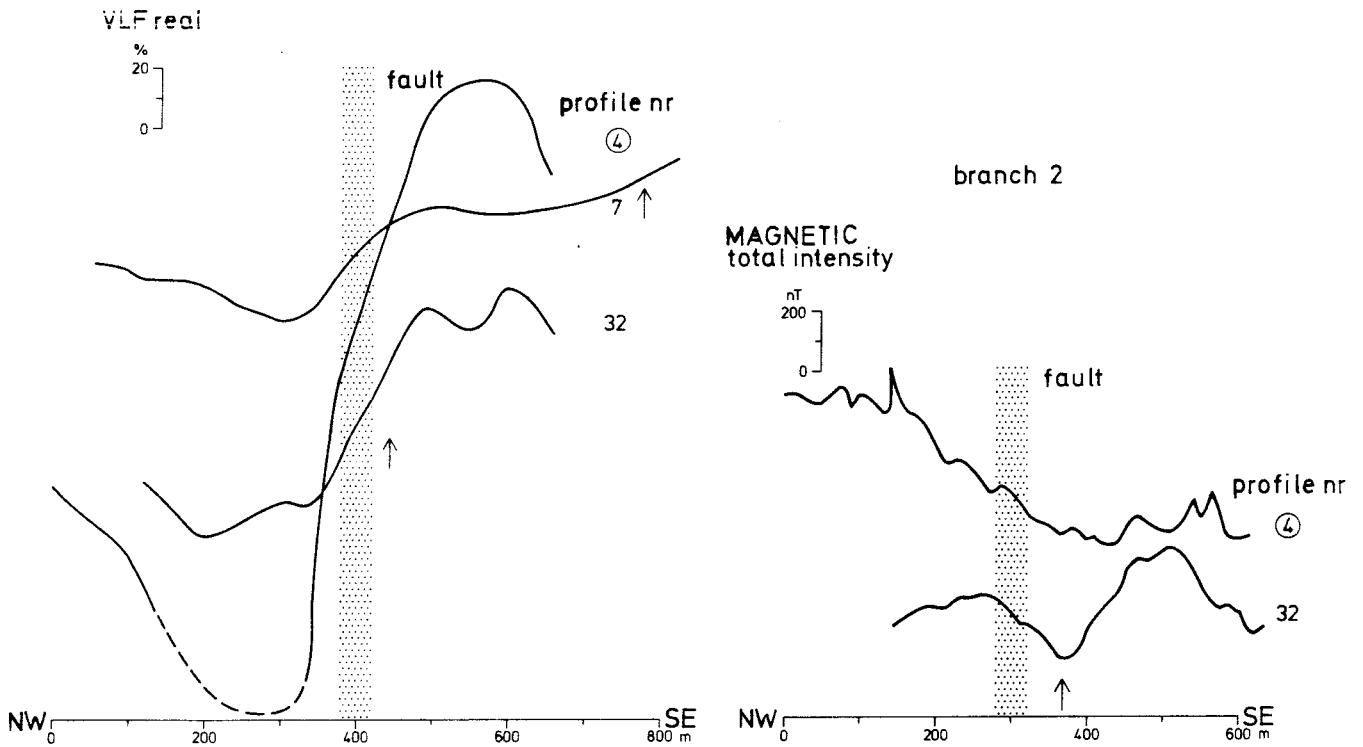
Fig. 11. Branch 2. In this branch, the recent fault movement is
independent of older zones. A strong electric anomaly, similar
to the formerly described, appears in profiles 4 and 32. In
profile 32, the water-bearing zone is situated about 40 m to
the east of the fault. The parallel magnetic dislocation SE of
the fault also gives an electric anomaly (arrow). The
measurements imply that oxidation not yet has occurred in the
young fault, despite its high water content. The scarp is at
its highest (6 - 7 m) in the central part of the fault branch,
decreasing outwards (down to 3 - 4 m).
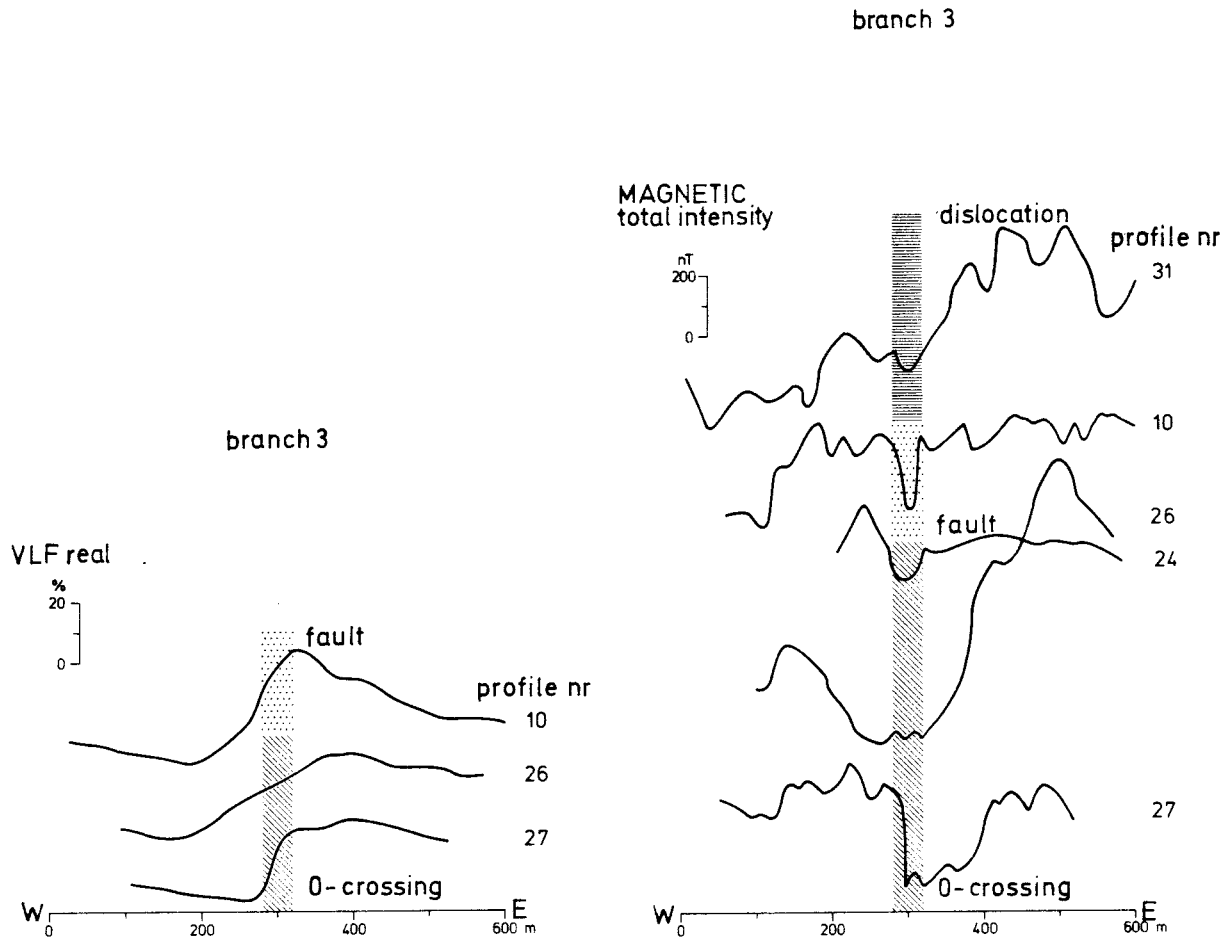
Fig. 12. Branch 3. Profile 10, crossing this fault branch, exhibits both electric and magnetic indications. The dislocation, within which the fault is situated, has been investigated along further profiles, showing distinct magnetic features. Electric indications occur in the southernmost part. The height of the scarp decreases northwards from a maximum of 8 - 10 m, located in the southern part. To the south, the scarp decreases abruptly to 2 m.

Fig. 13. Branch 4. (see next page) Profile measurements in the western part of this branch show strong electric indications. The Slingram anomalies are assymmetric, indicating a southeasterly dip in profile 12, and a northeasterly in profile 13. This holds despite that the fault follows the NW-trending regional dislocation zone (which is steeply dipping). Here, the recent fault is principally a thrust towards the NW - such block motion may originate from a lateral activation of the regional zone. The fault branch exhibits high and varying scarps. Note that the magnetic minima, visible in profiles 12 and 6, are assymmetric contact minima, indicating a southern-southeasterly dip of the causing magnetic body.
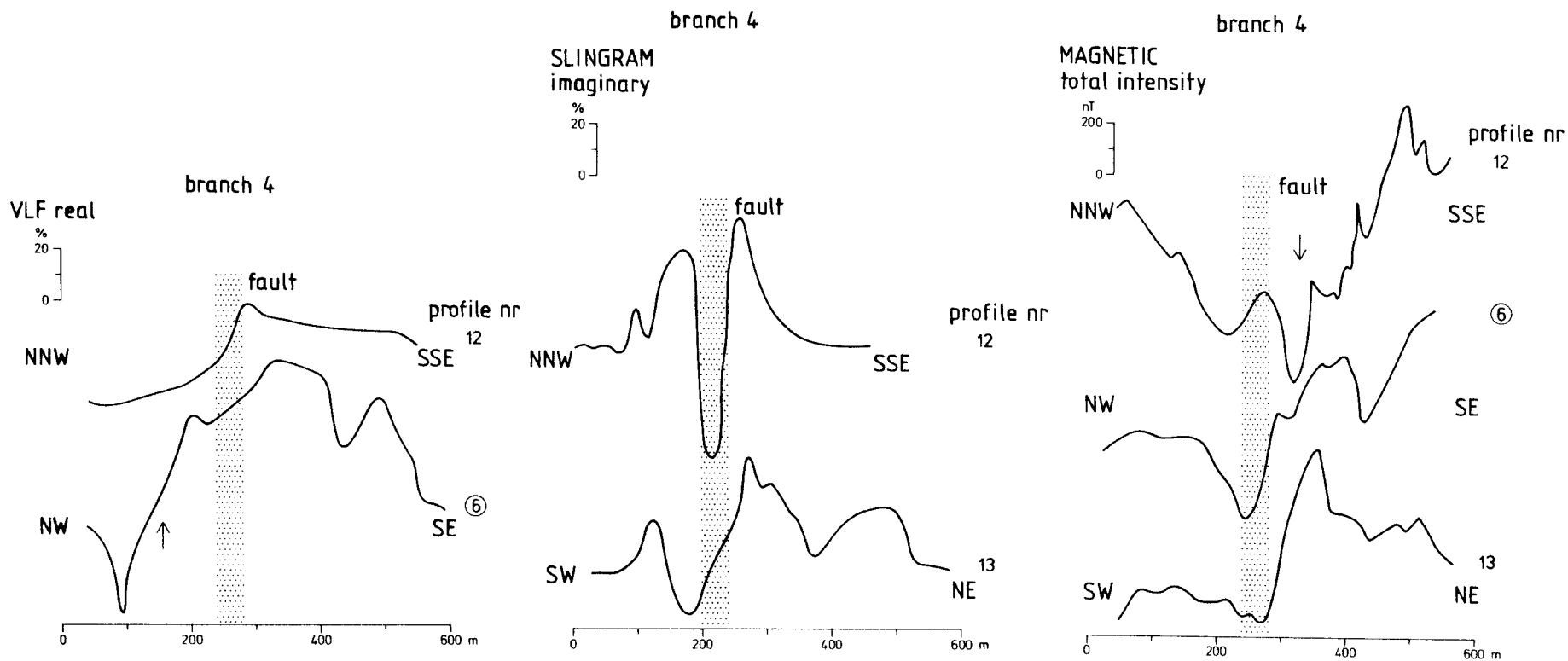
Figure 13. Stacked ground geophysical profiles over the fault branch nr. 4.
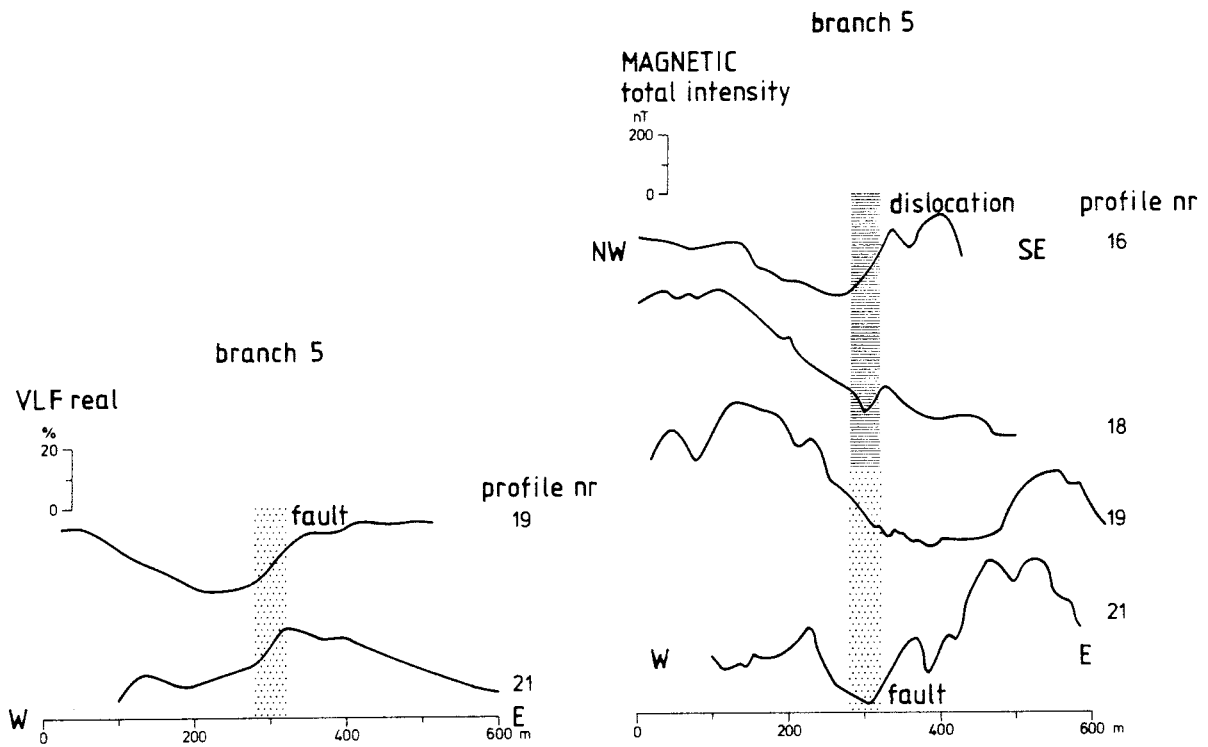
Fig. 14. Branch 5. Distinct electric indications appear in the southern
part of this branch. This also holds for the southern extension
of the fault. As for branch 1, the plausible interpretation is
that the throw of the fault gradually decreases within the
extending dislocations. To the south, the scarp decreases from
c. 5 - 7 m to about 2 m, within an area where several NW-
trending, topographic lineaments appear.

4.2 Comparison of some magnetic profiles across NW-trending dislocation zones

The stacked profiles shown in fig. 15 give a good notion of the character of these dislocations. One observes the great differences of width (100 - 300 m). At the broader zones, e.g. profile 30, a moderate contact minimum is developed on the northeastern side of the southwestern border of the zone, indicating that the zone dips steeply. The linear negative anomalies have an amplitude of 300 - 600 nT, which implies a substantial depth extent (up to 800 m) of the oxidation causing the anomaly. Through magnetic model calculations, one may obtain more exact estimates of dip angle and depth extension.
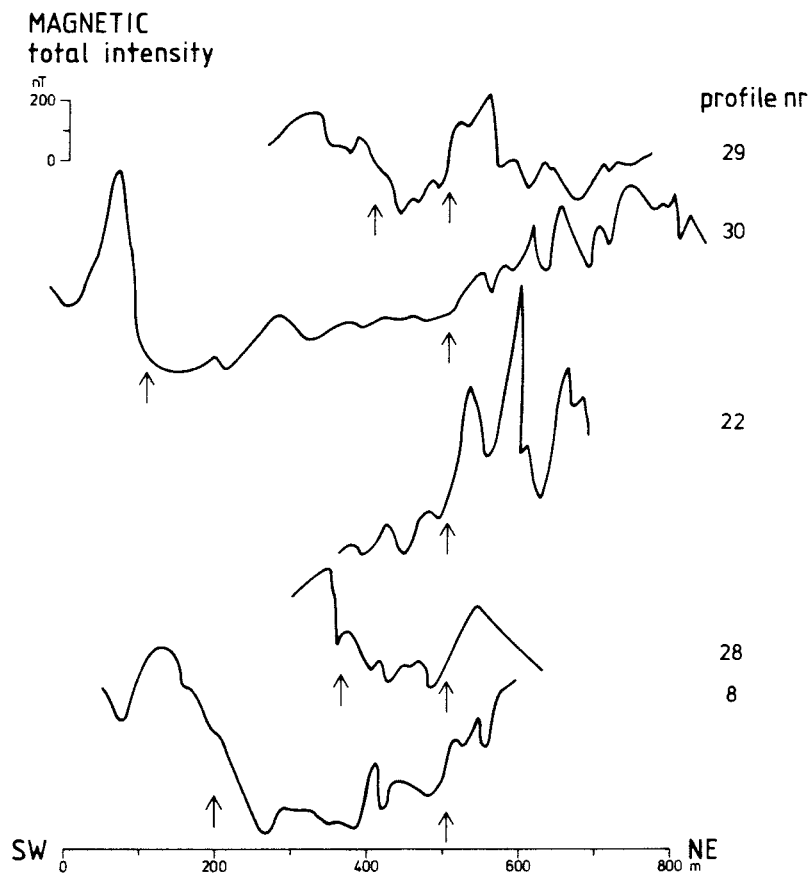
Fig. 15. Ground magnetic profiles over NW-trending dislocation zones
(oxidation zones), characterized by negative magnetic
anomalies of different width.

4.3 Comparison of the Slingram profile measurements

Figure 16. Stacked Slingram
profiles from different parts of
the late quaternary fault.

SLINGRAM
imaginary
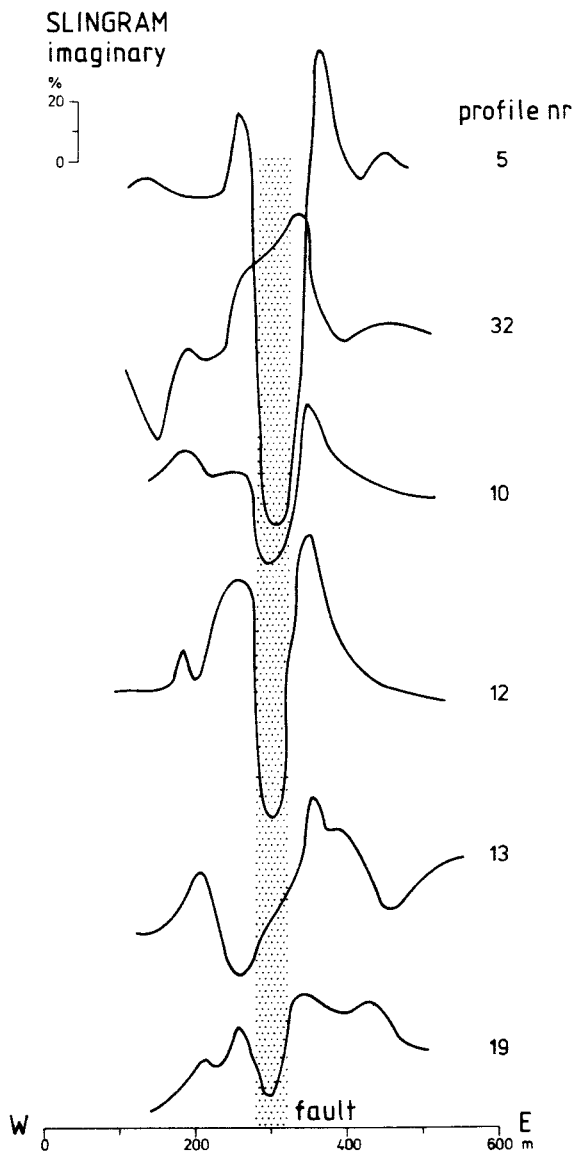
In figure 16, Slingram anomalies
over different branches of the
fault are compared. Throughout,
distinct, asymmetric indications
are observable, the asymmetry
indicating an easterly dip of the
branches of the fault.

4.4 Presentation of the profiles where several geophysical methods have been applied. The profiles are shown in figures 17 - 22.
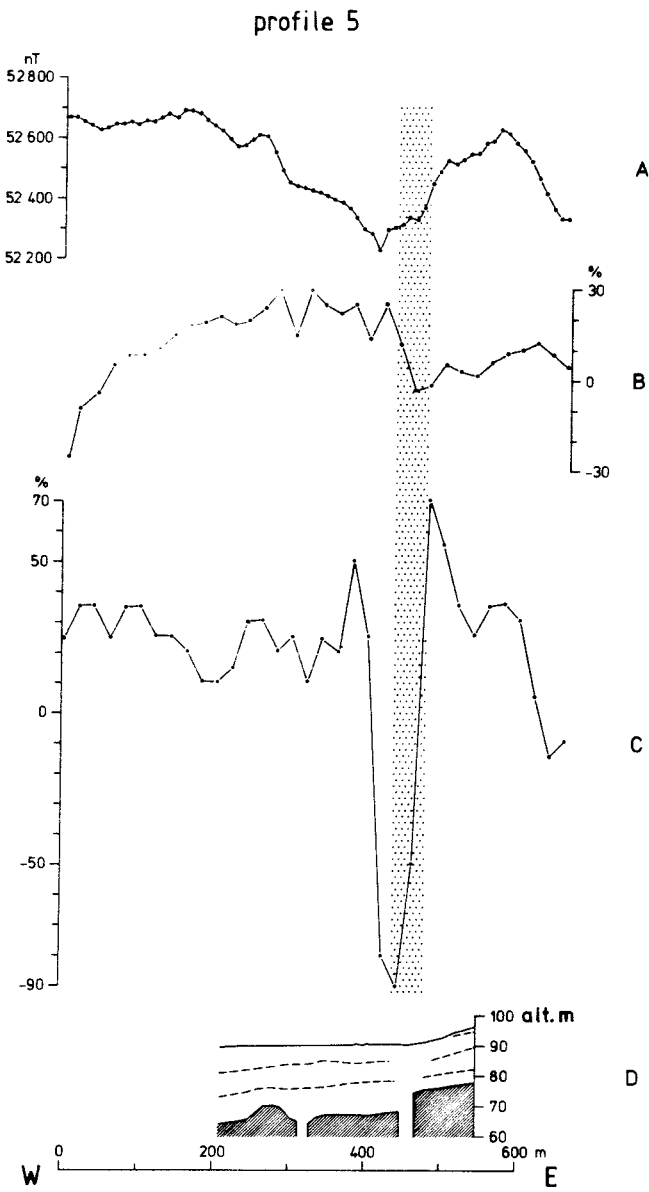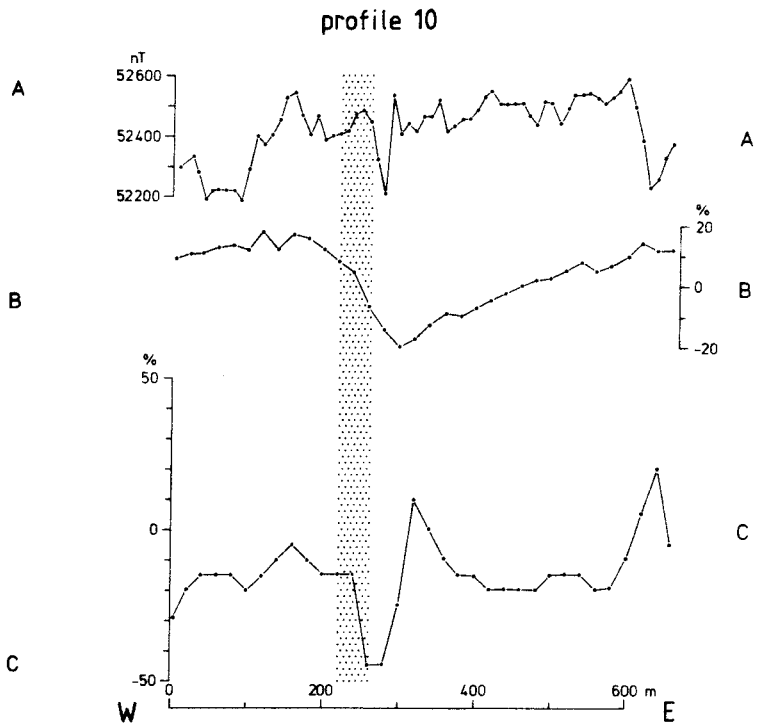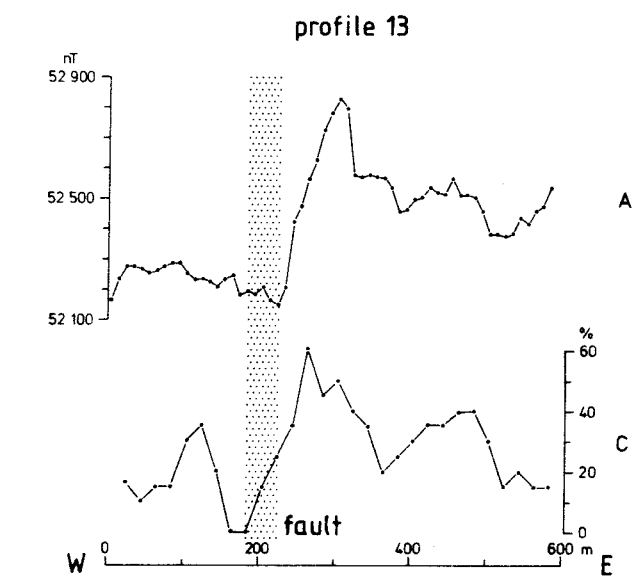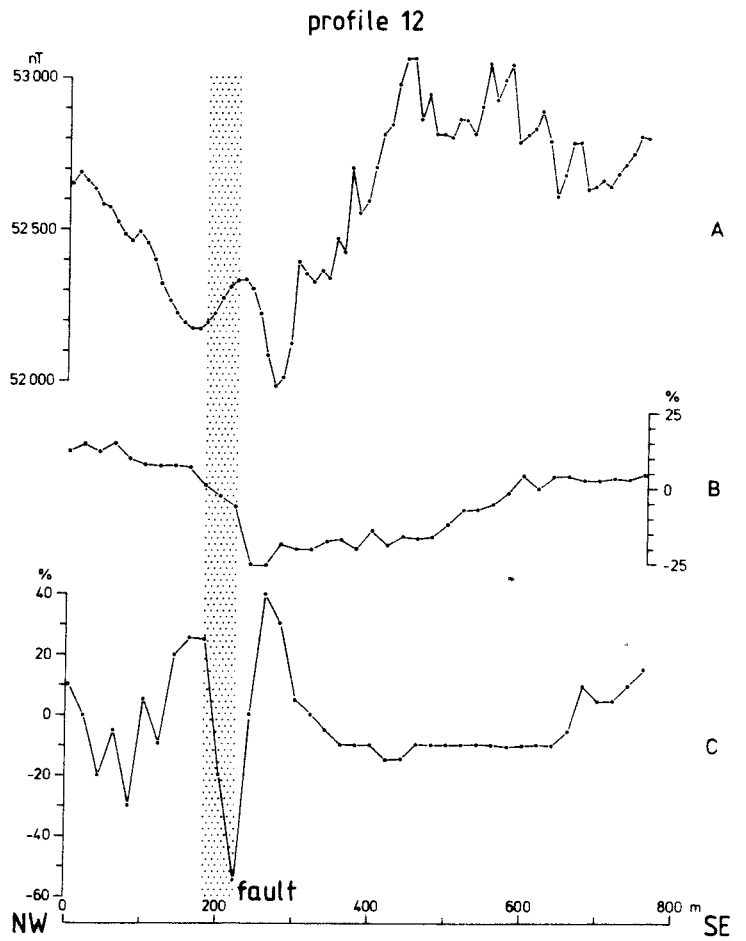
Figures 17-20. Ground geophysical profile measurements. A magnetic total intensity, B VLF real, C Slingram imaginary, D seismic interpretation.

profile 32

profile 19

fault
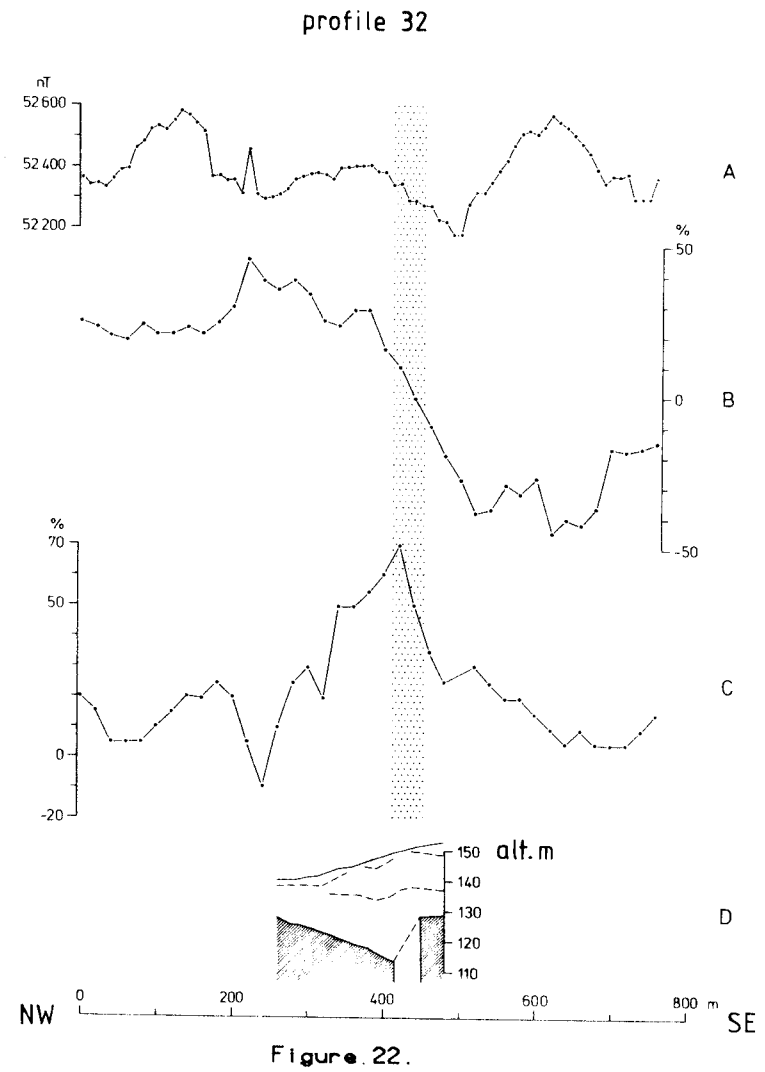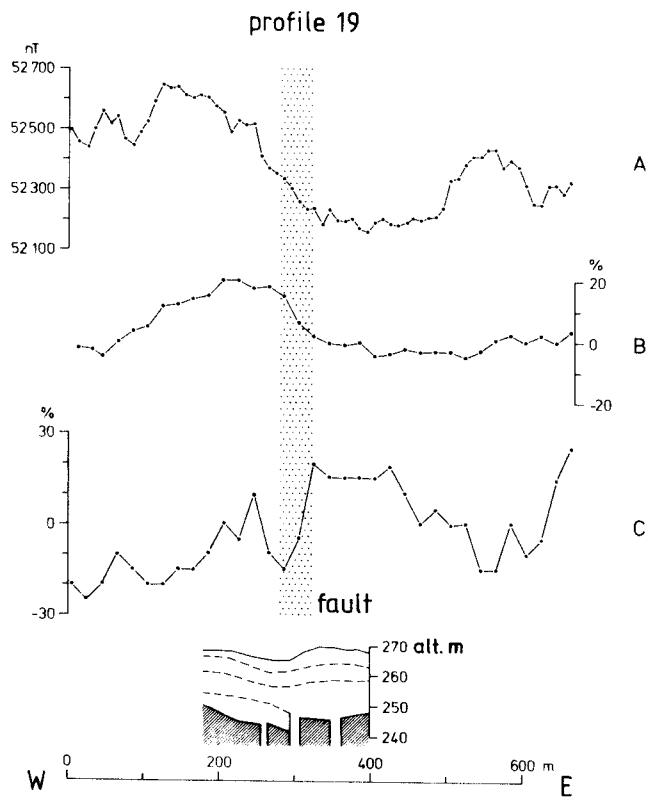
Figure 21.

Figure 22.

Figures 21-22. Ground geophysical profile measurements. A magnetic total intensity,
B VLF real, C Slingram imaginary, D seismic interpretation.

30

K   L   M

27   27

26   26
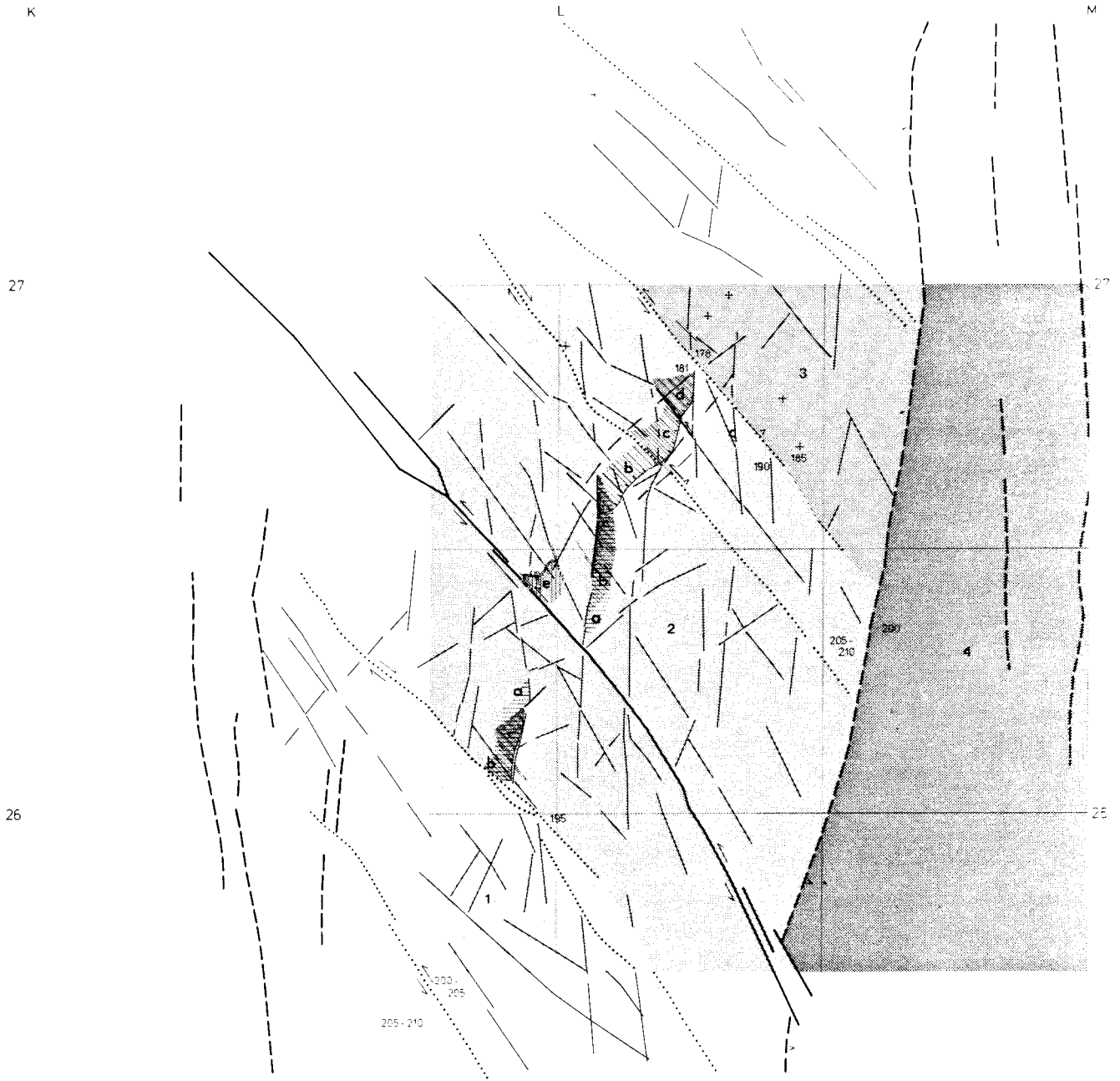
RECENT BLOCK MOVEMENTS

interpreted from changes of the highest coastline level:

    ——→ increasing subsidence

  1   2 **3**   possible relative subsidence c. 5 m

  █████ **4** most recent subsidence 5 - 10 m

interpreted from late quaternary faults:

  b **c** **d** ——→ increasing post glacial subsidence

  0 - 2 2 - 5 5 - 8 m

  a／ possible preglacial subsidence

  e possible thrust

  ⌐⌐⌐⌐ late quaternary fault

        change of scarp height

  + landslide

 195 highest coastline level

OLDER BLOCK MOVEMENTS

  ———— most recent ⎫

  — — —   ⎬ major regional fault

  ········· oldest ⎭

  ⟋ ᵥ block displacement

  ———— major secondary fracture systems

Figure 23. Summary of a tentative tectonic interpretation
in the Lansjärv region.

4.5 Short description of the separate branches of the Lansjärv fault

In the following, a short description is given of each of the separate branches of the fault, cf. fig. 6. (Also summarized in fig. 23).

1. The northernmost branch is a somewhat winding, nearly NNE-trending fault, with a downthrown northwestern block. In the north, it discontinues within a N-S-trending dislocation. Its central part crosses a few NW-trending dislocations. At the cross-points, the throw of the fault increases by steps from c. 6 m in the SW to c. 9 m in the NE. To the southwest, it deviates about 200 m towards the NW from the dislocation. The branch is discontinued by a NW-trending dislocation.

2. This branch is similar to the foregoing, and constitutes its extension in the strike direction. The branch winds around a northeasterly direction, and has a downthrown northwestern block. It follows no dislocation zones, though such a zone exists c. 500 m to the SSE of the fault. It crosses several NW-trending dislocations, and is discontinued by a N-S-trending dislocation.

3. The third branch differs from the two above by its straighter trend, and by entirely following a N-S-striking dislocation. The branch also discontinues within this dislocation zone. The eastern block has subsided. The scarp height decreases from c. 7 m to c. 2 m where the fault crosses a few NW-trending dislocations.

4. This part is entirely isolated, and has a very winding course. The eastern part trends to the ENE. The northwestern block is downthrown. The western part of the branch follows a NW-trending, regional major dislocation zone, within which it also ceases after about 2 km. To the north, it crosses a few NW-trending dislocations, and is discontinued by a NNE-trending dislocation.

5. The southernmost branch is also wholly isolated. It almost entirely follows a N-S-trending dislocation, within which it ceases in the south. To the north, it is discontinued by a NE-trending dislocation. The western block has subsided. In the southern part of the branch, the scarp height changes stepwise from 7 m to 2 m in an area with several NW-trending topographic lineaments.

Table 5. Characteristics of separate branches of the Lansjärv fault.

Branch	group	strike	length (km)	follows disloc. trend, km	crosses disloc. trend	ceases at dislocat. trend	ceases within disloc trend.	change of scarp height in disloc. trending
1	b	NNE	7.5	N-S 2.5	NW	NW or N-S	N-S	NW
2	b	NE	7	-------	NW	N-S or NW	------	------
3	a	N-S	6	N-S 6	NW,NE	---------	N-S	NW
4	c	ENE	6.5	NW 2	N, NW	NNE	NW	NW,N
5	a	N-S	6	N-S 5.5	NW,NE	NE	N-S	NW
Total			33	16				
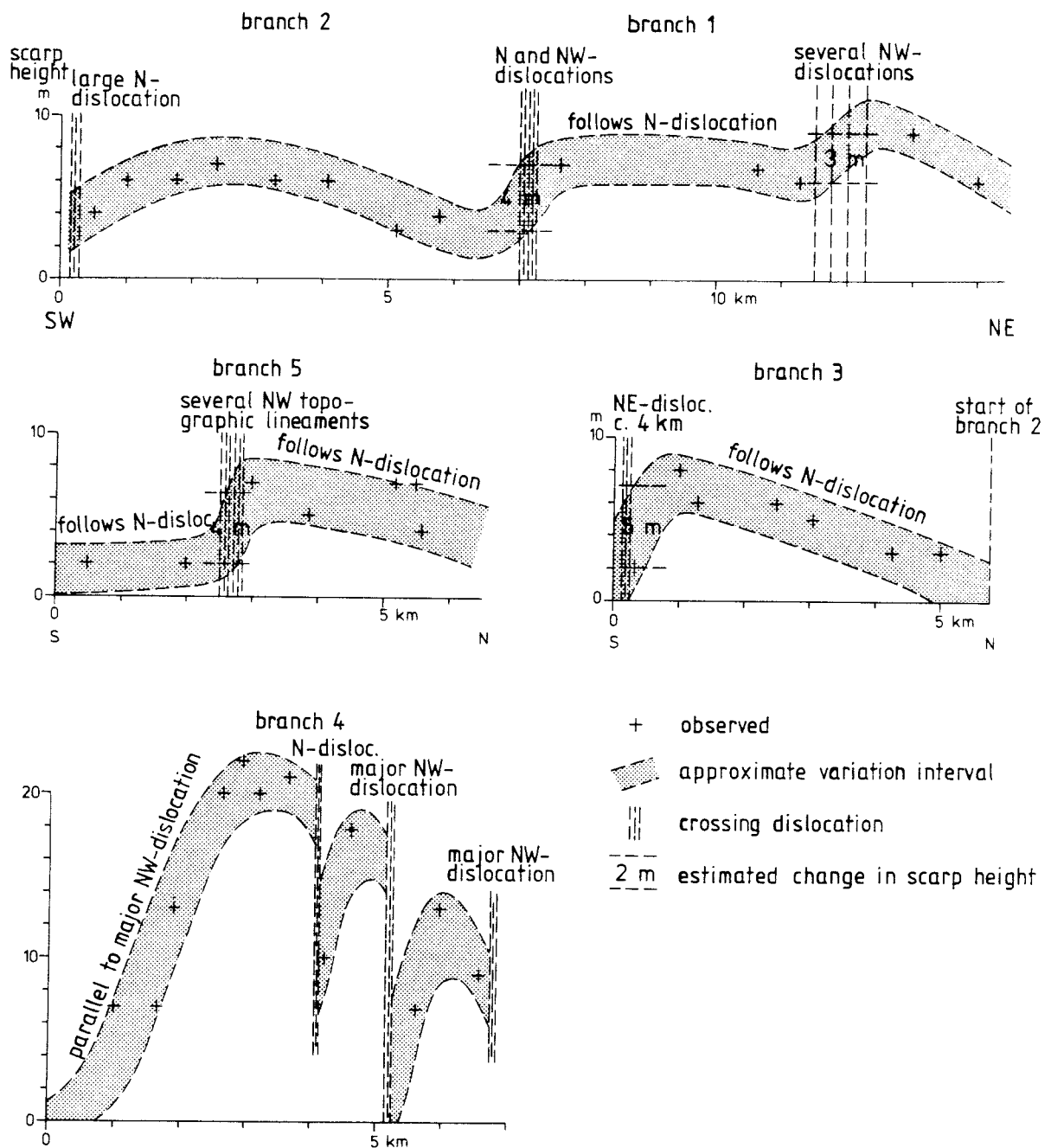
Fig. 24. Changes of scarp height in the different branches of the Lansjärv fault.

Changes in the scarp height are outlined in fig. 24. The scarps of recent faults within N-trending dislocation zones are low in the south, greatly increase to their maximum height at the crossing of possible NW-trending fracture zones, and then gradually decrease towards the north.

The two more NNE-striking fault branches exhibit abrupt changes of scarp height at the crossings of NW-trending, larger dislocations. At both branches, the scarp height increases by 3-4 m to the NE.
The fault branch nr.4 has a winding course, and a great variation in scarp height. It is uncertain, whether these changes are connected to the crossing of other dislocations. If this branch is interpreted as a sequence of thrusts, with the maximum apparent throw at the front edge of the thrust lobe, it may be divided into 3 partly separate lobes, the throw of which gradually decreases towards the NE.

The late quaternary faults may be released along existing fractures of different magnitude. For instance, within the broad and extended regional faults, a throw of 5-10 m may be distributed over a 50 - 500 m wide zone, and thus the single displacement steps will be difficult to detect. Such a spreading of the movement also causes less secondary phenomena (e.g. landslides), as it allows for a more continuous stress release. At the minor zones, a recent displacement will be more concentrated and more easily detected.

A preliminary analysis of the highest coast-line estimations conducted by R. Lagerbäck (1982) shows, that level discrepancies of about 5 m exist across some NW-trending faults (zones 3,6,8,10, and, possibly, zone nr. 9) (cf. fig. 5). Across zone nr. 7, no such discrepancies of the HC-level occur, while the matter cannot be settled for the zones 12 and 13. The traceable changes of the HC imply a relative subsidence of the northeastern block along NW-trending faults, and a subsidence of the eastern block along N-trending faults. The change in scarp height of 3 - 4 m at the branches 1 and 2 of the Lansjärv fault across the zone nr. 9 may imply a subsidence of the northeastern block by this amount. In the northern part of fault branch 1, an increase in scarp height from about 6 m to 9 m occurs where the fault crosses a NW-trending, larger dislocation. In the southern part of fault branch 5, a resembling change sets in where the fault crosses a series of NW-trending, topographic lineaments.
Though the above indications imply the occurrence of recent movement along older faults, a more exhaustive investigation of HC-changes, in combination with seismic refraction lines across NW-faults, is required, if positive judgement of possible recent block movement along the older faults is to be achieved.

The occurrence of landslides within the Lansjärv region is concentrated to two areas, 8 - 10 km to the north of, and 8 - 10 km to the east of fault branch 1. Further indications occur 30 km to the NW, and 50 km to the NE. At a comparison with recent earthquakes, it appears that the effects, in the form of landslides etc., occur within 15 km from the epicenter, while the major faults formed in the event may have a different pattern of distribution (plausibly governed by older zones of weakness within the bedrock). Cf. figure 25 (Burford et al. 1981).
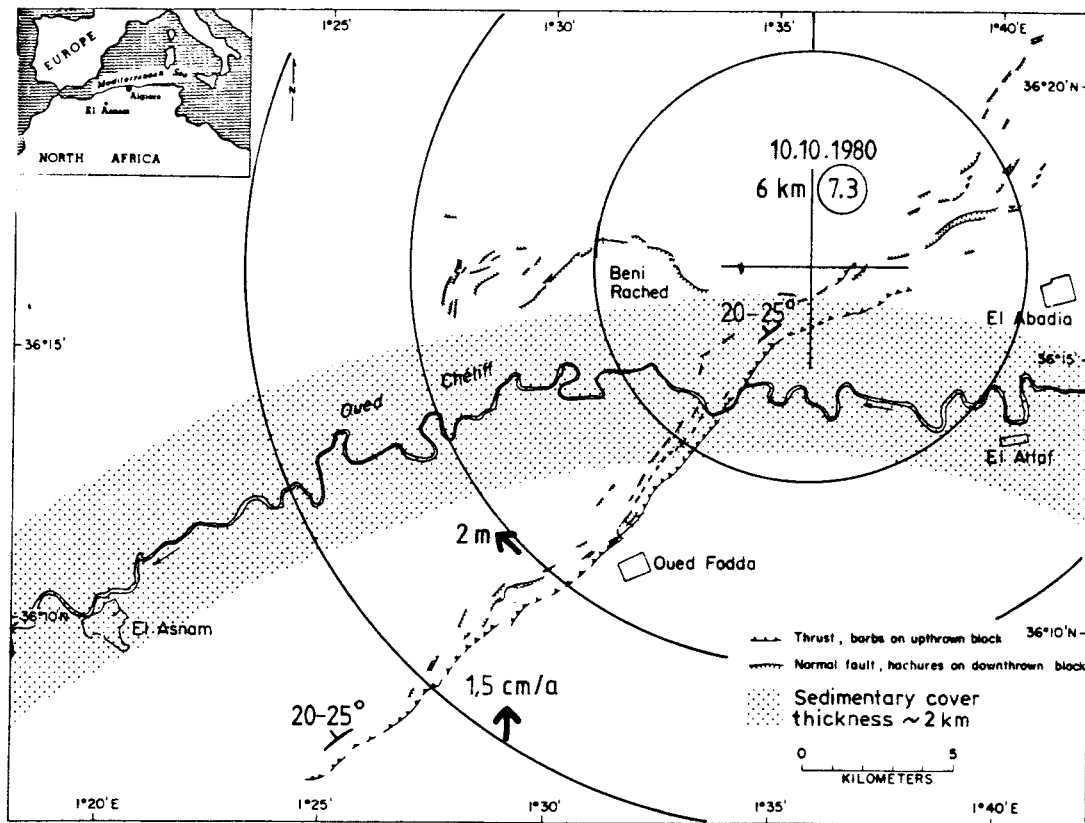
Figure 25. The earthquake at El Abadia 1980.10.10 (of magnitude 7.5) and the fault systems that developed in connection with the stress release.

To sum up, the following interpretation of the connection between late quaternary faults, their movement, and older fracture zones may be given:

-The late quaternary faults are of 3 different types:

a) Those that entirely follow older N-trending fracture zones (and cease within these zones), and whose throw decreases towards the north,

b) Those only partly following older fracture zones, but whose throw changes abruptly at the crossing of major NW-trending, older fracture zones, and

c) Fault branch 4, interpretable as a series of thrusts towards the NW.

-Since the type b often crosses NW-trending, older zones, the faults of type b probably cease at N-trending (rather than NW-trending) zones.

-Both N- and NW-trending older zones have probably been activated in connection with the late quaternary block movements.

-The three different types of late-quaternary faults represent different kinds of block motion during phases of the glaciation and the deglaciation. Group a apparently also comprises older motion, causing

the preglacially weathered rock to remain on the downthrown side. Group
b includes recent block displacement, developed after the erosion of
preglacially weathered material.

-The fault branch nr. 4 differs from a) and b) above by its higher and
more varying scarps, and by being distinctly connected to movements
within an older, NW-trending fault.

-The observed difference between faults of the types a) and b), and the
fault branch nr. 4, as regards type of movement and relation to older
zones may imply that three different events, of different stress field,
have caused the observed pattern.

-the occurrence of landslides to the north and to the east of branches 1
and 2 (type b)) is interpreted as resulting from these faults being
more independent of older zones.

-The outer landslide area is too far from the late quaternary faults in
the Lansjärv region to have a connection to these. In addition, several
major regional zones lie in between (nrs. 12,8, and 13).

-possible leaps of the HC occur mainly along fault nr. 10, that crosses
the landslide area and limits the late quaternary faults to the north.

4.6 Discussion of possible mechanisms

May motion along the major regional fault zones be the cause of the
observed late quaternary faults?

In particular, lateral displacement may easily be obscured within the
broad fault zones. Since these often constitute river valleys, much of
the effects have disappeared through erosion.

The following two cases are discussed:

a) A vertical motion of the earth's crust (e.g. adjustment to
   glaciation/deglaciation), and

b) A twisting of the crust (adjustment of its form to the spherical
   plate motion).

In both cases, it is assumed that the crust moves as a set of minor
blocks, bordered by major faults and their secondary fracture systems.

a: Normally, the adjustment of the crust proceeds continuously along all
   existing fracture zones. At extremely rapid changes of load, an
   additional component of motion occurs locally. This is illustrated in
   the sketch below. In the simplest case, at least two fracture trends
   are involved. In plane, these shear surfaces are conformal around the
   center of the load change. In the case where the ice cover rapidly
   recesses towards the WNW, the eastern block will rise relative to
   the western one (and reversely if the process acts at the western
   border of the ice cover). Thus, after complete deglaciation, a
   graben-like fault pattern remains. Gradually, these displacements are
   neutralized, as a reversed movement sets in (an uplift of the

previously glaciated area), owing to the viscosity of the asthenosphere. The hitherto mapped late quaternary faults only partly fit into a graben pattern. (Neither do they fit the present uplift.) An interpretation of case a, as caused by deglaciation, is presented in fig. 26. As far as is known, no other contemporary process would give rise to vertical block motion.

fault, barbs towards downthrown block
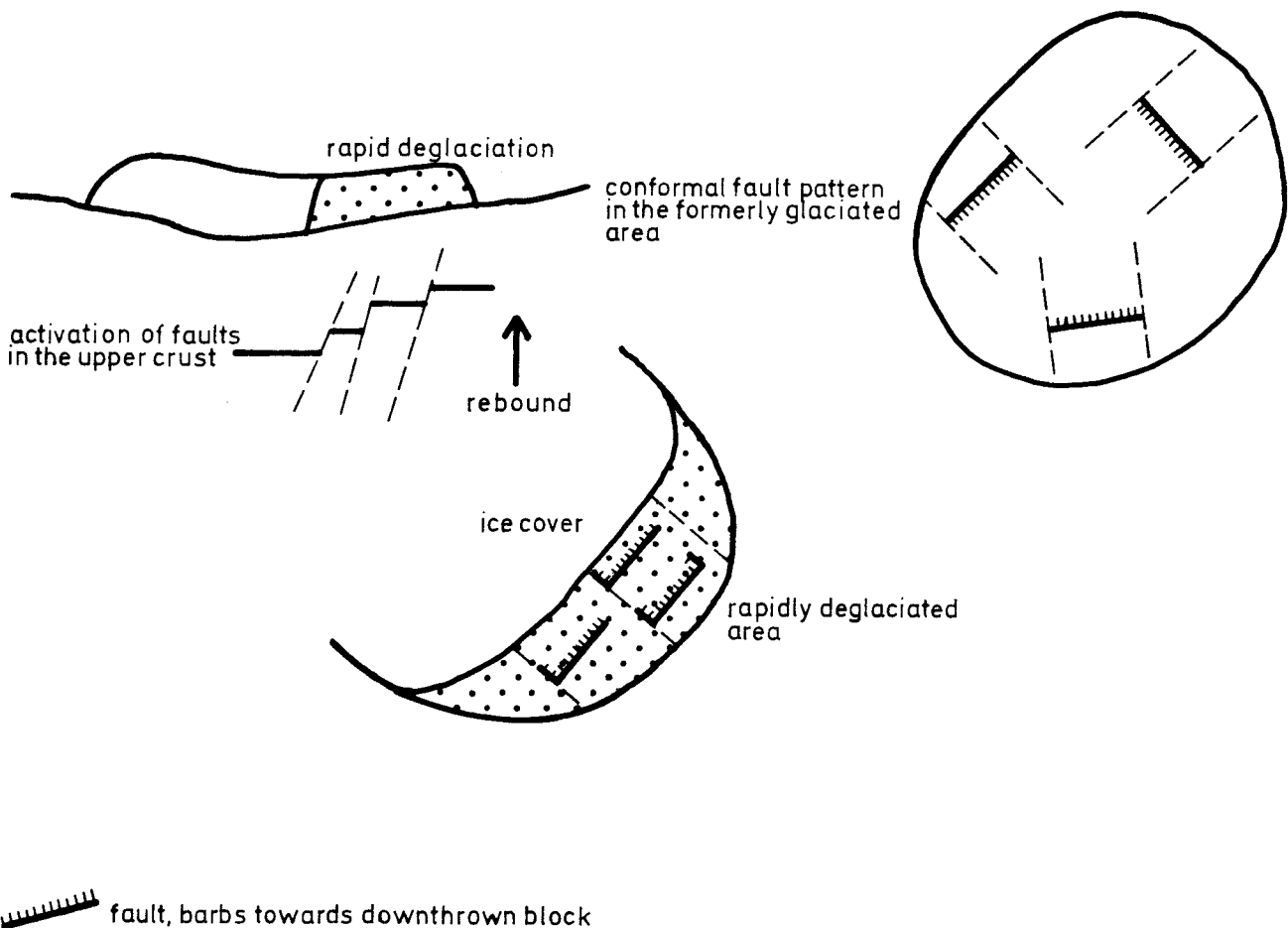
Figure 26. Outline of possible fault patterns during phases of relatively rapid deglaciation.

b: Also in this case, the adjustment normally proceeds along all existing fractures. However, there is a distinct tendency of the movements to accumulate in some zones, since motion in certain directions is more efficient for the required twist. Though the movements always occur simultaneously in several fractures, they are of different character in different areas and at different fault planes (Hill 1982). Figure 27 presents the expected pattern of movements (which partly is observed in the cited paper). The pattern may be arbitrarily rotated, but the pattern shown in the figure fits closest to the observations made in the Lansjärv area. Hence, one may conclude that the NW-trending faults, observed from the Bay of

Bothnia to the coast of northwestern Norway, form parts of a major
dextral lineament, where, from time to time, the northeastern block
moves southwards, with side-effects in the form of N-trending
normal faults (subsidence of the western block), and of northerly
thrusts. If this is the case, microseismic movements will be manifest
within the area, and, furthermore, must statistically fit into the
pattern demanded by the model (fig. 27).
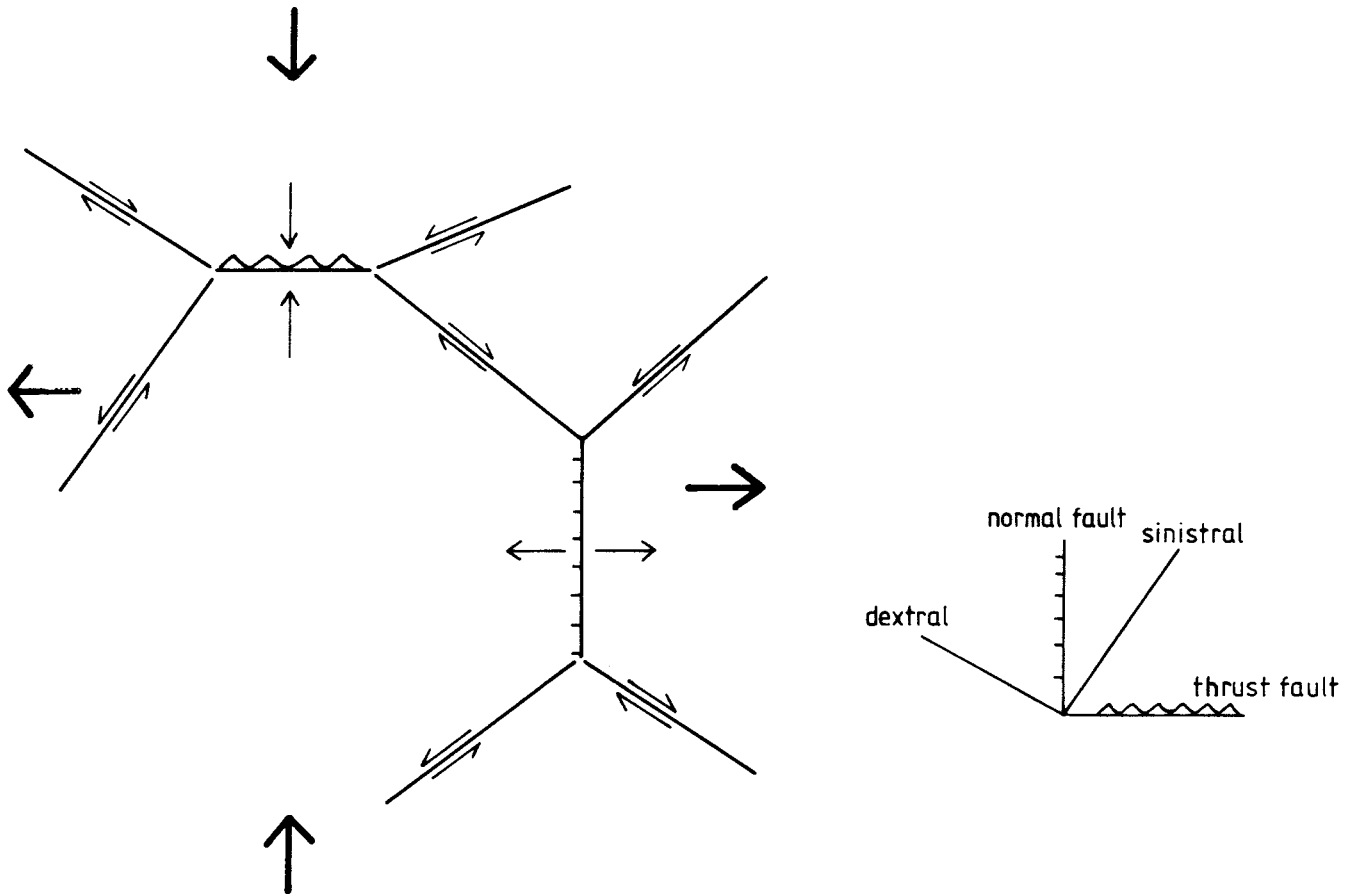
Figure 27. Internal block movements during compression in a N-S
direction provided that the crust is divided into suitable,
minor blocks.

Of course, it is not unlikely that both cases, a and b, occur. For the
determination of the cause of the late quaternary faults, both a mapping
of the deglaciation process, and an investigation of possible present
block movements, are necessary. It may also be added, that in the
literature, other tentative explanations of complex fracture systems
exist.

5. THE CONNECTION OF THE LATE QUATERNARY FAULT NW OF KÄRKEJAURE (MAP AREA 30K NV) TO OLDER FRACTURE ZONES (By Herbert Henkel)

As a basis for the regional interpretation, a preliminary magnetic map material, to the scale of 1 : 200 000, with a resolution of 50 nT has been used (this map was produced for the Nordkalott project). For the local interpretation, a revision of the older aeromagnetic survey was made. This way, a map of 40 nT equidistance was obtained.

The separate branches of the late quaternary fault, in total 15 km of length, entirely follow a major regional, NNE-trending dislocation zone. Up to now, this zone has escaped detection, depending on its small angle to the strike direction of the local structures, and on the low resolution of the printed aeromagnetic maps. This fault zone is over 125 km long, and up to 3 km wide. The accumulated block displacement is very large, in part consisting of an apparent dextral component amounting to at least 6 km (and up to 9 km), and in part of a subsidence of the eastern block. A 25 km wide swarm of dolerite dikes, some of which reaching the length of 20 km, occur partly parallel to the fault zone. The dike-swarm consists of several generations. One of these follows an older structural trend, bending to the NNE.

The major regional fault systems are shown in figure 28, and the local dislocation systems in the vicinity of the recent fault in figure 29. The trend distribution of the regional fault systems is shown in figure 30. Trends between N5E - N15E dominate. Subordinately, the trends N45W - N30W and N30E - N50E occur.

Around the Kärkejaure gabbro, a nearly 6 km wide zone of numerous disturbancies appears. The disturbancies are caused by the intrusion of the gabbro, (their frequency increases towards the gabbro). Older structures are bent outwards around the gabbro by a series of thrust faults. This deviation is also observed around the otherwise linear, and probably fault-caused gradient, that forms the eastern boundary of the western, high magnetic area. However, repeated block movements have followed the existing trends within the zone of disturbancies caused by the gabbro (this zone constituting but a local, rather superficial part of the crust).

Within the zone of disturbance from the gabbro, the late quaternary motion is split upon two faults, and is less regular compared to the northernmost part of the fault. In the north, the late quaternary fault ceases within the older fault zone. In the southern part, it follows a minor, NE-trending dislocation zone for about 1.5 km. The eastern block has subsided. Thus, the fault NW of Kärkejaure is comparable to the third branch of the Lansjärv fault, that also entirely follows an older, NNE-trending zone, and where the eastern block has subsided.

Though the late quaternary movement has occurred within a major, older fracture zone, it apparently is concentrated in a particular part of this zone. This may be further checked through detailed seismic investigation.

MAGNETIC DISLOCATIONS
MAJOR REGIONAL ZONES
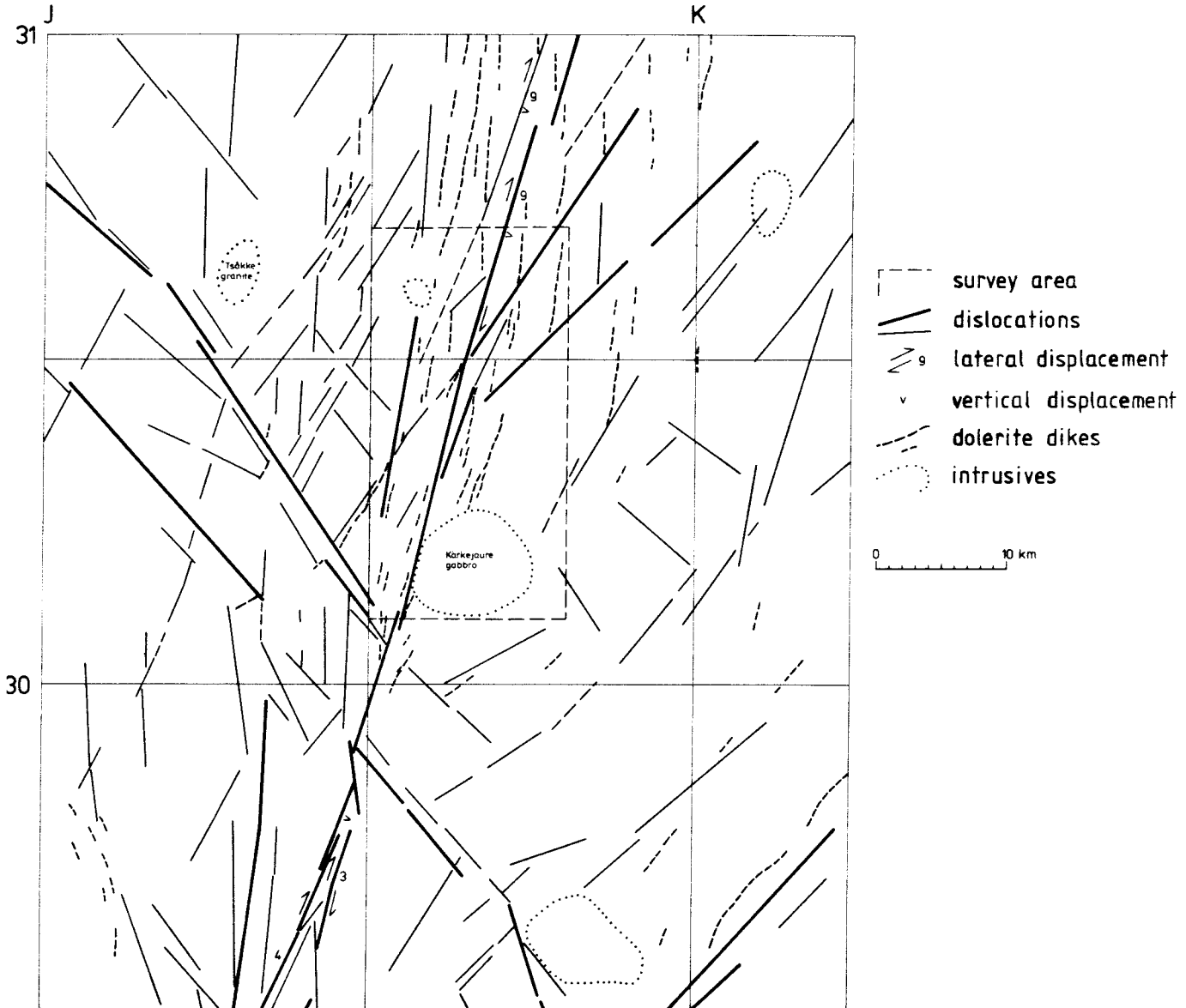
Figure 28. Major magnetic dislocation zones in the Kärkejaure area.

41

MAGNETIC DISLOCATIONS 30K SOPPERO, 6-9 a-c

dolerite dikes
magnetic dislocations
late-quaternary fault
reference structures
zones of disturbancies from
the Kärkejaure-gabbro
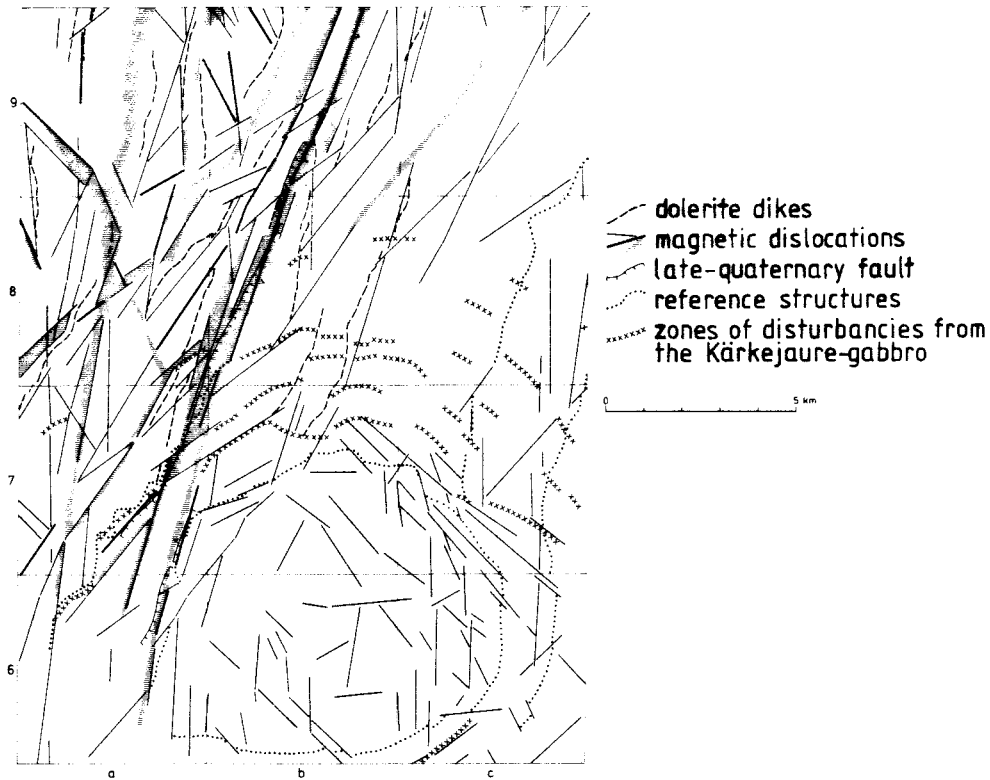
Figure 29. Magnetic dislocations and some reference structures in the
area 30k 6 - 9 a - c.

Figure 30. Direction frequency
spectrum of all magnetic
dislocations in the region of
Kärkejaure. The angular
resolution is 5 degrees.

3031K
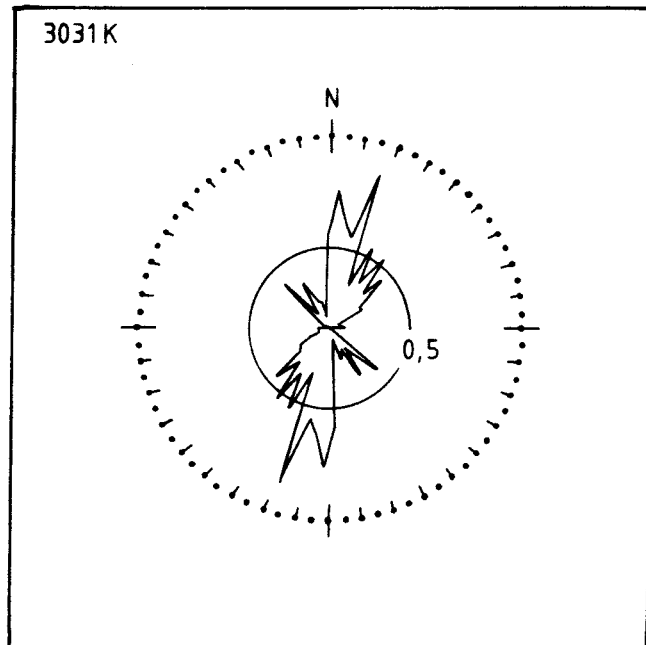
6. SEISMIC REFRACTION PROFILES AT LANSJÄRV (By Herbert Henkel)

In the Lansjärv area, seismic refraction measurements were made along the three profiles depicted in figure 31 (for location of the profiles, see fig.2.
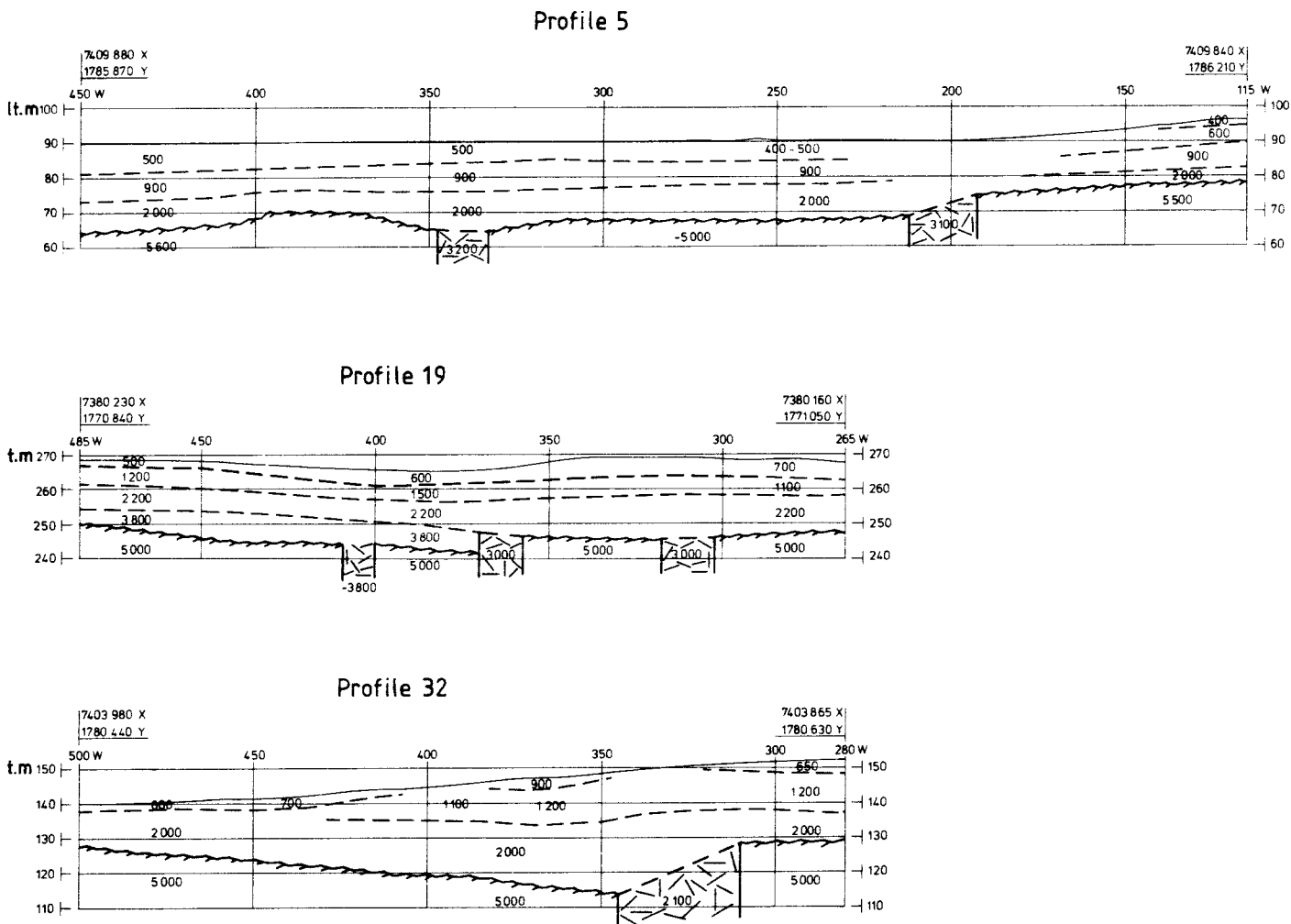
Figure 31. Seismic profiles at Lansjärv.

Scale H=L 1:2000

In profile 19, where the late quaternary fault follows an older fracture zone, the situation is similar to the one at Tjårrojåkka, i.e. the subsided eastern block has an upper layer of low-velocity rock beneath the moraine:

height of quaternary scarp   4 m,
scarp of low velocity rock   6 m,
scarp of unweathered rock   6 m,
width of the fault zone   12 m.

At profile 5, where the late quaternary movement has occurred within an older fracture zone, low velocity rock is absent:

> height of quaternary scarp   5 m,
> scarp of unweathered rock   6 m,
> width of the fault zone   19 m.

Profile 32 is located close to an older NW-trending fracture zone, that crosses the profile obliquely. The late quaternary displacement is less than the level difference of unweathered rock:

> height of quaternary scarp   4.5 m,
> scarp of unweathered rock   14.5 m,
> width of the fault zone   35 m.

Though the zone containing the recent fault is unusually broad, it is probable that the late quaternary movement has taken place in a narrow area in the northwestern part of the zone, where the level of subsoil water changes. The greater level difference of the unweathered rock, as compared to the quaternary scarp, implies that the adjacent blocks have moved in the same direction at several events, though after the glacial erosion that removed the preglacially weathered rock (i.e. the low velocity rock).

7. AIRBORNE ELECTROMAGNETIC SURVEYS OVER LATE QUATERNARY FAULTS

(by L. Eriksson)

A study of the airborne electromagnetic VLF surveys (RAMA maps), that kindly have been placed at our disposal by LKAB, shows that practically all observed cases of regionally occurring late quaternary block movement conicide with fairly strong VLF anomalies. In general, the correlation of observed topographic effects to detected electric conductors is very good, implying that these recent movements are corresponded by at present open and, thus, water-bearing fracture systems.

In this context, it may be pointed out that such highly conductive fracture systems are frequent in the precambrian bedrock. At a rough estimate, the spacing between major zones of a certain trend is a little more than one km. Our knowledge is best concerning the zones that trend in the direction in which the method is most sensitive, i.e. the direction towards the transmitter, in this case about NW.

The frequency of fracture zones does not fluctuate much in different kinds of rock, whereas the amplitude of the anomalies, which depends on the conductivity contrast, may be less within some 'tighter' types of rock, e.g. veined gneisses.

Electric, as well as magnetic, evidence suggests that these fracture systems are developed over a very long period of time, and that the late quaternary motion closely associates to fracture systems of a considerably longer history. Only in some exceptional cases, observed late quaternary faults deviate from conductive zones by hundreds of meters. The deviation may be due to local thrusting near an otherwise steep tectonic zone.

Usually, the zones are very extended and continuous, their length being of the order of 1 - 5 km. The occurring discontinuities may indicate perpendicular fracture systems, that do not cause distinct anomalies due to the 'blind angle' of the applied method. However, the observed late-quaternary zones trend quite favourably relative to the transmitter direction. As regards the dip angle of the zones, the fact that they remain linear, despite substantial differences in topographic level, indicates that they generally are vertical or steeply dipping.

In some cases, e.g. at Vieto, we have been able to make more precise dip determinations, based on the ground measurements, earlier made for ore prospecting in the area. Here, the Slingram survey reveals a negative, symmetric anomaly, indicating an almost vertical, fairly conductive, about 10 m wide zone. The conductor coincides with a precipice towards the east. By the increase in background levels, an enhanced conductivity of the adjacent rock to a distance of 125 m from the fault is indicated. This may imply that the late quaternary movement has caused a local increase in fracturing within a probably much older tectonic zone.

Figure 32. The appearance of the Pärvie fault on the RAMA (airborne VLF) map south of Torneträsk railway station, map area 30J SW.   1 km

In the southern part of the area, parallel precipices towards the west occur. These are not accompanied by corresponding negative anomalies, which indicates that these recent movements have not caused a corresponding fracturing.

One of the most prominent RAMA anomalies yet encountered, the Sparvguld anomaly, located near Svärdsjö in Dalarna, has for several reasons been very thoroughly investigated, even by core-drilling. Cores from a 200 m deep hole, inclined towards the center of the anomaly, give clear-cut geological evidence of a prolonged, fracture-historic evolution. This evolution is documented by brecciation, several kinds of fracture mineralization, impregnation with rock pitch, and probably also by the signs of late-quaternary motion, in the form of abundent, open fracturing.

At present, a closer examination of the water-conductivity of the zone is made by well-drilling at several places. Also, the escarpments occurring in the quaternary deposit will be investigated. This zone appears to be well suited for the further and more detailed study of: fracture-historic evolution, fracture mineralogy, relation of gases to fracture tectonics (artesic water occurs in the drill hole, indicating that the zone is sealed upwards by the soil layer) etc.

AITEJÅKKA

P 2960 N   Late quaternary fracture zone
Slingram imaginary 18 kHz - 60 m
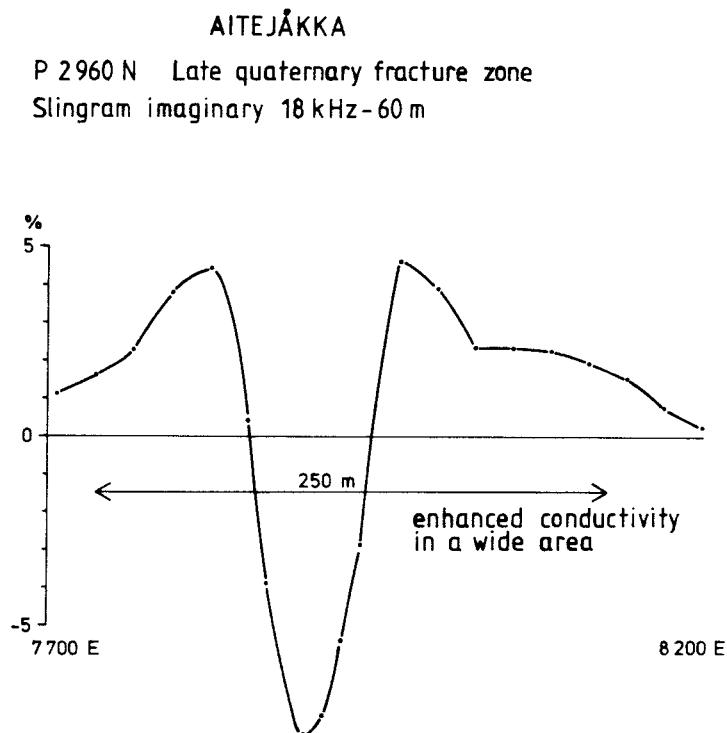
Figure 33. Slingram profile P 2960 N (18 kHz, 60 m coil distance, imaginary component) over the AitejÅkka zone, cf. fig. 34.
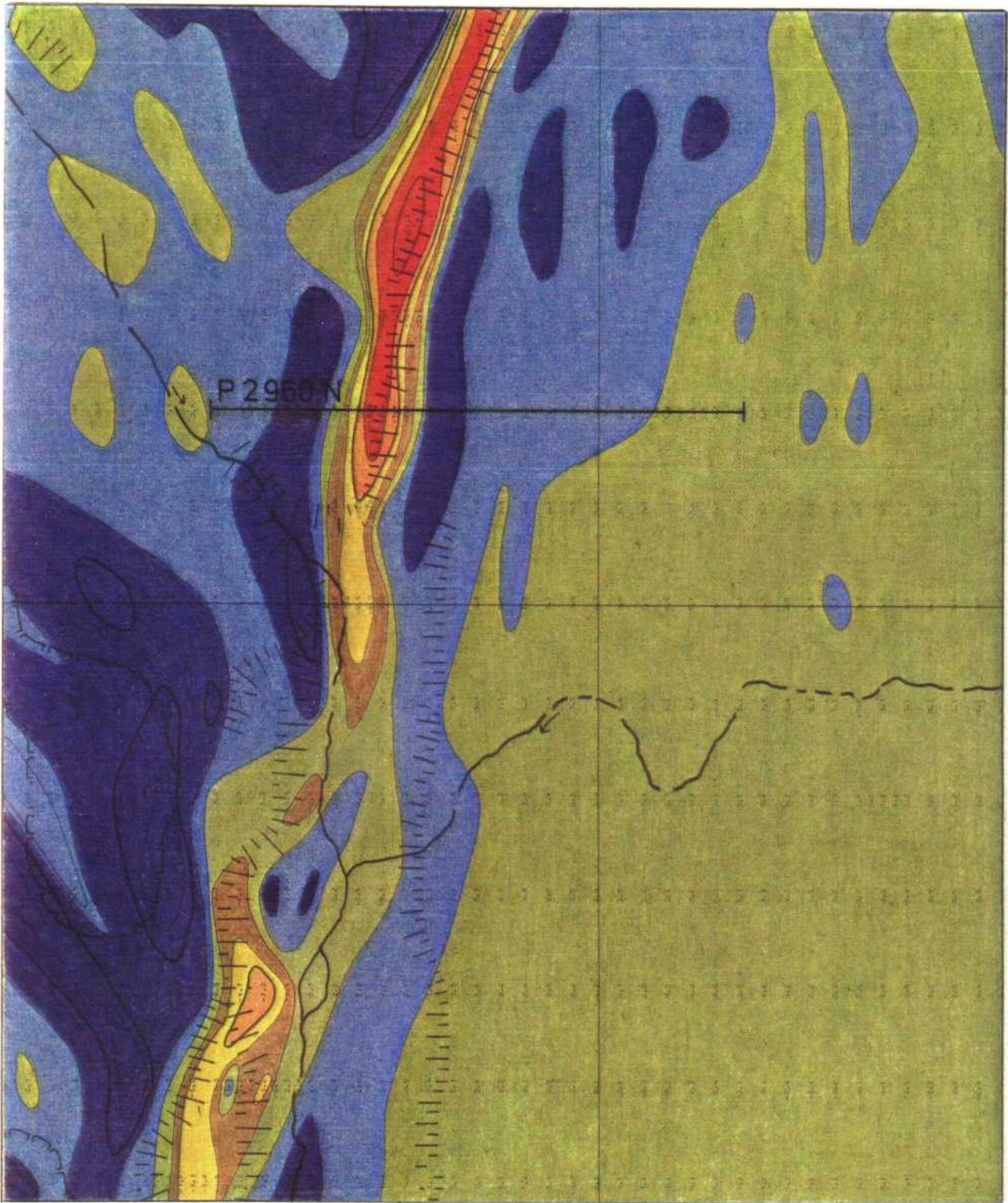
Figure 34. Slingram survey (18 kHz, coil distance 60 m, imaginary
component), over a late quaternary fault to the west of
Kiruna.

8. EVALUATION OF GEOPHYSICAL MEASUREMENTS OVER THE PÄRVIE FAULT

(By L. Johansson)

Abstract

The Pärvie fault, 150 km long and running parallel to the eastern border of the Caledonides through the map areas 28-29I, 29-31J, and which is regarded to be of late quaternary age, has been the subject of geophysical investigation. For the survey, older material from earlier ore prospecting has been used, augmented by supplementary surveys, including refraction seismics.

The investigations, conducted in the survey area Tjårrojåkka, (29I 2-3, h-i) have led to the following conclusions:

> The pärvie fault at Tjårrojåkka is situated in an older tectonic zone, where block movement, preceding the late quaternary displacement discernible from the topography, has occurred. The preglacial block displacement amounts to at least 10 m (vertical) and the late quaternary to 6-7 m.

> The Pärvie fault, generally characterized by a downthrown western block, dips steeply at Tjårrojåkka. At a shorter, parallel fault at Aitejåkka (29J 6-7, c-d), 10 km east of Pärvie, the eastern block has subsided. The dip of the latter fault is on the average 85" to the west.

> At Tjårrojkka, the Pärvie fault has but a small water content. This does, however, not preclude the presence of water-conducting, minor fractures.

8.1. Introduction

On the assignment of PRAV, SGU has undertaken an investigation of an area crossed by the 150 km long Pärvie fault. The survey area is situated about 50 km WSW from Kiruna.

The area, named Tjårrojåkka, has been the subject of ore prospecting, with the application of most of the usual geophysical methods, in the 1960's and -70's. This offers the opportunity to investigate the properties of the Pärvie fault, and possibly also to estimate its dip angle, i.e. to make out a 3-dimensional image of the fault.

The investigation has been undertaken mainly under the management of SGU, though after the division of SGU in July 1982, it has been completed at SGAB in Luleå.

8.2. The Tjårrojåkka survey area

8.2.1. Location

The area is located in the map area 29I Kebnekaise 2-3, h-j, see fig.
35. The area investigated in this project is located in sub-area 2i.

Figure 35. The map area 29I
SE with the
Tjårrojåkka
survey area.
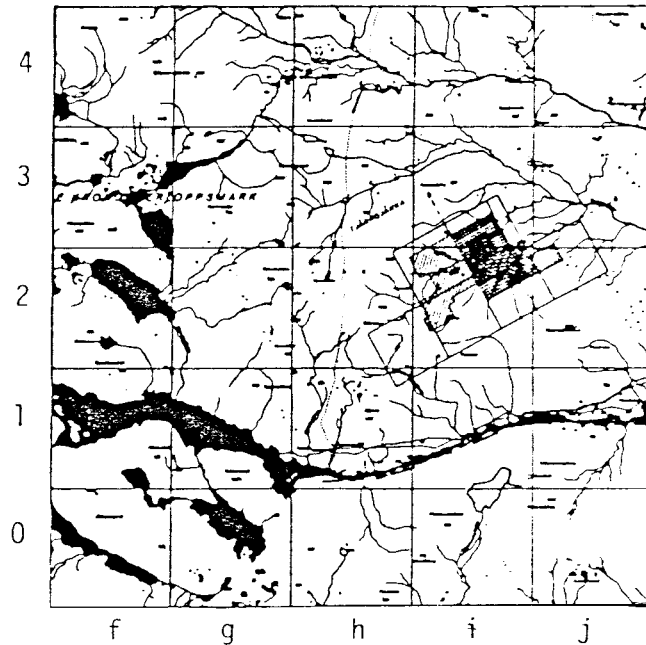
8.2.2 Geophysical measurements at Tjårrojåkka

In connection with ore prospecting campaigns in the 1960's and -70's,
the area has been the subject of geophysical investigations, with the
application of magnetic, electromagnetic (Slingram), and electric
methods. For the augmentation of these measurements, electromagnetic
(VLF) and seismic surveys have been undertaken. The areal extent of the
applied methods is shown in fig.36.
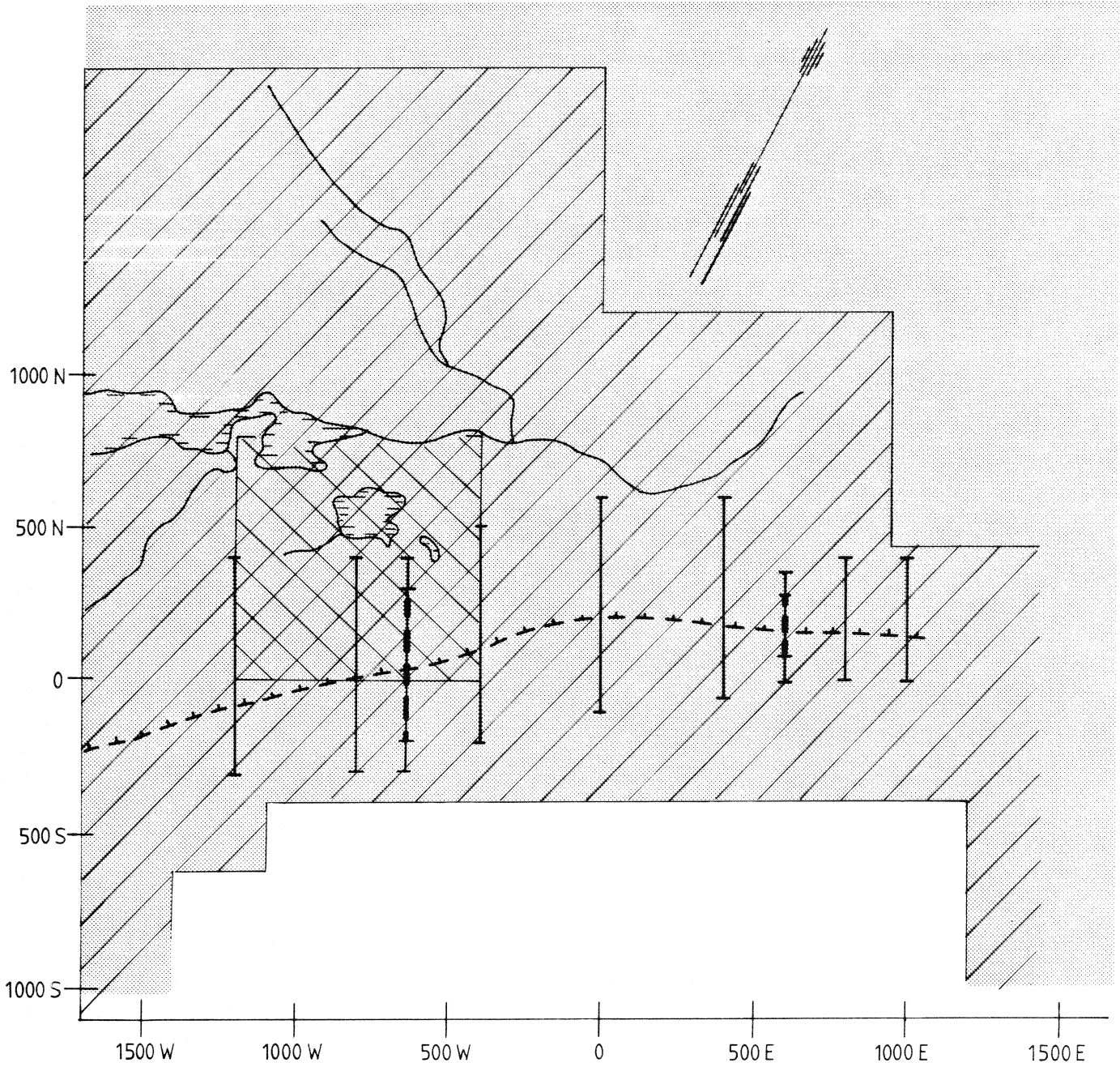
MEASUREMENTS

TJÅRROJÅKKA

SLINGRAM 18 kHz – 60 m

MAGNETIC VERTICAL FIELD

IP AND RESISTIVITY

VLF PROFILE

SEISMIC PROFILE

PÄRVIE FAULT

SCALE 1:10 000

0   100   200   300   400   500 m
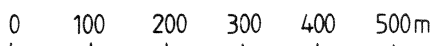
Figure 36.
The Tjårrojåkka survey area.

8.3. The aeromagnetic map

The aeromagnetic map (cf.fig. 37) of the Tjårrojåkka area shows the occurrence of several strong magnetic anomalies caused by high content of magnetite in the bedrock. The pattern formed by the anomalies is interrupted by magnetic dislocations of substantial length, showing systematic displacement of the anomaly pattern, or by other zones of lower magnetization (for cause, cf. chapter 3). Fig.37 shows the relation of the Pärvie fault to some magnetic dislocation zones.

South of the investigated area, the Pärvie fault follows an older fault zone. 600 m north of the southern border of the area, this older zone deviates northwards from the Pärvie fault. The stress distribution within the bedrock has caused the latter to turn eastwards, following another, less extended, magnetic dislocation.

East of the survey area, the appearance of the fault becomes more complex. This appears to be connected to changes in the direction of the fault and the related influence on the stress pattern.
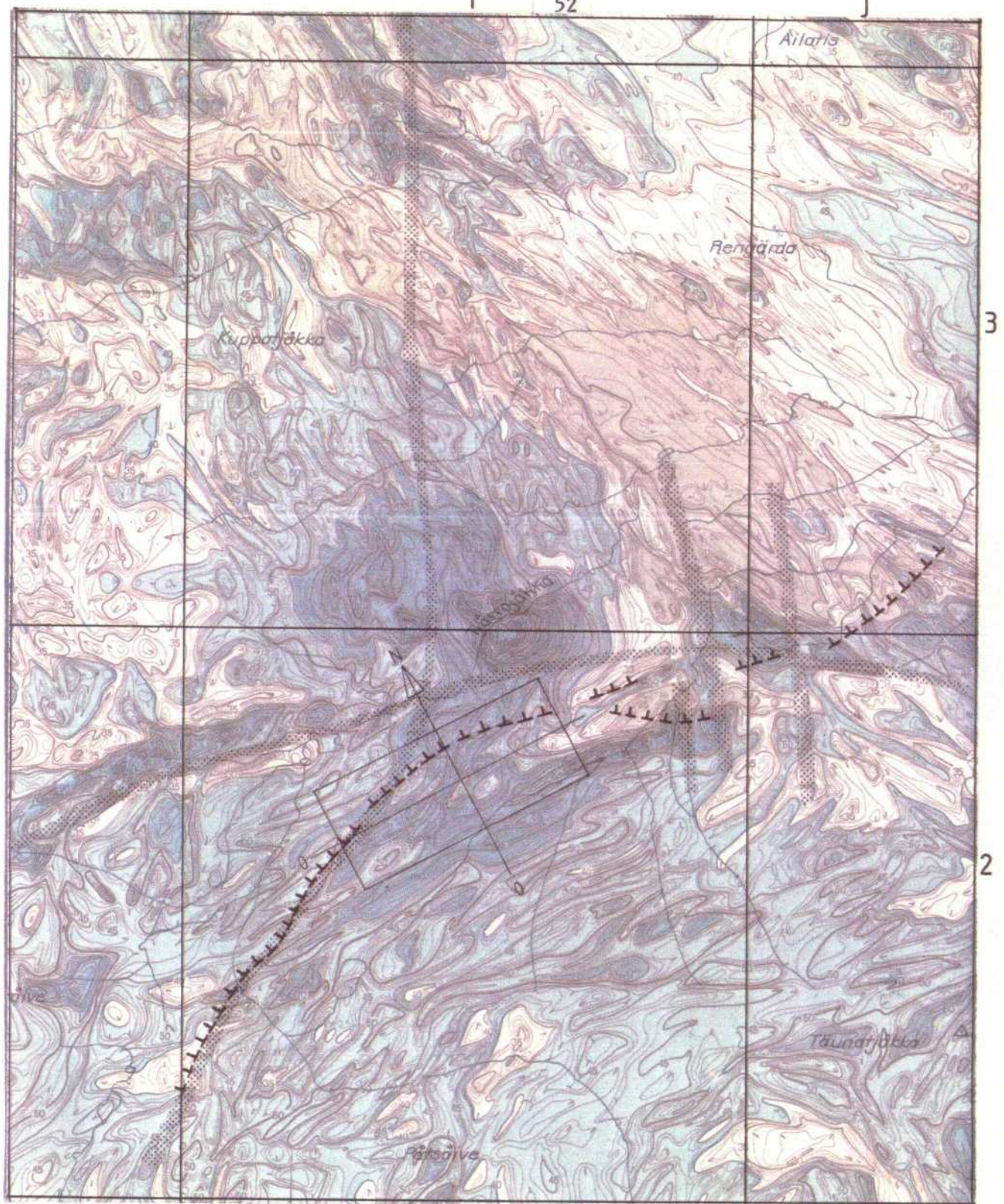
TJÅRROJÅKKA

AEROMAGNETIC MAP
(PART OF 29I KEBNEKAISE SO)

⊥⊥⊥⊥ THE PÄRVIE FAULT
(ACCORDING TO LAGERBÄCK AND
F. WITSCHARD 1982)

THE TJÅRROJÅKKA SURVEY AREA
AND LOCAL COORDINATE SYSTEM

Figure 37. Aeromagnetic map
of the Tjårrojåkka region.

Fluxgate magnetometer år 1963–64
Medelflyghöjd 30 m
Linjeavstånd 200 m

Färgschema:

Anomali:
+ 5.000 gamma
+ 2.000 gamma

Normalvärde   + 500 gamma
51.500 gamma   −500 gamma

8.4. Electromagnetic survey

Within the area, VLF measurements have been made along 9 profiles
crossing the Pärvie fault. Previously, the whole area has been surveyed
using Slingram 18 kHz, coil distance 60 meters.

Figs. 38 and 39 show the results from the VLF measurements, except for
two profiles, coinciding with seismic ones. Figs.40 and 41 show VLF and
Slingram results from these profiles, 640 W and 600 E. A compilation of
the results into an interpretation map of the survey area is presented
in fig. 44.

——— REAL COMPONENT

– – – IMAGINARY COMPONENT

P   LOCATION OF THE PÄRVIE FAULT
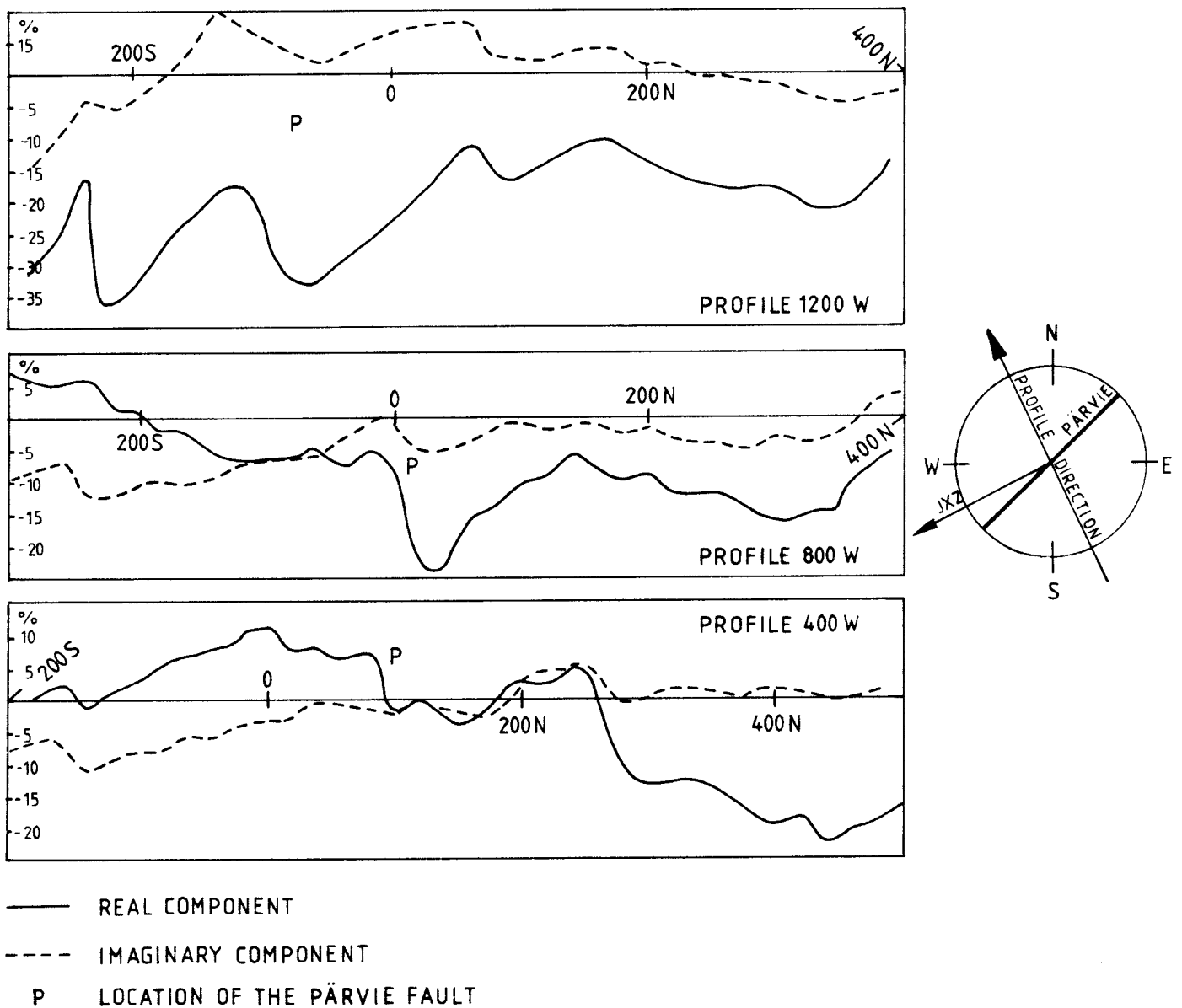
Figure 38. VLF profiles at Tjårrojåkka.

TJÅRROJÅKKA
VLF PROFILES

The Pärvie fault is indicated by the electromagnetic survey as a poorly
conductive zone, the conductivity being slightly higher in the western
part, where the tectonic zone connected to the fault is broader.

Along the profiles 1200 W - 400 W, the anomaly from the steeply dipping
Pärvie fault is superimposed by the anomaly from a flat-lying conductor,
situated to the NW of the fault. This conductor is also visible from the
Slingram measurements along profile 640 W, fig. 40, where the flat
conductor is indicated by a higher level of both components.

REAL COMPONENT

IMAGINARY COMPONENT

P   LOCATION OF THE PÄRVIE FAULT
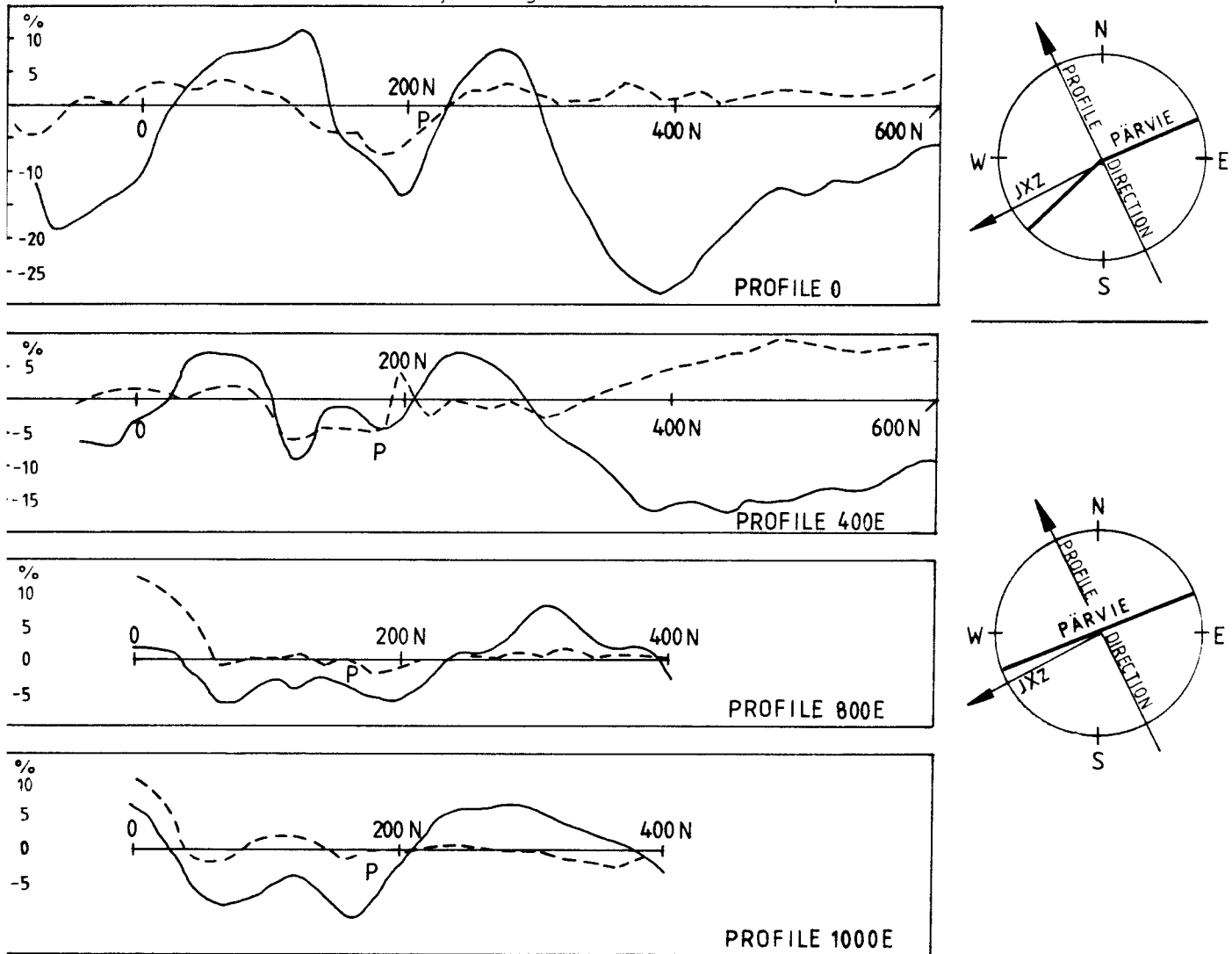
Figure 39. VLF profiles at Tjårrojåkka.
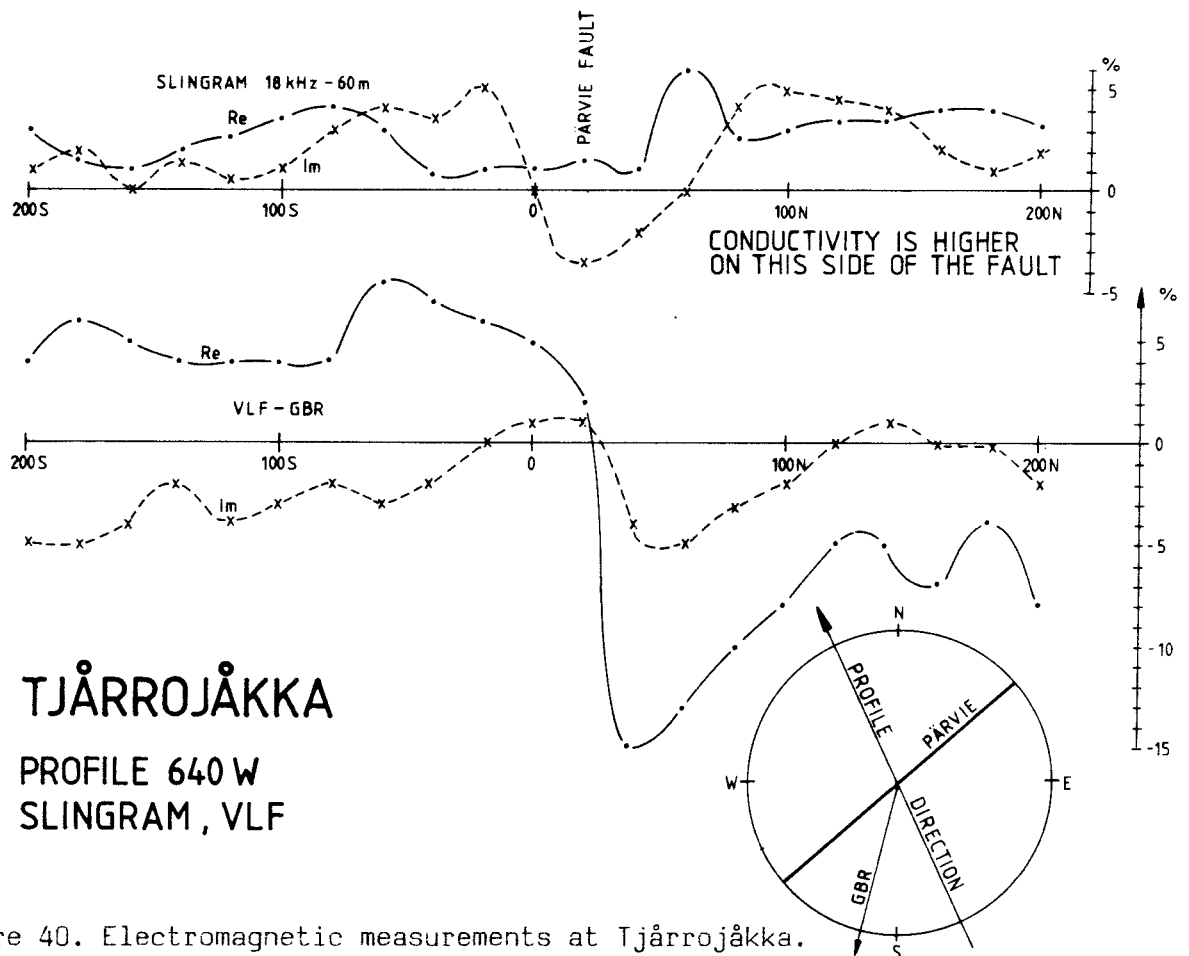
Figure 40. Electromagnetic measurements at Tjårrojåkka.

East of the origin (figs. 38 and 39), the VLF survey does not indicate the anomaly from a flat conductor near the fault. However, the Slingram indication remains, the lower amplitude of the anomaly suggesting a thinning out of the conductive stratum.

At Aitejåkka (fig. 45) within the map area 29J Kiruna, another late-quaternary fault, striking north-south, runs parallel to the Pärvie fault. The fault at Aitejåkka follows an older tectonic zone forming the border between syenite east of the fault, and greenstones on the western side. Slingram measurements at Aitejåkka indicate the fault as a moderately conductive tectonic zone. Cf. fig. 39.

In many cases, dip determination of sheet-like conductors can be made from electromagnetic measurements. At Tjårrojåkka, nearby anomalies interfere with the anomaly from the fault, precluding a more precise dip determination than 75" - 105". At Aitejåkka, however, the anomaly from the fault is fairly undisturbed over long distances. A systematic evaluation shows that the zone dips steeply westwards, plunging under the raised block. The dip angle is estimated to 85" +/- 10". At some localities, for about 10% of the strike length of the fault, a steep eastward dip is indicated.

56
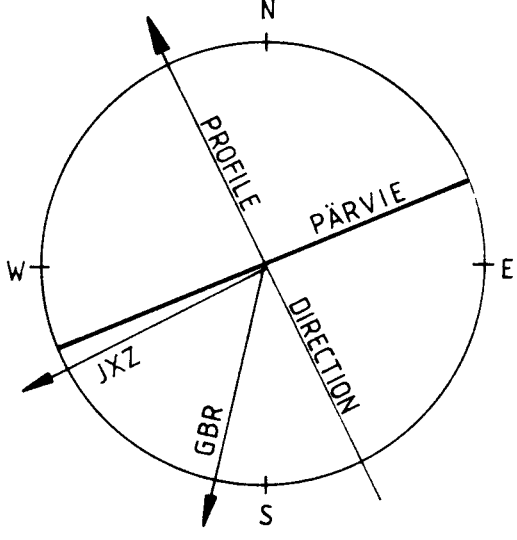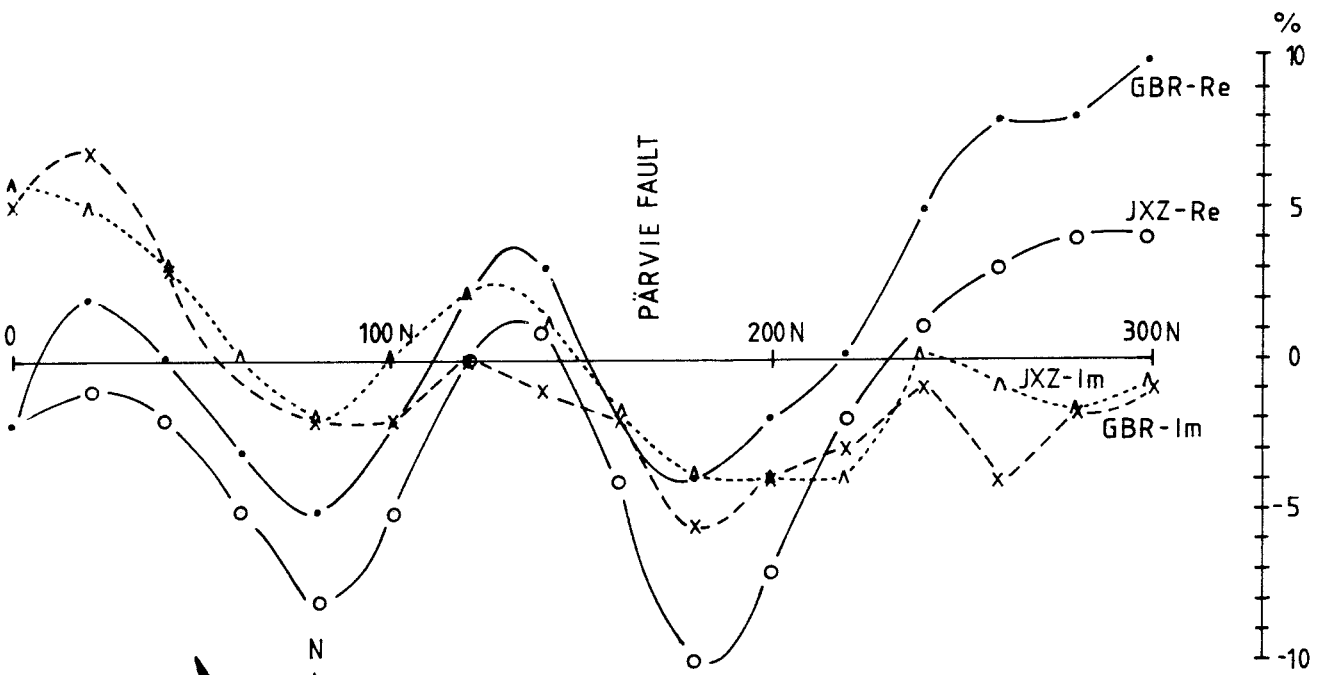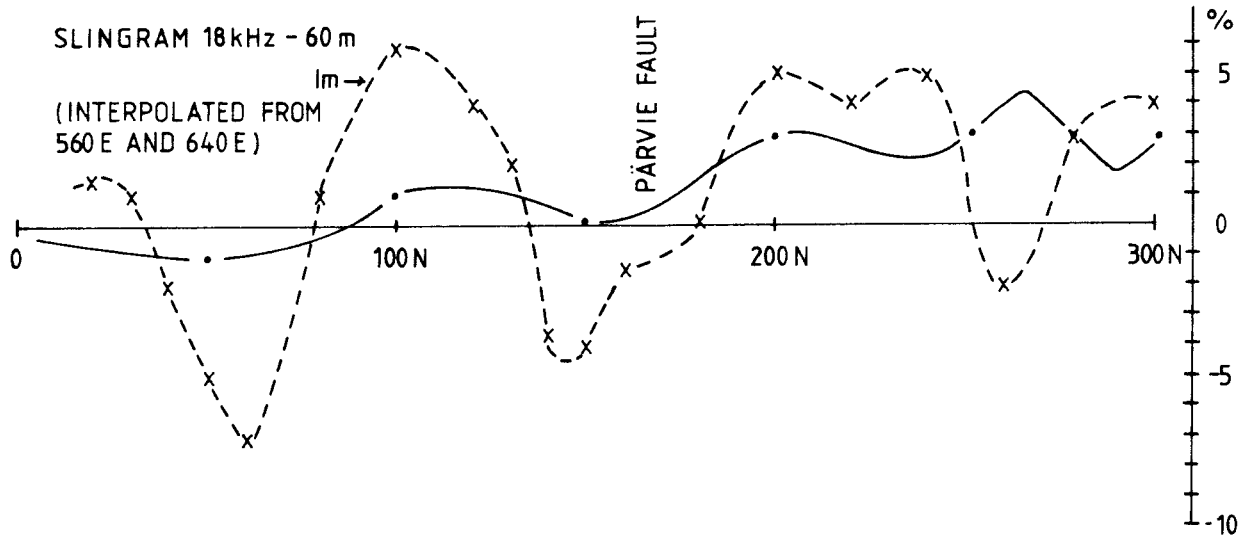
Figure 41. Electromagnetic measurements at
Tjårrojåkka.

8.5. Electric survey

A minor part of the Tjårrojåkka area has previously been investigated
regarding resistivity and IP-effect (see fig. 36). The Pärvie fault
appears in the resistivity survey as a zone of low resistivity and low
to normal IP-effect. The reduction in IP-effect, known from surveys of
other tectonic zones, is attributed to weathering of polarizable
minerals and the change in current distribution caused by an increase of
the conductive surface.

8.6. Seismic survey

Seismic refraction investigations have been made along two profiles
crossing the Pärvie fault, at 640 W (see fig. 42 for interpretation),
and at 600 E (fig. 43). The profiles have been leveled at a relative
accuracy of 0.1 m. The absolute accuracy of altitude is +/- 5 m.
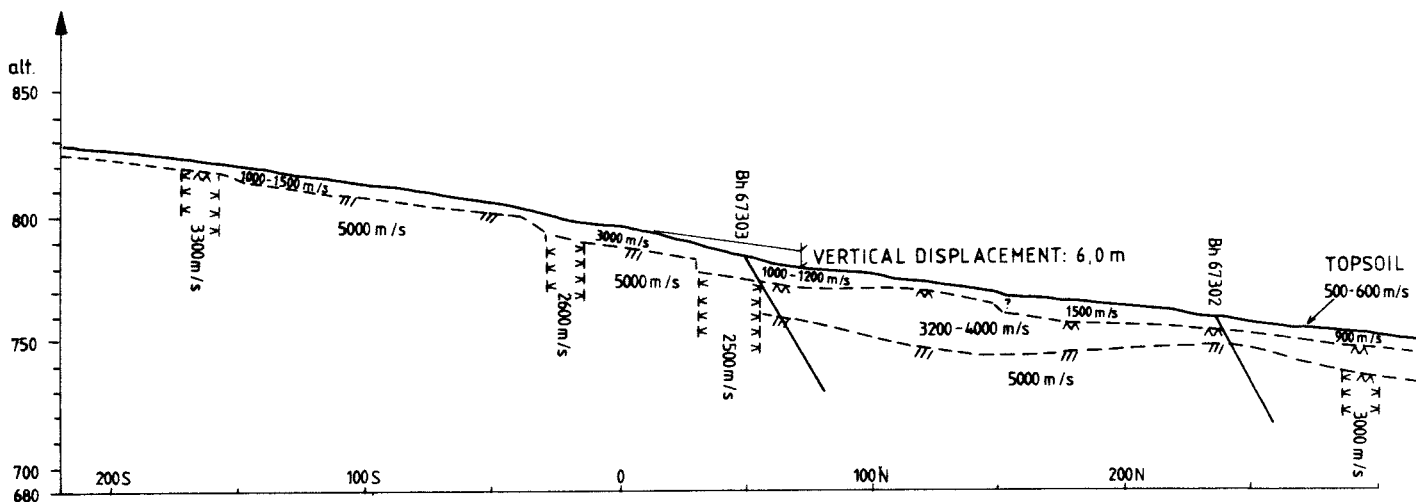
TJÅRROJÅKKA   SEISMIC PROFILE 640 W

—ᴧᴧ—   SURFACE OF FRACTURED OR WEATHERED ROCK
—ᴧᴧ—   SURFACE OF UNWEATHERED ROCK
ᴷ ᴴ   FRACTURE ZONE
ᴷ ᴴ

Figure 42. Interpretation of seismic profile 640 W.

At the profile 640 W, a tectonic zone, about 25 m wide, has been
indicated by the reduced seismic propagation velocity through fractured
rock. Additional tectonic zones, reaching the width of 15 m, have also
been indicated.

The overburden is 4 - 10 m thick, including an upper, less consolidated
layer of 1 m thickness. As no water level is indicated in the moraine,
the level of subsurface water is taken to be below or just above the
bedrock surface.

On the upper side of the fault, a seismic velocity in the bedrock of 5000 m/s is obtained. Below the fault, the unweathered rock is covered by weathered rock, indicated by propagation velocities of 3200 - 4000 m/s. The depth extension of the weathering is 5 - 20 m. The bore hole Bh67303 is located close below the Pärvie fault. The core logging reveals considerable fracturing and alteration to a vertical depth of 21.8 m, in good agreement with the seismically estimated depth of 20 m. From the bore hole Bh67302, this relation has not been demonstrated, as rock types change, and one cannot from the core log decide which changes are related to rock types and which are caused by surface weathering.

At the profile 640 W, the vertical throw of the fault has been seismically estimated to about 7 m. The step in the topography amounts to 6.0 m. Other steps in the bedrock surface occur on both sides of the fault, the one on the upper side appearing to be rather local, while at the lower side, the step coincides with a topographic escarpment, extending for 1,5 km (as interpreted from aerial photography) in the southwestern elongation of the northeastern part of the Pärvie fault.

TJÅRROJÅKKA   SEISMIC PROFILE 600 E

—ᴧᴧ— SURFACE OF FRACTURED OR WEATHERED ROCK
—ᴫ— SURFACE OF UNWEATHERED ROCK
ᴋ ᴎ
ᴋ ᴎ   FRACTURE ZONE
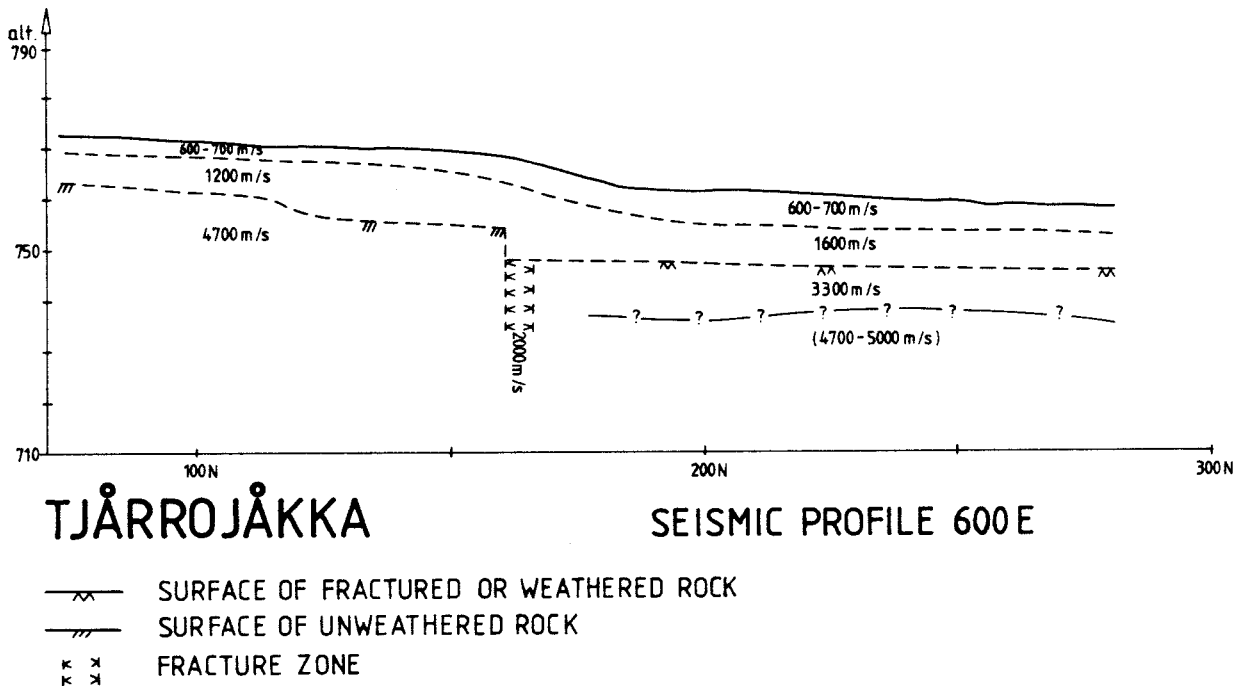
Figure 43. Interpretation of seismic profile 600 E.

The seismic investigation at profile 600 E shows the same main features as profile 640 W. Data from profile 600 E (corresponding from 640 W in brackets):

Width of the Pärvie tectonic zone, about 5 m (25 m)

Thickness of overburden, 9 - 13 m SE of the fault and 12 - 14 m on the NW side (4 - 10 m on both sides)

Depth extension of weathered rock NW of the Pärvie fault 5 - 10 m

(5 - 20 m) . The depth extension has seismically been estimated
as exceeding 5 m but no depth limit has been obtained. From the
results of the electromagnetic survey, the depth of weathering is
interpreted as not exceeding 10 m.

The vertical displacement at profile 600 E is seismically established
to be about 6 m (about 7 m). The topographic escarpment is 6.4 m
(6.0 m).
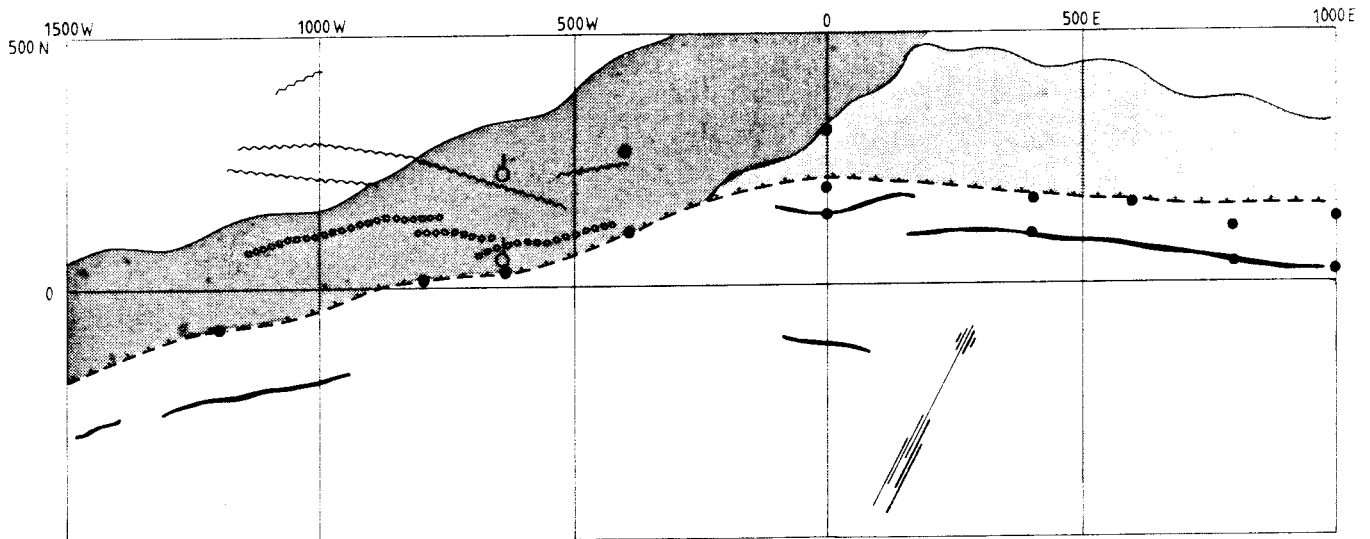
INTERPRETATION MAP OF THE TJÅRROJÅKKA AREA

_._._ THE PÄRVIE FAULT
WATER-BEARING FRACTURE ZONES:
⌒⌒⌒ INDICATED BY RESISTIVITY MEASUREMENTS
‾‾‾ INDICATED BY SLINGRAM 18 kHz-60 m
 • INDICATED BY VLF PROFILE MEASUREMENTS
♂ DRILL HOLE

oooo SULPHIDE MINERALIZATION, INDICATED BY
IP MEASUREMENTS
DEPTH EXTENT OF ROCK WEATHERING:

☐ 5-10 m

▨ 5-20 m

Figure 44. Interpretation map of the Tjårrojåkka area.

8.7. Conclusions

The investigations show, that at the examined part of the Pärvie fault,
block movement has occurred at, in the least, two separate events,
separated by the erosion of more than 10 m of weathered rock. The latest
block movement has on other criteria, not presented in this context,
been proved to be of late-quaternary age. The total vertical
displacement, taken as the difference in altitude of unweathered rock on
respective sides of the fault, exceeds 18 m. The displacement preceding
the development of the present rock surface amounts to at least the
remaining depth of weathered rock in the vicinity of the fault, i. e. a
minor portion of the total block movement has occurred in late-
quaternary age.

The Pärvie fault follows older tectonic zones, but strikes out new paths
where stress conditions have demanded. Within the surveyed area, the
fault switches from a prominent, old tectonic zone into another, less

developed one.

At Tjårrojåkka, the Pärvie fault has only a minor water content, as indicated by the weak electromagnetic anomalies. The water flow in the fault zone can, however, not be estimated, as small, open fissures, though carrying plenty of water, will not be detected owing to their low product of width and conductivity.

The fault at Aitejåkka is reversed and mainly dipping steeply to the west (85").

The Pärvie fault at Tjårrojåkka is steeply dipping. No more precise dip determination has been practicable.

Figures 45 and 46. Late quaternary fault at Aitejåkka. The southern part of Fig. 46 is also shown in Fig. 34.
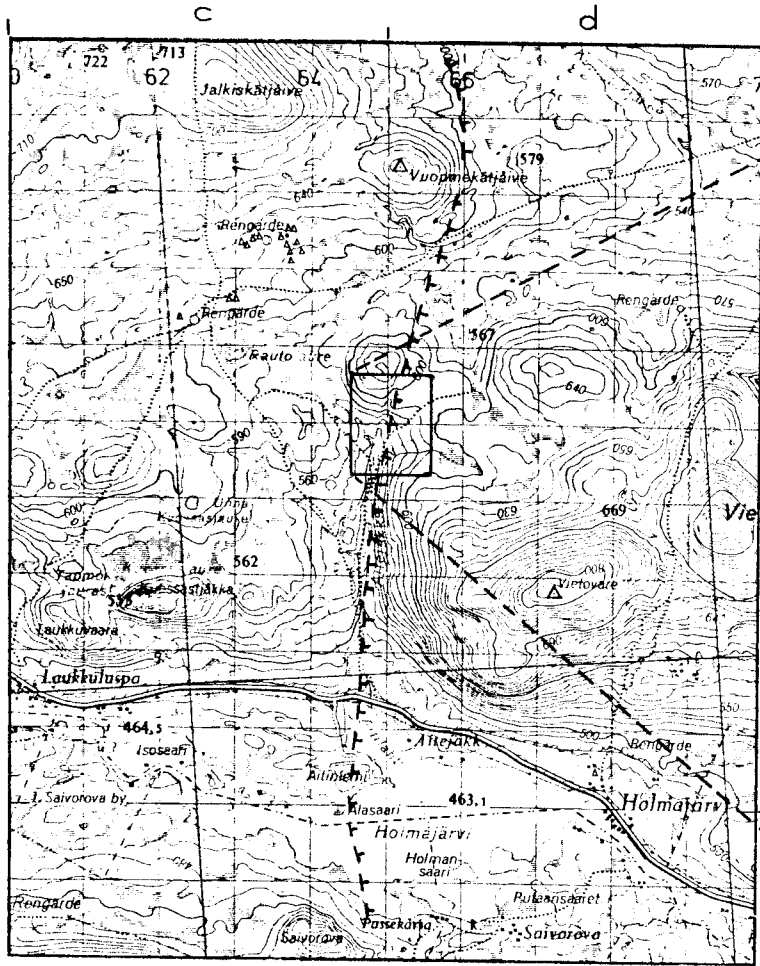
Figure 45. Part of the topographic map 29J
Kiruna (6-7, c-d)
⊤ ⊤ ⊤ fracture zone
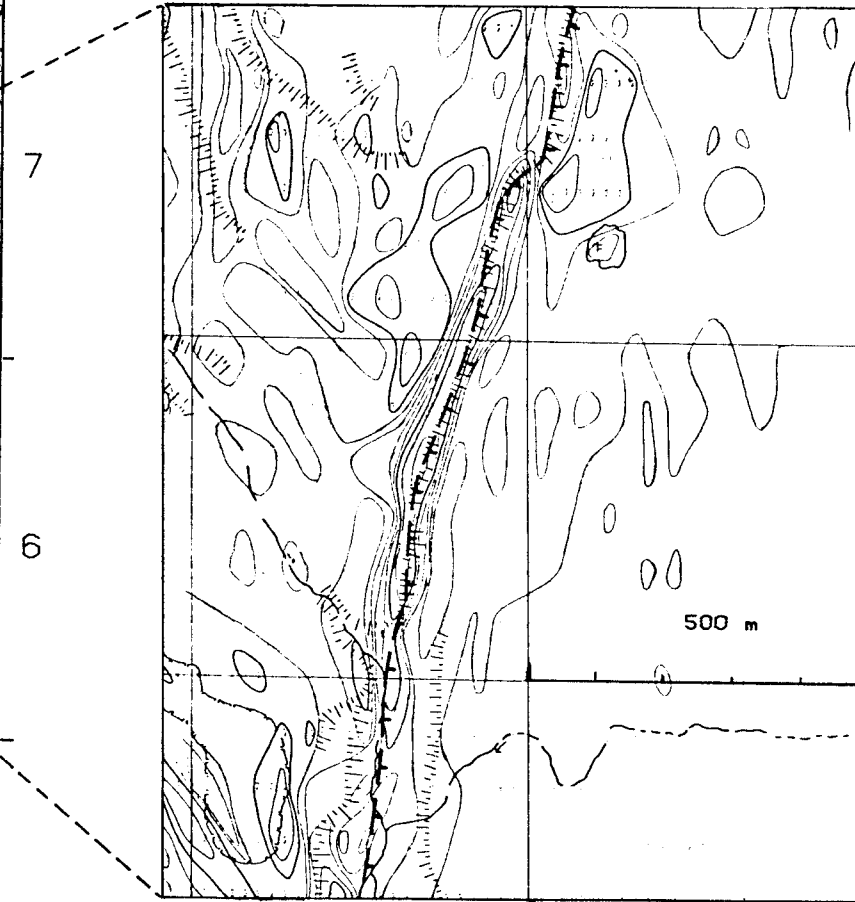
Figure 46. Slingram imaginary 18 kHz - 60 m. Indication over a water-bearing fracture zone (⊤ ⊤ ⊤⊤).

61

9. CONCLUSIONS AND RECOMMENDATIONS

The major regional, older fracture zones can be mapped out by aeromagnetic interpretation. However, large enough areas (at least 100 x 100 km) must be interpreted in the same context. Furthermore, a sufficiently detailed map material must be produced - this is particularly important in areas of low magnetic rocks. Without these conditions, the interpretation of accumulated block displacement, and of the interaction between separate fracture zones, will be too unreliable. In areas where airborne VLF-measurements are at hand, a good overview of the occurrence of major water-bearing fracture zones is obtained. Magnetic and VLF interpretation complement each other in areas with low magnetic rocks, and regarding the unfavourable trend of the VLF method (Henkel and Eriksson 1980).

The present study is the first attempt at a detailed, regional out-mapping and analysis of major fracture zones. Many of the faults appearing on certain of the published geological maps of Norrbotten have but a sporadic connection to existing structures. An evaluation of their regional distribution and character of movement is not feasible, since the presented fault patterns are different within each map area.

The surveys and the interpretation made at Lansjärv, Kärkejaure, and Tjårrojåkka prove that the recent late quaternary motion is composed of several phases, with the same type of movement. Thus, the late-quaternary movements may be part of a long-term tectonic process, interfering with the recent glacial motion in the earth's crust. Estimation of the more recent accumulated displacement of separate faults is feasible only from detailed seismic profiles.

The recent block movements also differ by the way they have engaged older tectonic zones. In favourable conditions (i.e. magnetic bedrock and/or abundant magnetic reference structures), the older zones may be mapped out to fine detail by aeromagnetic interpretation. Thus, the NNE-trending late quaternary faults entirely follow major regional faults (e.g. at Kärkejaure), or the secondary fractures of such fault systems that trend in this direction (e.g. at Lansjärv). On the other hand, the more northeasterly trending late quaternary faults frequently cross areas without older fracture zones. The discontinuation of the recent faults, and changes of their scarp height, is often connected to the passage of N- or NW-trending local or regional older fracture zones and faults. Thus, it is likely that these zones are partially involved in the late quaternary block motion.

It is beyond the scope of this work to establish a tectonic-kinematic hypothesis of the cause of the recent block movements, and their interaction with older fracture zones. For the achievement of such a hypothesis, the following is suggested:

-A check of the block movement at he major regional faults, through interpretation (by model calculations) of the available gravity and magnetic data.

-Further study of the connection of other late quaternary faults to
older structures, so that a more statistic description of these
connections can be made.

-A number of seismic refraction lines, each about 200 m of length, for
the mapping of the width and the type of displacement of the other
late-quaternary faults. At these sites, VLF, magnetic and Slingram
measurements should also be made over at least 600 m, for the
estimation of dip and water content.

-Recording of possible microseismic activity within an area where late
quaternary faults occur, over a longer period of time, in order to
detect any contemporary creep. The Lansjärv area is suitable for such
an investigation.

-Excavation of a late quaternary fault, for a closer study of its effects
on the moraine and the bedrock. Here, too, the Lansjärv area is
suggested.

-A more accurate mapping of the highest shore-lines in the Lansjärv
area, and a study of the deglaciation of Norrbotten.

-The publication of a summary of the present study in an international
paper.

10. REFERENCES

Burford, R.O., et al. 1981: Last October 7.3 quake in Algeria reviewed. Geotimes May 1981.

Carlsson, A., and Olsson, t. 1982: High rock stresses as a consequence of glaciation. Nature 298-5876 pp. 739-742.

Henkel, H, & Guzman, M., 1977: Magnetic features of fracture zones. Geoexploration 15, 173-181.

Henkel, H., 1979: Dislocation sets in northern Sweden. GFF 100, 271-278.

Henkel, h., and Eriksson, L., 1980: interpretation of low altitude airborne magnetic and VLF measurements for identification of fracture. In Subsurface Space, edited by Magnus Bergman. Pergamon Press 1980.

Henkel, H., 1982: Stora gabbro intrusioner i norra Sverige. SGU Sekt. f. regional geofysik. Rapport 8108.

Hill, D.P., 1982: Contemporary block tectonics: California and Nevada. Journ. Geoph. Res. 87, pp. 5430-5433.

Lagerbäck, R., and Witschard, F., 1982: Neotektonik i Norrbotten, kvartär- och berggrundsgeologisk dokumentation. SGU, sektionen för kvartärgeologi. Rapport 1982.08.15.

Stanfors, R., 1973: Mienstrukturen – en kryptoexplosiv bildning i Fennoskandias urberg. Doctoral thesis at the University of Lund.

LIST OF KBS's TECHNICAL REPORTS

TR 83-03   Smectite alteration
            Proceedings of a colloquium at State University of
            New York at Buffalo, May 26-27, 1982
            Compiled by Duwayne M Anderson
            State University of New York at Buffalo
            February 15, 1983

TR 83-04   Stability of bentonite gels in crystalline rock -
            Physical aspects
            Roland Pusch
            Division Soil Mechanics, University of Luleå
            Luleå, Sweden, 1983-02-20

TR 83-05   Studies in pitting corrosion on archeological
            bronzes - Copper
            Åke Bresle
            Jozef Saers
            Birgit Arrhenius
            Archaeological Research Laboratory
            University of Stockholm
            Stockholm, Sweden 1983-01-02

TR 83-06   Investigation of the stress corrosion cracking of
            pure copper
            L A Benjamin
            D Hardie
            R N Parkins
            University of Newcastle upon Tyne
            Department of Metallurgy and Engineering Materials
            Newcastle upon Tyne, Great Britain, April 1983

TR 83-07   Sorption of radionuclides on geologic media -
            A literature survey. I: Fission Products
            K Andersson
            B Allard
            Department of Nuclear Chemistry
            Chalmers University of Technology
            Göteborg, Sweden 1983-01-31

TR 83-08   Formation and properties of actinide colloids
            U Olofsson
            B Allard
            M Bengtsson
            B Torstenfelt
            K Andersson
            Department of Nuclear Chemistry
            Chalmers University of Technology
            Göteborg, Sweden 1983-01-30

TR 83-09   Complexes of actinides with naturally occurring
            organic substances - Literature survey
            U Olofsson
            B Allard
            Department of Nucluear Chemistry
            Chalmers University of Technology
            Göteborg, Sweden 1983-02-15

TR 83-10   Radiolysis in nature:
            Evidence from the Oklo natural reactors
            David B Curtis
            Alexander J Gancarz
            New Mexico, USA February 1983

TR 83-11   Description of recipient areas related to final
           storage of unreprocessed spent nuclear fuel
           Björn Sundblad
           Ulla Bergström
           Studsvik Energiteknik AB
           Nyköping, Sweden 1983-02-07

TR 83-12   Calculation of activity content and related
           properties in PWR and BWR fuel using ORIGEN 2
           Ove Edlund
           Studsvik Energiteknik AB
           Nyköping, Sweden 1983-03-07

TR 83-13   Sorption and diffusion studies of Cs and I in
           concrete
           K Andersson
           B Torstenfelt
           B Allard
           Department of Nuclear Chemistry
           Chalmers University of Technology
           Göteborg, Sweden 1983-01-15

TR 83-14   The complexation of Eu(III) by fulvic acid
           J A Marinsky
           State University of New York at Buffalo, Buffalo,NY
           1983-03-31

TR 83-15   Diffusion measurements in crystalline rocks
           Kristina Skagius
           Ivars Neretnieks
           Royal Institute of Technology
           Stockholm, Sweden 1983-03-11

TR 83-16   Stability of deep-sited smectite minerals in
           crystalline rock - chemical aspects
           Roland Pusch
           Division of Soil Mechanics, University of Luleå
           1983-03-30

TR 83-17   Analysis of groundwater from deep boreholes in
           Gideå Sif Laurent
           Swedish Environmental Research Institute
           Stockholm, Sweden 1983-03-09

TR 83-18   Migration experiments in Studsvik
           O Landström
           Studsvik Energiteknik AB
           C-E Klockars
           O Persson
           E-L Tullborg
           S Å Larson
           Swedish Geological
           K Andersson
           B Allard
           B Torstenfelt
           Chalmers University of Technology
           1983-01-31

TR 83-19 Analysis of groundwater from deep boreholes in
          Fjällveden
          Sif Laurent
          Swedish Environmental Research Institute
          Stockholm, Sweden 1983-03-29

TR 83-20 Encapsulation and handling of spent nuclear fuel for
          final disposal
          1   Welded copper canisters
          2   Pressed copper canisters (HIPOW)
          3   BWR Channels in Concrete
          B Lönnerberg, ASEA-ATOM
          H Larker, ASEA
          L Ageskog, VBB
          May 1983

TR 83-21 An analysis of the conditions of gas migration from
          a low-level radioactive waste repository
          C Braester
          Israel Institute of Technology, Haifa, Israel
          R Thunvik
          Royal Institute of Technology
          November 1982

TR 83-22 Calculated temperature field in and around a
          repository for spent nuclear fuel
          Taivo Tarandi
          VBB
          Stockholm, Sweden April 1983

TR 83-23

TR 83-24 Corrosion resistance of a copper canister for spent
          nuclear fuel
          The Swedish Corrosion Research Institute and its
          reference group
          Stockholm, Sweden April 1983

TR 83-25 Feasibility study of EB welding of spent nuclear
          fuel canisters
          A Sanderson
          T F Szluha
          J Turner
          Welding Institute
          Cambridge, United Kingdom April 1983

TR 83-26 The KBS UO_2 leaching program
          Summary Report 1983-02-01
          Ronald Forsyth
          Studsvik Energiteknik AB
          Nyköping, Sweden February 1983

TR 83-27 Radiation effects on the chemical environment
          in a radioactive waste repository
          Trygve Eriksen
          Royal Institute of Technology
          Stockholm, Sweden April 1983

TR 83-28 An analysis of selected parameters for the BIOPATH-
          program
          U Bergström
          A-B Wilkens
          Studsvik Energiteknik AB
          Nyköping, Sweden April 1983

TR 83-29 On the environmental impact of a repository for spent
          nuclear fuel
          Otto Brotzen
          Stockholm, Sweden April 1983

TR 83-30 Encapsulation of spent nuclear fuel -
          Safety Analysis
          ES-konsult AB
          Stockholm, Sweden April 1983

TR 83-31 Final disposal of spent nuclear fuel -
          Standard programme for site investigations
          Compiled by
          Ulf Thoregren
          Swedish Geological
          April 1983

TR 83-32 Feasibility study of detection of defects in thick
          welded copper
          Tekniska Röntgencentralen AB
          Stockholm, Sweden April 1983

TR 83-33 The interaction of bentonite and glass with aqueous
          media
          M Mosslehi
          A Lambrosa
          J A Marinsky
          State University of New York
          Buffalo, NY, USA April 1983

TR 83-34 Radionuclide diffusion and mobilities in compacted
          bentonite
          B Torstenfelt
          B Allard
          K Andersson
          H Kipatsi
          L Eliasson
          U Olofsson
          H Persson
          Chalmers University of Technology
          Göteborg, Sweden April 1983

TR 83-35 Actinide solution equilibria and solubilities in
          geologic systems
          B Allard
          Chalmers University of Technology
          Göteborg, Sweden 1983-04-10

TR 83-36 Iron content and reducing capacity of granites and
          bentonite
          B Torstenfelt
          B Allard
          W Johansson
          T Ittner
          Chalmers University of Technology
          Göteborg, Sweden April 1983

TR 83-37   Surface migration in sorption processes
            A Rasmuson
            I Neretnieks
            Royal Institute of Technology
            Stockholm, Sweden March 1983

TR 83-38   Evaluation of some tracer tests in the granitic
            rock at Finnsjön
            L Moreno
            I Neretnieks
            Royal Institute of Technology, Stockholm
            C-E Klockars
            Swedish Geological, Uppsala
            April 1983

TR 83-39   Diffusion in the matrix of granitic rock
            Field test in the Stripa mine. Part 2
            L Birgersson
            I Neretnieks
            Royal Institute of Technology
            Stockholm, Sweden March 1983

TR 83-40   Redox conditions in groundwaters from
            Svartboberget, Gideå, Fjällveden and Kamlunge
            P Wikberg
            I Grenthe
            K Axelsen
            Royal Institute of Technology
            Stockholm, Sweden 1983-05-10

TR 83-41   Analysis of groundwater from deep boreholes in
            Svartboberget
            Sif Laurent
            Swedish Environmental Research Institute
            Stockholm, Sweden April 1983

TR 83-42   Final disposal of high-level waste and spent
            nuclear fuel - foreign activities
            R Gelin
            Studsvik Energiteknik AB
            Nyköping, Sweden May 1983

TR 83-43   Final disposal of spent nuclear fuel - geological,
            hydrological and geophysical methods for site
            characterization
            K Ahlbom
            L Carlsson
            O Olsson
            Swddish Geological
            Sweden May 1983

TR 83-44   Final disposal of spent nuclear fuel - equipment
            for site characterization
            K Almén, K Hansson, B-E Johansson, G Nilsson
            Swedish Geological
            O Andersson, IPA-Konsult
            P Wikberg, Royal Institute of Technology
            H Åhagen, SKBF/KBS
            May 1983

TR 83-45 Model calculations of the groundwater flow at
          Finnsjön, själlveden, Gideå and Kamlunge
          L Carlsson
          Swedish Geological, Göteborg
          B Grundfelt
          Kemakta Konsult AB, Stockholm
          May 1983

TR 83-46 Use of clays as buffers in radioactive repositories
          Roland Pusch
          University of Luleå
          Luleå May 25 1983

TR 83-47 Stress/strain/time properties of highly compacted
          bentonite
          Roland Pusch
          University of Luleå
          Luleå May 1983

TR 83-48 Model calculations of the migration of radio-
          nuclides from a repository for spent nuclear fuel
          A Bengtsson
          B Grundfelt
          Kemakta Konsult AB, Stockholm
          M Magnusson
          I Neretnieks
          A Rasmuson
          Royal Institute of Technology, Stockholm
          May 1983

TR 83-49 Dose and dose commitment calculations from ground-
          waterborne radioactive elements released from a
          repository for spent nuclear fuel
          U Bergström
          Studsvik Energiteknik AB
          Nyköping, Sweden May 1983

TR 83-50 Calculation of fluxes through a repository caused
          by a local well
          R Thunvik
          Royal Institute of Technology
          Stockholm, Sweden May 1983

TR 83-51 GWHRT - A finite element solution to the coupled
          ground water flow and heat transport problem in
          three dimensions
          B Grundfelt
          Kemakta Konsult AB
          Stockholm, Sweden May 1983

TR 83-52 Evaluation of the geological, geophysical and
          hydrogeological conditions at Fjällveden
          K Ahlbom
          L Carlsson
          L-E Carlsten
          O Durano
          N-Å Larsson
          O Olsson
          Swedish Geological
          May 1983

TR 83-53   Evaluation of the geological, geophysical and
            hydrogeological conditions at Gideå
            K Ahlbom
            B Albino
            L Carlsson
            G Nilsson
            O Olsson
            L Stenberg
            H Timje
            Swedish Geological
            May 1983

TR 83-54   Evaluation of the geological, geophysical and
            hydrogeological conditions at Kamlunge
            K Ahlbom
            B Albino
            L Carlsson
            J Danielsson
            G Nilsson
            O Olsson
            S Sehlstedt
            V Stejskal
            L Stenberg
            Swedish Geological
            May 1983

TR 83-55   Evaluation of the geological, geophysical and
            hydrogeological conditions at Svartboberget
            K Ahlbom
            L Carlsson
            B Gentzschein
            A Jämtlid
            O Olsson
            S Tirén
            Swedish Geological
            May 1983

TR 83-56   I: Evaluation of the hydrogeological conditions
                 at Finnsjön
            II: Supplementary geophysical investigations of
                 the Sternö peninsula
            B Hesselström
            L Carlsson
            G Gidlund
            Swedish Geological
            May 1983

TR 83-57   Neotectonics in northern Sweden -
            geophysical investigations
            H Henkel
            K Hult
            L Eriksson
            Geological Survey of Sweden
            L Johansson
            Swedish Geological
            May 1983

TR 83-58   Neotectonics in northern Sweden - geological
            investigations
            R Lagerbäck
            F Witschard
            Geological Survey of Sweden
            May 1983

TR 83-59   Chemistry of deep groundwaters from granitic
            bedrock
            B Allard
            Chalmers University of Technology
            S Å Larson
            E-L Tullborg
            Swedish Geological
            P Wikberg
            Royal Institute of Technology
            May 1983

TR 83-60   On the solubility of technetium in geochemical
            systems
            B Allard
            B Torstenfelt
            Chalmers University of Technology
            Göteborg, Sweden 1983-05-05

TR 83-61   Sorption behaviour of welldefined oxidation
            states
            B Allard
            U Olofsson
            B Torstenfelt
            H Kipatsi
            Chalmers University of Technology
            Göteborg, Sweden May 1983

TR 83-62   The distribution coefficient concept and aspects
            on experimental distribution studies
            B Allard
            K Andersson
            B Torstenfelt
            Chalmers University of Technology
            Göteborg, Sweden May 1983

TR 83-63   Sorption of radionuclides in geologic systems
            K Andersson
            B Torstenfelt
            B Allard
            Chalmers University of Technology
            Göteborg, Sweden May 1983

TR 83-64   Ion exchange capacities and surface areas of some
            major components and common fracture filling
            materials of igneous rocks
            B Allard
            M Karlsson
            Chalmers University of Technology
            E-L Tullborg
            S Å Larson
            Swedish Geological
            May 1983